



Faculty of Engineering

Master of Science in Hydrocarbon Processing Engineering

DISSERTATION TITLE

Numerical Simulation Study on Liquefied Natural Gas and Boil-off Gas Behaviour Changes, Boil-off Gas Recovery and Conversion to CNG fuel at LNG Receiving Terminal.

A Dissertation by

NGIRUWONSANGA Emmanuel

Location of Submission:

Maputo, Mozambique

Year of Submission:

October 2024



Faculty of Engineering

Master of Science in Hydrocarbon Processing Engineering

DISSERTATION TITLE

Numerical Simulation Study on Liquefied Natural Gas and Boil-off Gas Behaviour Changes, Boil-off Gas Recovery and Conversion to CNG fuel at LNG Receiving Terminal.

A Dissertation by

NGIRUWONSANGA Emmanuel

Supervisors

Dr. Alberto Bila and Dr. João Chidamoio

Location of Submission:

Maputo, Mozambique

Year of Submission:

October 2024

DECLARATION OF DOCUMENT ORIGINALITY

"I declare that this dissertation has never been submitted to obtain any degree or in any other context and is the result of my own individual work. This dissertation is presented in partial fulfillment of the requirements for the degree of Master of Science in Hydrocarbon Processing Engineering, from the Universidade Eduardo Mondlane".

Submitted by: **Emmanuel NGIRUWONSANGA**

ABSTRACT

As the energy market continues to grow, the liquefied natural gas has attracted attention as a cheap and environmentally friendly option to carry natural gas for distant markets. As a result, the liquefied natural gas supply chain has also witnessed a steady increase. The boil-off gas (BOG) generated at LNG receiving terminals is significant and industry practice is to flare and vent it to the atmosphere, which causes environmental damage. This work proposes a technical strategy to minimize the flaring and venting of excess BOG by using it as an alternative fuel for CNG-powered vehicles at the LNG receiving terminal. Dynamic simulation studies were carried out to quantify and recover the dynamic generation of BOG during LNG regasification, ships unloading and holding mode, under hourly ambient temperature between 26th May and 13th June 2024 for the hypothetical Maputo LNG receiving terminal of a 200,000 m³ aboveground full containment LNG storage tank. The heat ingress and BOG recovery at the LNG receiving terminal were simulated with LNG and generated BOG property changes analysis. Whilst the BOG conversion into CNG was investigated with the use of multistage compressor. The model was simulated for BOG generated by three different LNGs to analyse the resulted CNG suitable for to be used as vehicle fuel. The simulation results show that BOG recovered from lean, medium and rich LNG respectively is 315913.51kg, 290373.34kg and 307147.70kg during LNG regasification, 186482.32kg, 156570.73kg, and 173210.30kg during ships unloading with 168628.30kg, 140249.76kg and 159199.1kg solely during LNG pumping and piping, and 22462.53kg, 22370.38kg, and 19279.79kg during holding mode. A 100% excess BOG produced were recovered. During LNG regasification, lean, medium, and rich LNG storage tank served 361 hours, 383 hours and 406 hours respectively with a constant 200,000 kg hourly LNG regasification. During ships unloading mode, lean, medium and rich LNG storage tank took 15.2497 hours, 15.2496 hours, and 15.2492 hours to get at 95% storage capacity. The ships unloading mode produced more CNG hourly, more energy consumption for a CNG kilogram produced during ship unloading mode except in medium LNG, and CNG from lean and medium LNG's BOG are on spec to be used as a vehicle fuel.

Keywords: Liquefied Natural Gas, LNG receiving terminal, boil-off gas, BOG conversion, multistage compressor, Compressed Natural Gas.

RESUMO

À medida que o mercado de energia continua a crescer, o gás natural liquefeito (GNL) vem se mostrando uma opção barata e ecologicamente correcta para transportar gás natural para mercados distantes. O gás de evaporação (BOG) gerado nos terminais de descarga de GNL é significativo e a prática da indústria é queimá-lo e ventilá-lo para a atmosfera, o que causa danos ambientais. Este trabalho propõe uma estratégia técnica para minimizar a queima e ventilação do excesso de BOG, utilizando-o como combustível alternativo para veículos movidos a gás natural comprimido (GNC) nos terminais de descarga de GNL. Estudos de simulação dinâmica foram realizados para quantificar e recuperar a geração dinâmica de BOG durante a regaseificação de GNL, descarrea e modo de retenção de navios, sob temperatura ambiente horária entre 26 de maio e 13 de junho de 2024 para o terminal de descarga de GNL hipotético de Maputo, com um tanque de armazenamento de GNL de 200.000 m³ de contenção total acima do solo. A entrada de calor e a recuperação de BOG no terminal de descarga de GNL foram simuladas com a análise das mudanças nas propriedades do GNL e do BOG gerado. Enquanto isso, a conversão de BOG em GNC foi investigada com o uso de um compressor multi estágio. O modelo foi simulado para o BOG gerado por três diferentes GNLs para analisar o GNC resultante adequado para ser usado como combustível para veículos. Os resultados da simulação mostram que o BOG recuperado de GNL magro, médio e rico, respectivamente, é de 315913,51 kg, 290373,34 kg e 307147,70 kg durante a regaseificação de GNL, 186482,32 kg, 156570,73 kg e 173210,30 kg durante a descarga de navios, com 168628,30 kg, 140249,76 kg e 159199,1 kg exclusivamente durante o bombeamento e tubulação de GNL, e 22462,53 kg, 22370,38 kg e 19279,79 kg durante o modo de retenção. Foi recuperado 100% do excesso de BOG produzido. Durante a regaseificação de GNL, os tanques de armazenamento de GNL magro, médio e rico serviram por 361 horas, 383 horas e 406 horas, respectivamente, com uma regaseificação constante de 200.000 kg por hora de GNL. Durante o modo de descarga de navios, os tanques de armazenamento de GNL magro, médio e rico levaram 15,2497 horas, 15,2496 horas e 15,2492 horas para atingir 95% da capacidade de armazenamento. O modo de descarga de navios produziu mais GNC por hora, com maior consumo de energia por quilograma de GNC produzido durante o modo de descarga de navios, exceto no GNL médio, e o GNC proveniente do BOG de GNL magro e médio está conforme as especificações para uso como combustível para veículos.

Palavras-chave: Gás Natural Liquefeito, terminal de recebimento de GNL, gás de evaporação, conversão de BOG, compressor de múltiplos estágios, Gás Natural Comprimido.

DEDICATION

To my beloved family,

This thesis is dedicated to you. Your unwavering support, endless encouragement, and boundless love have been my rock throughout this journey. Without your sacrifices, patience, and faith in my potential, none of this would have been possible. You are my inspiration and my strength, and for that, I am eternally grateful.

ACKNOWLEDGEMENTS

First and foremost, I extend my deepest gratitude to Almighty God for granting me the strength, wisdom, and perseverance to complete this work and my studies as well.

“I can do all things through Christ who strengthens me.”

Philippians 4:13.

To my family, your unwavering support and love have been my anchor. Your encouragement has propelled me forward every step of the way.

A special thank you to my supervisors, Dr. Alberto Bila and Dr. João Chidamoio, whose guidance, expertise, and patience have been invaluable. Your insights have shaped this work, and your mentorship has been a cornerstone of my academic journey.

To my lecturers, thank you for imparting your knowledge and fostering a stimulating learning environment, your dedication to education has greatly contributed to my growth.

Finally, to my classmates, thank you for camaraderie and collaborative spirit. Together, we have navigated challenges, celebrated successes, and created lasting memories.

TABLE OF CONTENTS

ABSTRACT	ii
DEDICATION	iv
ACKNOWLEDGEMENTS	v
LIST OF TABLES	xi
ACRONYMS	xiii
CHAPTER I	1
INTRODUCTION	1
1.1. Background	1
1.2. Problem statement	6
1.3. Research Objectives	7
1.3.1. Main objective	7
1.3.2. Specific objectives	7
1.4. Motivation	7
CHAPTER II	8
LITERATURE REVIEW	8
2.1. LNG receiving terminal	8
2.1.1. Docking facilities	8
2.1.2. Storage tanks	9
2.1.3. BOG management facilities	12
2.1.4. Regasification units	12
2.1.5. Pumping system	13
2.1.6. Safety and environmental systems	14
2.2. Boil-off gas sources, recovery and use	15
2.2.1. Sources of BOG source during receiving terminal operational modes	15
2.2.2. Boil-off gas recovery	17
2.2.3. Boil-off gas use	18
2.3. CNG	19
CHAPTER III	22
RESEARCH MATERIAL AND METHODOLOGY	22
3.1. Research material	22
3.1.1. Software	22
3.1.2. Equation of state	22

3.1.3. Operation conditions.....	23
3.1.4. Designed Receiving terminal.....	26
3.2. Research methodology.....	29
3.2.1. Heat ingress.....	30
3.2.2. BOG management.....	34
3.2.3. Safety and control	35
3.2.4. LNG, BOG and CNG properties.....	36
CHAPTER IV.....	37
RESULTS AND DISCUSSION.....	37
4.1. Heat ingress.....	37
4.1.1. Heat ingress to the LNG storage tank.....	37
4.1.2. Heat ingress in piping and pumping	54
4.2. LNG and BOG properties changes	58
4.2.1. Composition.....	59
4.2.2. Molecular weight	77
4.2.3. Density	83
4.2.4. Heat capacity.....	87
4.2.5. Heating value	91
4.2.6. Thermal conductivity	96
4.3. Recoverable BOG	100
4.4. BOG management.....	102
4.5. CNG properties	104
4.6. Validation	108
CHAPTER V.....	109
CONCLUSION AND RECOMMENDATION	109
5.1. Conclusion	109
5.2. Future study recommendation.....	109
REFERENCES	110
ANNEXES.....	117
I. Depicted temperature and solar radiation	117
II. Collected Maputo average wind speed	123
CURRICULUM VITAE	Error! Bookmark not defined.

LIST OF FIGURES

Figure 1. Flowchart of BOG recovery and conversion into CNG fuel at receiving terminal.....	5
Figure 2. Aboveground single, double, and full containment LNG tanks (Coyle & Patel, 2005).	11
Figure 3. Membrane tank wall make-up (Rötzer, 2016).....	12
Figure 4. Simulated LNG regasification flowchart.....	25
Figure 5. Simulated ships unloading mode flowchart.	25
Figure 6. Simulated LNG holding mode flowchart.	26
Figure 7. Hourly BOG excess formation from lean LNG during LNG regasification from receiving terminal tank.	38
Figure 8. Hourly BOG excess formation from medium LNG during LNG regasification from receiving terminal tank.	39
Figure 9. Hourly BOG excess formation from rich LNG during LNG regasification from receiving terminal tank.	40
Figure 10. Relationship of bottom heat leaks and the LNG temperature changes during LNG regasification.....	41
Figure 11. Hourly BOG excess released from lean LNG during LNG storage tank filling at receiving terminal.	42
Figure 12. Hourly BOG excess released from medium LNG during LNG storage tank filling at receiving terminal.	43
Figure 13. Hourly BOG excess released from rich LNG during LNG storage tank filling at receiving terminal.	44
Figure 14. Relationship of bottom heat ingress and LNG temperature change.....	44
Figure 15. Relationship between tank wall and roof heat ingress and the height of lean LNG column.....	46
Figure 16. Relationship between tank wall and roof heat ingress and the height of LNG column.	47
Figure 17. Relationship between tank wall and roof heat ingress and the height of LNG column.	48
Figure 18. Relationship of heat, ambient temperature and hourly BOG excess released from receiving terminal lean LNG storage tank.	48

Figure 19. Relationship of heat, ambient temperature and hourly BOG excess released from receiving terminal medium LNG storage tank.....	49
Figure 20. Relationship of heat, ambient temperature and hourly BOG excess released from receiving terminal rich LNG storage tank.	50
Figure 21. Relationship between tank wall and roof heat ingress and the height of lean LNG column.....	50
Figure 22. Relationship between tank wall and roof heat ingress and the height of medium LNG column.....	51
Figure 23. Relationship between tank wall and roof heat ingress and the height of LNG column.	52
Figure 24. Relationship of tank bottom heat ingress and LNG temperature change.....	53
Figure 25. Relationship between heat ingress into run-down pipelines and ambient temperature.	56
Figure 26. Relationship between BOG formation and heat ingress through piping and pumping of the LNG.	58
Figure 27. Lean LNG compositional change during LNG regasification.	60
Figure 28. Medium LNG compositional change during LNG regasification.	61
Figure 29. Rich LNG compositional change during LNG regasification.	61
Figure 30. BOG composition changes during lean LNG regasification.	63
Figure 31. BOG composition changes during medium LNG regasification.	64
Figure 32. BOG composition changes during rich LNG regasification.	64
Figure 33. Lean LNG compositional change during storage tank loading.	67
Figure 34. Medium LNG compositional change during storage tank loading.	67
Figure 35. Rich LNG compositional change during storage tank loading.	68
Figure 36. BOG composition changes during lean LNG storage tank loading.	69
Figure 37. BOG composition changes during medium LNG storage tank loading.....	70
Figure 38. BOG composition changes during storage tank loading with rich LNG.....	70
Figure 39. Lean LNG compositional change during storage tank holding mode.	72
Figure 40. Medium LNG compositional change during storage tank holding mode.	72
Figure 41. Rich LNG compositional change during storage tank holding mode.	73
Figure 42. BOG composition changes during lean LNG storage tank holding mode.	74

Figure 43. BOG composition changes during medium LNG storage tank holding mode.....	75
Figure 44. Rich LNG compositional change during storage tank holding mode.	75
Figure 45. Molecular weight and volume changes during lean LNG regasification.	78
Figure 46. Molecular weight and volume changes during LNG storage tank filling.	81
Figure 47. Molecular weight and volume changes during holding mode for lean LNG.	82
Figure 48. BOG molar and mass density changes during LNG regasification.....	84
Figure 49. BOG molar and mass density changes during LNG ships unloading.	85
Figure 50. BOG molar and mass density changes during LNG holding mode.	86
Figure 51. BOG specific and mass heat capacity changes during LNG regasification mode.	88
Figure 52. BOG specific and mass heat capacity changes during LNG unloading from the ship.	89
Figure 53. BOG specific and mass heat capacity changes during LNG holding mode.....	91
Figure 54. Higher heating value changes during LNG regasification mode.	92
Figure 55. Lower heating value changes during LNG regasification mode.	92
Figure 56. Higher heating value changes during LNG ships unloading mode.....	93
Figure 57. Lower heating value changes during LNG ships unloading mode.....	94
Figure 58. Higher heating value changes during LNG holding mode.....	95
Figure 59. Lower heating value changes during LNG holding mode.....	95
Figure 60. Thermal conductivity of BOG during LNG regasification.	97
Figure 61. Thermal conductivity of BOG during LNG ships unloading mode.	98
Figure 62. Thermal conductivity of BOG during LNG holding mode.	99
Figure 63. Study results comparison of BOG generation and methane content relationship during holding mode.	108
Figure 64. Mozambican map of average wind speed at 100m (Badger et al., 2024).	123

LIST OF TABLES

Table 1. In-ground and aboveground LNG storage tank differences (Mokhatab et al., 2014).	10
Table 2. Difference between onshore and offshore regasification units.	13
Table 3. LNG composition and initial storage temperature used.....	23
Table 4. LNG ship carrier fabric, insulation and their thickness.	27
Table 5. LNG storage tank material, thermal conductivity, thickness, and absorptivity.	28
Table 6. Hourly heat ingress into LNGs from the pumps and pumped LNG volume.	55
Table 7. Initial LNG and BOG composition inside storage tank during LNG regasification.	59
Table 8. Initial LNG and BOG composition inside storage tank during ship unloading.....	65
Table 9. Ship unloaded lean LNG composition.	66
Table 10. Final LNG and BOG composition inside storage tank after ship unloading.	71
Table 11. Final LNG and BOG composition inside storage tank at the end of LNG holding mode.	76
Table 12. Initial and final molecular weight and volume of LNG during regasification.....	78
Table 13. Initial and final molecular weight and volume of LNG during storage tank loading from ships.	79
Table 14. Initial and final molecular weight and volume of LNG during storage tank holding mode.	81
Table 15. Initial and final mass and molar density of LNG during LNG regasification.	83
Table 16. Initial and final mass and molar density of LNG during storage tank loading.	85
Table 17. Initial and final mass and molar density of LNG during holding mode.	86
Table 18. Initial and final heat capacities of LNG during LNG regasification.....	87
Table 19. Initial and final heat capacities of LNG during ships unloading mode.	89
Table 20. Initial and final heat capacities of LNG during holding mode.	90
Table 21. Initial and final heating values of LNG during LNG regasification.	91
Table 22. Initial and final heating values of LNG during ships unloading.	93
Table 23. Initial and final heating values of LNG during holding mode.....	94
Table 24. Initial and final thermal conductivity of LNG during LNG regasification.	96
Table 25. Initial and final thermal conductivity of LNG during ships unloading.....	98
Table 26. Initial and final thermal conductivity of LNG during holding mode.....	99
Table 27. BOG conversion to CNG simulation results.....	102

Table 28. Conversion performance assessment.	103
Table 29. The resulted CNG composition for each LNG in all simulated modes.	104
Table 30. Produced CNG properties and its comparison to typical CNG properties' range.	106
Table 31. Used temperature and solar radiation (AccuWeather, 2024; Tutiempo network, 2024).	117

ACRONYMS

TWh: terra watt hour

bcm: billion cubic meters

LNG: liquified natural gas

BOG: boil-off gas

CNG: compressed natural gas

BOR: boil-off gas rate

kWh: kilowatt hour

LP: low pressure

GIIP: good international industrial practices

EHS: environmental, health and safety

barg: bar gauge

STV: shell and tube vaporiser

ORV: open rack vaporizer

SCV: submerged combustion vaporiser

LKP: lee-kesler-plöcker equation of state

BWRS: benedict-webb-rubin-starling equation of state

MON: motor octane number

VLV: valve

BCE: before common era

PIP: piping

API: american petroleum institute

CHAPTER I

INTRODUCTION

1.1. Background

Day-to-day, energy seeking solutions are unveiled due to the increase in the world population and economic growth. The search for ever cleaner energy solutions is becoming increasingly frequent due to global warming driven by the use of fossil fuels, the increase in the world's population and economic growth.

A long time ago, people used to burn wood to get the energy they needed in their daily life. Later, they started to use wind energy to sail across water bodies. Waterfalls were then used to produce electricity. Currently, the population's life depends on energy. There are various sources of energy including renewable and non-renewable resources. Renewable energy sources are yet to be enhanced to take over non-renewable sources. In 2022, 80.45% (143939 TWh) of energy consumed across the world was from non-replenishable sources. These are mostly fossil fuel and some radioactive minerals. Non-replenishable energy sources are petroleum, natural gas, coal, and uranium. Natural gas contributed 22.03% of the non-renewable energy sources. In the last ten years (2012 to 2022), natural gas consumption has increased from 25030 TWh to 39413TWh, which is equivalent to 36.5% increase, and it is expected to continue increasing (Hannah et al., 2024). In 2016, around 28.55% of the energy consumption was solely for transport sector (NEED, 2018). Since 2010, demand for natural gas in transport domain has increased up to 27.3% over the last twelve years, from 2010 to 2022 (International Energy Agency, 2023).

Natural gas is a fossil fuel that is primarily made up and small quantities of lighter hydrocarbons, such as ethane and propane. In its raw state, natural gas also contains non-hydrocarbon species such as nitrogen, carbon dioxide, hydrogen sulfide as well as helium may also present depending on the reservoir source (Al Ghafri et al., 2021). Natural gas reservoirs are often discovered in remote areas, and for this reason liquefied natural gas (LNG) dominates the natural gas energy market due to its ease of transport to distant locations and cheaper storage facilities.

In modern society, it has become a key energy source in the global energy transition for several reasons, including low cost, low CO₂ emission into the atmosphere and established distribution

network. Natural gas contributes 50 to 60% less CO₂ production than coal and 15 to 20% fewer greenhouse gas emissions than gasoline in vehicle engines (Al Ghafri et al., 2021).

Conversion of natural gas into liquid form is carried out by cooling it down to its normal boiling point of -160°C at atmospheric pressure; the main objectives of liquefaction process are to ease natural gas transportation for distant markets and storage. The liquefaction process shrinks the volume of natural gas by 600 times the volume natural gas would occupy at standard conditions. This makes it cost-effective transportation and storage possible (Al Ghafri et al., 2021; Dobrota et al., 2013).

Usually, LNG is transported and stored in tanks as a cryogenic liquid, or as a liquid that is below its boiling point, mostly at -163°C. Although LNG storage tanks are insulated, it does not completely stop heat ingress inside the tank due to the temperature difference between the LNG and the ambient temperature. Therefore, the heat ingress from the surrounding environment is unavoidable during LNG loading, transportation, storage tanks and distribution. This heat ingress causes LNG to evaporate, which is known as Boil-Off Gas (BOG). Furthermore, the heat ingress, alters the LNG quality, and quantity as well as the loading pressure of the LNG, as it turns portion of LNG to gaseous phase (Rahmania & Purwanto, 2020).

The BOG generation changes composition, volume, and pressure within LNG facilities and carrier tanks. The amount BOG depends on LNG quality, design and operational conditions of the LNG carrier such as ships and tanks. For safety reasons, the BOG is continuously removed from the tanks to avoid risks of an increase in LNG storage pressure, which could have serious consequences and render the storage system unsafe. Usually, the recovered BOG is used as fuel for liquefaction plant at the loading terminal, or re-liquefied or even burned during vessels transportation, vent or sent to regasification process after compression at receiving terminal (Dobrota et al., 2013; Włodek, 2019).

At receiving terminal, part of BOG is retrieved from storage tank and sent to the ship to balance pressure and optimize the LNG unloading process while the remaining part is flared or vented to atmosphere. Additional portion of BOG is re-condensed and mixed up with re-gasified LNG in a gas send-out pipeline. The BOG retrieved in storage tank at receiving terminal has many sources of formation: ship's unloading, pumping, heat ingress in storage tank, ambient temperature around

the pipes, pressure drop and mixing unloaded LNG with existing LNG stock in storage tanks (Dobrota et al., 2013).

Studies have been carried out to minimize, recover and use the BOG that is being flared, vented and burnt at receiving terminal. Liu et al. (2010) conducted thermodynamic analysis-based design and operation for BOG flare minimization at LNG receiving terminals. It was found that four-stage LNG regasification system (i.e. stage comprises of compressor, condenser and a pump) of the superstructure conceptual designed model is the most least energy consuming for recovering BOG generated at receiving terminal. Li & Li (2016) conducted dynamic simulation on receiving terminal and optimize the formation of BOG fluctuations. The result of optimization by tank pressure adjustment for different conditions appropriately, one compressor capacity conformed with BOG quantity, flaring and compressors' energy consumption was reduced. Wu et al. (2019) performed optimization and application for the recondensation process of boil-off gas in a liquefied natural gas receiving terminal. Their model was optimized by changing operating variable, recirculation and branch flow rate were introduced as variable, and effective operation variables were evident after optimization.

Thermodynamically based analysis has shown that BOG flare optimal minimization at receiving terminal can be achieved in stages. It was then proven that the optimum BOG minimization must be done in four stages LNG regasification system. Each stage had a compressor and condenser served for liquefying BOG into LNG before vaporization of LNG. The study was done by recovering, compressing, and mixing BOG with vaporized LNG. The mixture was sent into the gas distribution pipeline network. Evidently, the increase of stage numbers to five and six would be effective but would increase operating costs. The increase in stages means the increasing number of compressors. Compressor's energy consumption was found to cover 30% of the energy consumption of LNG unloading process. Despite the optimal design with certainly low energy consumption, BOG flaring and capital cost, operating cost remained higher beyond equilibrium line because of use of many compressors. Therefore, it had recommended for further study to completely cease flaring BOG and reduce operating cost (Liu et al., 2010).

The boil-off formation rate model has been established and studied using evaporation model, it has shown that for proper implementation of the developed model to monitor gas phase movement inside the tank, BOR valued to 0.11% weight of LNG inside the tank per day. It is below amount

found by other researchers by using other methods with 0.15% per day by International Marine Organization (IMO). Further studies for handling BOG and unloading/loading contribution were recommended to understand and tackle BOG generated (M. S. Zakaria et al., 2013).

The study of boil-off rate (BOR) relationship with LNG composition and temperature has been reported. It revealed that LNG with higher nitrogen (from 2%) associates with higher BOR than lean and rich LNG. This is because nitrogen has low bubble temperature and rich LNG has slightly higher boiling point due to the presence of heavy components such as ethane and propane (Włodek, 2019). In contrast, the LNG composition is inconsistent since it varies within a reservoir, unloaded from different ships, different location and other factors such as ageing. Furthermore, the temperature continues to rise because of global warming. Proper ways of regulating boil-off rate towards constant and use of BOG use are recommended to be studied.

For small scale LNG facilities, the cogeneration plant showed to be an alternative BOG management with re-liquefaction together as backup. It has the capability of processing all BOG in most demanding instinct. This work has suggested an in-ground tank and recommended further study on a dynamic simulation of the loading and unloading tank at receiving terminal to understand, envision, and maximize the suitable BOG solutions for the terminal (Alexandra & Antunes, 2018).

Dynamic optimization of the Boil-Off Gas (BOG) fluctuations at an LNG receiving terminal has been carried out and provides its recommendation towards effective minimization of BOG. It has shown that proper adjustment of LNG tank's operating pressure against different conditions resulted from ambient or receiving terminal's activity, BOG's quantity can be kept to single compressor's capacity and 0.19 million cubic meter can be saved from being flared per year. Therefore, not the easy control of recondenser gained but also BOG compressor's energy consumption and power can be saved with 4.2% and 0.19 million kWh with 0.14 million US dollars annual saving (Li & Li, 2016).

M. Ibrahim. Khan & Islam (2007) have conducted a study on energy saving by BOG prediction efficiently and BOR impact in a full containment LNG storage tank. Heat leakage, BOG generation, and BOR have been found out to depend on the LNG level in tank.

During the study of rollover phenomena in LNG storage tank, the LNG density was found to continuously decrease as the time that LNG is being stored increases and abruptly rose and fell during rollover occurrences (Z. Zakaria et al., 2019).

Previous works have defined, traced BOG sources and propose ways to minimize BOG flaring and venting as well as optimize BOG usage at receiving terminal; One way is to recover BOG and condense it into LNG. However, excess BOG has been flared to avoid safety operational problems. Therefore, more studies are required to research to understand the LNG and BOG behaviour changes, and the best practices for capturing BOG and reducing gas flaring and venting at the LNG receiving terminal.

This work proposes a new technical strategy to minimize the flaring and venting of excess BOG at the receiving terminal by converting BOG into an alternative fuel for CNG-powered vehicles at the LNG receiving terminal. A dynamic simulation will be employed to evaluate and recover dynamic BOG generation during the LNG unloading, storage, piping, and pumping stages in Figure 1. The recovered BOG at the LNG receiving terminal is then subjected to multi-stage compression to be used as an alternative fuel for CNG-powered vehicles.

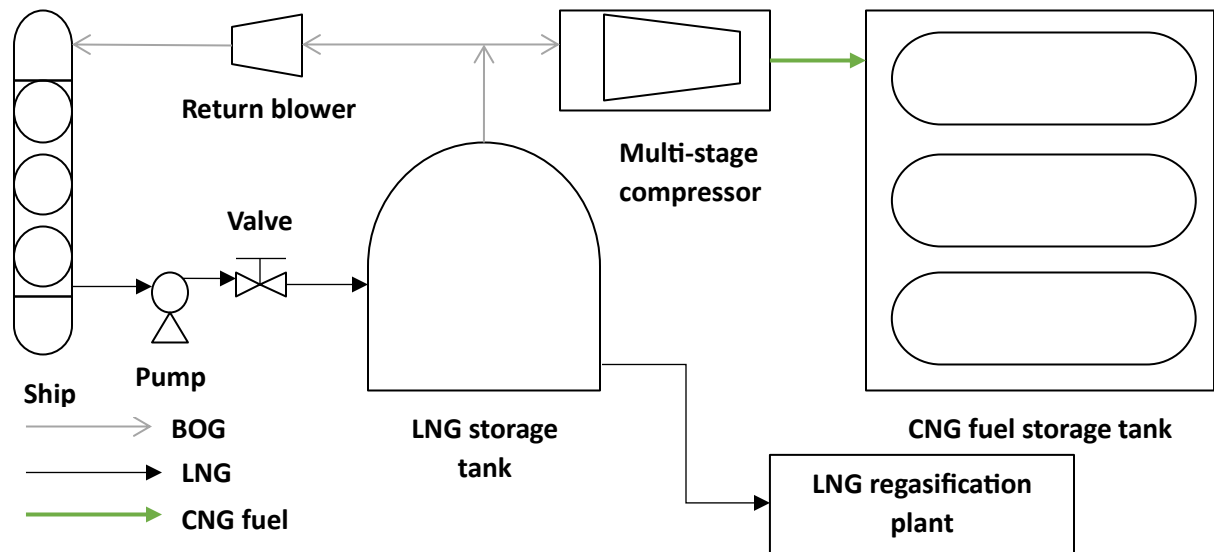


Figure 1. Flowchart of BOG recovery and conversion into CNG fuel at receiving terminal.

1.2. Problem statement

For long distances, natural gas is most economically transported in liquid form through vessels across the whole world (Foss, 2012). During the loading, transport, and unloading of LNG, natural gas evaporates due to heat exchange between the LNG and its environment. This evaporation creates Boil-Off Gas (BOG), which alters the LNG volume over time. BOG typically ranges from 0.022 to 0.05% of the LNG storage tank per day (Włodek, 2019; Yang, 2006). Boil-Off Gas (BOG) from LNG, though relatively small, has notable economic and environmental impacts. As BOG increases, it raises the pressure in LNG tanks, leading to the need for continuous flaring and venting to maintain safe levels, resulting in economic losses and environmental harm. Since LNG is largely comprised of methane, the approximate LNG global warming potential is between 27 and 30 for 100 years. It lasts shorter than CO₂ but absorbs more energy than CO₂ (EPA, 2023). The flaring and venting of BOG are undesirable as it contributes to greenhouse gases emissions and environmental damage. In LNG supply chain, scholars have proposed that BOG can be recovered and used as fuel, or re-liquefied (Włodek, 2019).

The flaring and venting of Boil-Off Gas (BOG) result in economic losses and environmental pollution. BOG, primarily composed of lighter methane and nitrogen, decreases over time, leading to an increase in heavier hydrocarbons like ethane, propane, i-butane, n-butane, and i-pentane. This weathering process reduces LNG volume and energy density, but increases the higher heating value and Wobbe Index, still within gas turbine and engine specifications. Effective BOG recovery and efficient use are recommended to mitigate these supply chain impacts (Rahmania & Purwanto, 2020).

This work will assess all scenarios associated with BOG formation, LNG and BOG behaviour changes, and introduce new techniques for efficiently recovering and converting BOG into CNG fuel at receiving terminal. This study attempts to answer the following research questions:

1. How much BOG excess is generated from each source in the LNG value chain at the receiving terminal?
2. How much BOG is recovered and converted into CNG fuel?
3. How much energy is consumed by converting BOG into CNG fuel?
4. Is the conversion of BOG into CNG technically feasible?
5. Is the produced CNG fuel on spec?

1.3. Research Objectives

1.3.1. Main objective

This work proposes a technical strategy to minimize the flaring and venting of BOG excess by using it as an alternative fuel for CNG-powered vehicles at receiving terminal.

1.3.2. Specific objectives

- To develop a dynamic process model of LNG receiving terminal and BOG conversion into CNG;
- To perform heat ingress analysis at LNG receiving terminal tank;
- To investigate the changes of LNG and BOG composition and properties;
- To evaluate recoverable BOG and its management at the receiving terminal;
- To analysis of resulted CNG fuel specifications.

1.4.Motivation

The planet is facing severe climate change while it fears the nearing end of fossil resources; therefore, proper use of resources and sustainable innovative energy solutions are of vital concerns. BOG flaring and vent have been contributing adverse greenhouse gases through the result of CO₂ and unburned methane. CO₂ emission pollutes the atmosphere and BOG flaring is one of its sources. Methane is the major component of BOG. Despite the various uses of methane gas, its emission has a higher warming potential than CO₂ though it short-lived (EPA, 2023; The World Bank, 2022, 2023). This study is driven by environmental and financial concerns over gas flaring; therefore, an efficient capture of BOG and subsequent conversion into CNG fuel for use in vehicle as proposed.

CHAPTER II

LITERATURE REVIEW

As this study will solely deal with BOG management and its conversion at the receiving terminal, this chapter will mainly focus on receiving terminal operations, boil-off gas recovery and compressed natural gas.

2.1.LNG receiving terminal

An LNG receiving terminal is a natural gas downstream comprises of final stage of LNG supply chain before final distribution to end consumers. It is a facility designed to receive, store, and regasify LNG transported by ship cargo. The operations that take place at LNG receiving terminal are LNG unloading, storing, regasification, BOG recovery, and gas distribution. These terminals play a crucial role in the natural gas supply chain, enabling countries to import natural gas from regions where it is abundant.

An LNG receiving terminal comprises of docking facilities, storage tanks, BOG management facilities, regasification units, pumping systems, safety and environmental systems.

2.1.1. Docking facilities

Docking facilities are the specialized berths where LNG carriers can safely unload their cargo and equipped with specialized loading and unloading arms and hoses for transfer.

The facilities for berthing and unloading LNG, including all shore-side discharge arms and associated facilities, are known as the LNG jetty. The loading platform, breasting dolphin, and mooring dolphin make up the LNG Jetty's structure. The location of the LNG jetty must be sufficiently far from the population center. The exact depth, width, and alignment of the navigation channel must also be determined. Ignition-free safety zones must be identified. A suitable strength mooring system must be built. The safety transfer system must be installed using PERCs (Powered Emergency Release Couplers) and ERSs (Emergency Release Systems) (Turbaningsih & Yuanita, 2014).

LNG docking facilities are designed based on location, regulatory requirements, design criteria, site criteria, infrastructure availability, capacity intended, operational concerns, LNG sources, LNG characteristics, gas distribution criteria, owner's requirements, safety, and security considerations (Kaplan & Yang, 2003).

Before LNG unloading at receiving terminal, the unloading arms and rundown lines are cooled down to cryogenic temperature to avoid high LNG evaporation. The arms and pipelines are kept at low temperature by ship's unloaded LNG or LNG from storage tank. (Naji et al., 2019a). Arms and rundown lines are also kept at cryogenic temperature by continuous recirculating LNG in arms and pipelines from storage tank whenever there is no loading and unloading (M. S. Khan et al., 2020). When there are no continuous recirculation lines, ship's LNG is used to cool unloading arms and pipelines prior to unloading (Dobrota et al., 2013). Prior to unloading after arrival and mooring of the ship cargo, ship's BOG is drained via unloading arm to an empty storage tank and then to the flare. This is done to cryogenically cool down the temperature of unloading arms and pipes during receiving terminal start-up (Mokhatab et al., 2014).

LNG is unloaded from ship cargo through articulated unloading arms passing through rundown lines unto the receiving terminal storage tank. The flowrate of unloading LNG depends on the pressure and temperature difference between ship cargo tank and the LNG storage tank (Dobrota et al., 2013). While doing so, the loading arm returns through return blowers the displaced and formed BOG from the storage tank to the ship cargo tank. This procedure avoids the vessel's tanks pressure droppage, vacuum creation, and facilitates the LNG unloading process. This process is carried out until the LNG in ship cargo reaches the lowest allowable LNG volume in its tanks to keep it cool (Kurle et al., 2017).

Depending on the designed LNG receiving terminal size, docking facilities and jetty have limited ships unloading, storage and send-out capacity it cannot go beyond. Docking facilities can accommodate a ship cargo from 60,000m³ up to 250,000m³, store up to 250,000m³ and more for a single tank and with send-out capacity up to 2 billion standard cubic feet per day (Coyle & Patel, 2005).

2.1.2. Storage tanks

LNG storage tanks are insulated tanks that store LNG at very low temperatures (i.e., cryogenic temperature) to keep it in liquid form. They are typically designed with double walls for safety and to minimize LNG vaporization losses. The typical vaporization losses known as boil-off gas rate is 0.05% of the storage tank volume per day. LNG is stored at atmospheric pressure or slightly higher. Tank storage capacity can vary from 160,000m³ matching up the modern LNG carriers to more than 200,000m³ (Mokhatab et al., 2014). Currently, modern LNG storage tank at receiving

terminal can reach to 270,000m³ (Dobrota et al., 2013). LNG tanks are designed to comply with site and design criteria, environmental and safety requirements, regional geology, regulations, codes, and standard applicable design (Mokhatab et al., 2014). Tanks are divided in two major groups: in ground and above ground LNG storage tanks. The main difference is that in ground is built underneath the surface with less visibility while the above ground tanks are built and visible at the earth's surface. The detailed difference is summarised into the table 1 below. Aboveground tanks are mainly used, and the biggest LNG tanks are aboveground tanks (Long & Garner, 2004).

Table 1. In-ground and aboveground LNG storage tank differences (Mokhatab et al., 2014).

	In ground LNG tank	Above ground LNG tank
Containment	Single	Double
Insulation	Polyurethane and grass wool	Perlite and grass wool
Construction duration	4 to 5 years	3 years
Earthquake	More resistant	Resistant
Cost	Expensive	Cheap
Space	Save space	Require large space
Repairment	Hard	Easy

However, there are categories of LNG storage tank based on their designed structure, the most common are single, double, and full containment but there is a new coming design called LNG storage tank according to EN 1473, EN14620-1, NFPA 59A, and API 625 (Rötzer, 2016). All the categories of tanks are made of 9% nickel steel as the inner tank and differs with the further containment. Single, double, and full containment tanks are surrounded by carbon steel which encasing the insulation material mainly perlite while it is polyurethane insulation for membrane (Mokhatab et al., 2014).

- Single containment tank: it is surrounded by a bund wall with 20 m from the inner tank as the secondary containment in case of first containment failure as shown in figure 2 below. It cannot contain vapours or protect heat radiation in case of inner tank failure. In case of any ignition source, vapour dispersion in case of failure can cause catastrophic damage. It is cheap, faster to be built, requires large space and high premium insurance for its safety limitation (Rötzer, 2016).
- Double containment tank: the inner tank is surrounded by the tall concrete wall within 6 m to contain LNG and vapour dispersion in case of inner tank failure as it can be seen in

figure 2 below. It cannot contain vapours but provide a less heat radiation. Fire is restricted in upward direction in case of ignition. It also occupies small area compared to single containment (Rötzer, 2016).

- Full containment tank: it is a double containment tank with seal in annular gap between inner and secondary tank shown in figure 2 below. A pool fire and vapours are restricted inside the second containment in case of inner tank failure. It provides an enhanced safety with contained heat radiation, and it occupy a small space compared to other two. All the applicable connections are restricted to the top part of the tank while for the single and double containment tanks, connections are applied at the top and bottom. It is expensive with 10 to 20% more than single containment tank and require more time for construction (Mokhatab et al., 2014).

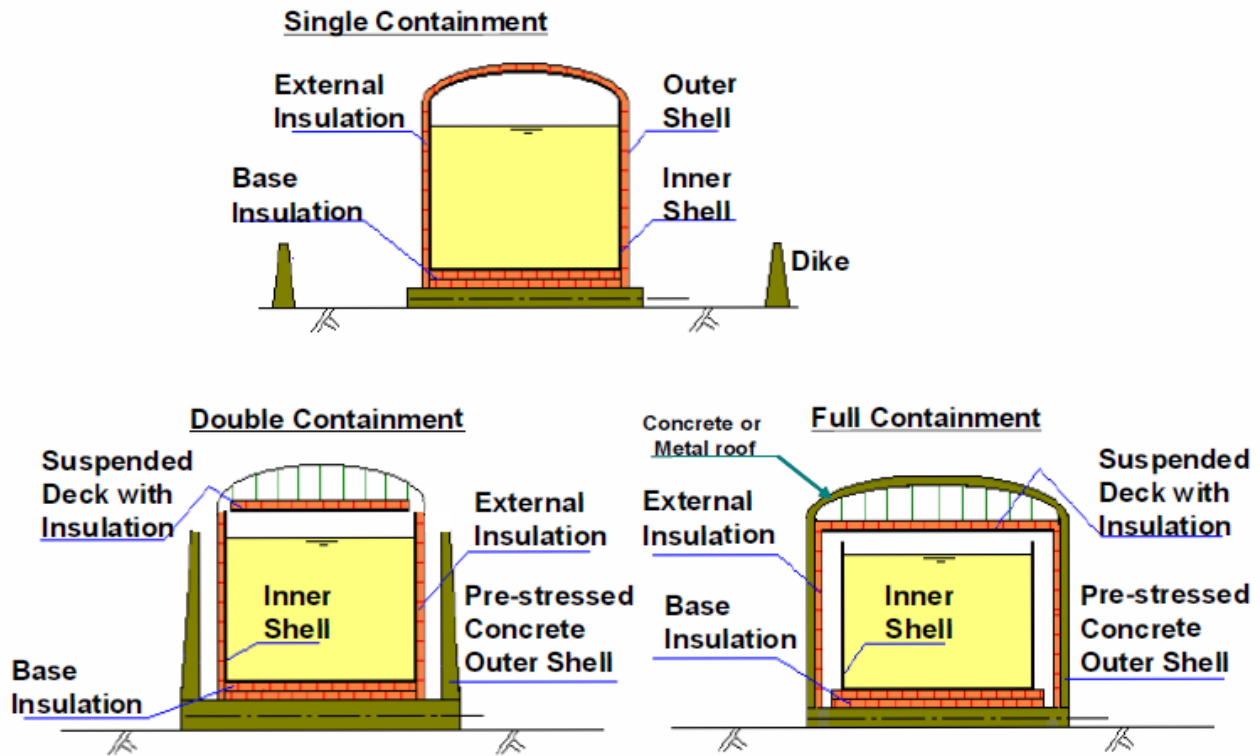


Figure 2. Aboveground single, double, and full containment LNG tanks (Coyle & Patel, 2005).

- Membrane tank: it is sometimes made of stainless steel instead of nickel steel, resistant to seismic activity and heat transfer, and mostly large. It is well gas tight due to its various barrier as shown in figure 3. The insulation space is continuously purged with nitrogen and monitored to ensure its continual functioning and vapour infiltration control (Rötzer, 2016).

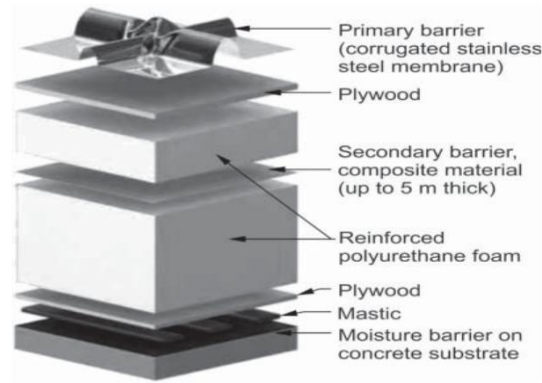


Figure 3. Membrane tank wall make-up (Rötzer, 2016).

2.1.3. BOG management facilities

LNG is a cryogenic liquid gas transported and stored at temperature below its boiling point. Due to heat leakage in LNG facilities such as in ship unloading, LNG regasification and holding operations, BOG continuously form and reduce the LNG quantity as well as altering its properties and composition (Bisen et al., 2018). Liquid and vapour are in thermal equilibrium in tanks. The tank temperature is controlled by liquid or LNG, pressure by vapour or BOG, and being liquid-gas equilibrium due to pressure, temperature and composition interdependency (Querol et al., 2010). BOG management facilities are facilities at LNG receiving terminal designed to handle boil-off gas for safety, environmental, regulation compliance and efficiency use of LNG. BOG management facilities comprise of gas recover system to capture BOG, compression unit for BOG processing and transportation, re-liquefaction or recondense unit to re-liquefy BOG and mix with LNG, fuel gas system to use BOG as energy source, and safety system to ensure safety by use of pressure relief valves and monitoring system to avoid overpressure, and emergency flaring (Dobrota et al., 2013).

2.1.4. Regasification units

Equipment that converts LNG back into gaseous form for distribution into the natural gas pipeline system. It often involves heating the LNG, typically using seawater or other heating methods. The pipeline system connects the terminal to the natural gas distribution network for transport to consumers including residential, commercial, and industrial consumers. There are many regasification techniques by use of different heating agent: ambient air, seawater, and combustion heat (Agarwal et al., 2017). The selection of regasification site base on the regional regulation, operational and environmental conditions and LNG regasification has to minimise the life cycle

cost as the LNG regasification industrial's requirement (Mokhatab et al., 2014). Currently, LNG regasification technologies being used employed onshore and offshore. LNG vaporisers in use are ambient air vaporisers, seawater vaporizers, combustion vaporizers and intermediate fluid vaporizers for onshore, and floating storage and regasification unit for offshore facilities (Agarwal et al., 2017). Intermediate fluid vaporizer can use air as heat source like ambient air vaporizers or use sea water like seawater vaporizers to heat ethylene or propylene glycol which serve as intermediate heat transfer fluid. There are three operational principal types for water-based vaporizers: open rack (ORV), shell and tube (STV), and submerged combustion vaporizers (SCV). The ORV and STV use sea water as heat source, they all use tubes with aluminium alloys for ORV and titanium fabric for STV, and STV is expensive but relatively compact to be employed even in floating and regasification units. SCV do not use sea water, they are employed where there is limited water resource and requires burning fuel to heat LNG in water bath. Currently, 90% of vaporizers are ORV and STV whereby ORV occupy 70% and STV with 20% due to their free and higher heat capacity energy source (Mokhatab et al., 2014). The working technology for onshore and offshore regasification unit are the same, the difference is where there are employed whereby one is land-based and another in marine-based (Agarwal et al., 2017).

Table 2. Difference between onshore and offshore regasification units.

	Onshore	Offshore
Construction and commission period	Up to 5 years	1 to 2 years
Cost	Expensive	Cheap
Size	Large	Small
Capacity	Large	Small
Flexibility	Rigid	Flexible

Beside differences in table 2, offshore regasification units are employed for temporary use or with space constrains while onshore units are vast and employed for long periods of time (Agarwal et al., 2017).

2.1.5. Pumping system

These systems facilitate the transfer of LNG from storage to the regasification units, where it is vaporized and pressurized. Pumps are completely submerged in send-out liquid and eventually reducing pump noise (Coyle & Patel, 2005). Electric submerged pumps are employed in storage tank for LNG is a dielectric fluid, and advantageously no tank penetration and mechanical seals

are required. Two submerged pumps are used during LNG regasification, low and high pressure send-out pump (Mokhatab et al., 2014).

- Low pressure send-out pump: a vertical retractable pump installed from the top of storage tank to pump out LNG for regasification with discharge of 8 to 10 barg. It may also be used to pump LNG in recirculating lines (i.e. jetty) to keep it cool when there is no ship unloading and mixing LNG inside the tank to avoid rollover (Mokhatab et al., 2014).
- High pressure send-out pump: a vertical multistage compact canned type of pump with submerged motor to pump LNG and recondensed BOG typical from 8 barg to send-out pressure requirement of 80 to 120 barg. BOG from heat generated by motor is removed by sensible LNG (Coyle & Patel, 2005; Mokhatab et al., 2014).

Before turning on the pump, the suction pot must be filled firstly and cooling pump down must be done slowly to avoid thermal stresses which can eventually damage the pump (Coyle & Patel, 2005).. The produced BOG in pumping is vented out to BOG condenser to avoid pump cavitation and locking of pump by vapours (Mokhatab et al., 2014).

2.1.6. Safety and environmental systems

Safety and environmental systems are comprehensive safety measures and environmental controls to manage the risks associated with LNG handling, including leak detection, fire suppression systems, emergency shutdown mechanisms, and containment measures. The environmental, health, and safety (EHS) guidelines provide measures to enhance safety and environmental awareness in LNG facilities. Each region has its own EHS guidelines to comply with. The EHS guidelines from Good International Industrial Practices (GIIP) provides the guidelines for LNG facilities including liquefaction facilities, vessels transporting, and receiving terminal (World Bank, 2017). General EHS provides regulations for the following.

- Environment addressing issues of threat to marine and land-based environment, hazardous material (i.e. that can be released from LNG facilities), wastewater and waste management, noise, air emissions, and LNG transport (i.e., pipeline and ship). The guidelines provide the benchmark for performance evaluation for emission and effluent, environmental monitoring program, and resource and energy usage (World Bank, 2007). The

environmental guidelines raise the awareness to protect and ensure sustainable environmental harmony.

- Occupational health and safety addressing issues of fire and explosion, roll-over, cold surfaces' contact, confined spaces (i.e., tanks) and chemical hazards. Benchmarks for evaluating the occupational health and safety guideline and monitoring, and accident and fatalities rate are also provided to ensure health and safety of workers, visitors, trainees, and anybody in LNG facility premises (World Bank, 2007).
- Community health and safety addressing issues associated with LNG facilities that can harm the community and security measures guideline to avoid such issues. These issues are gas leakage, heat radiation and flammable gas. Guidelines for an emergency preparedness, and response plan regarding neighbouring community and their infrastructure are also provided to ensure community health and safety (World Bank, 2007).

Terminal risks assessment is conducted prior, but continuous risk analysis should be implemented to ensure smooth, safety, and environmentally friendly operation. Risk analysis is not a straightforward but a dynamic with real-time evaluation (Alyami et al., 2014). Continuous risks assessment and analysis with implementation of EHS guideline enhance safety and environmental of LNG receiving terminal.

2.2.Boil-off gas sources, recovery and use

Under normal storage condition, BOG do not generate but due to continuous heat leakage, BOG generates. The surficial liquid cools by evaporating preferentially lighter components, liquid become dense than the surrounding and migrate to the tank bottom. This process continually take place as the heat continually ingress (British Petroleum & International Gas Union, 2011). The boil-off gas reduces LNG and alter it quality. Therefore, boil-off gas recovery is important for valuation of technical and financial aspects of LNG industry as well as LNG receiving terminal (Bisen et al., 2018).

2.2.1. Sources of BOG source during receiving terminal operational modes

The three operational modes at LNG receiving terminal contribute to BOG formation namely LNG regasification, ships unloading and holding mode.

2.2.1.1.Boil-off during LNG regasification mode

LNG regasification operation mode is a period between loading and unloading of LNG into the tank whereby the stored LNG is continuously being vaporized and distributed into distribution lines toward consumers (British Petroleum & International Gas Union, 2011). Although the storage tank is well insulated, heat ingress from surrounding environment is unavoidable because of large temperature difference between stored LNG and ambient temperature (Dobrota et al., 2013). Heat leaks through the tank roof, wall, and bottom by convection, conduction, and radiation. Since LNG is stored below its boiling point, any heat ingress leads to LNG vaporisation to cool itself up and eventually generate BOG. LNG and ambient pressure changes also cause BOG generation. During LNG regasification operation, BOG generation alter the quality of the LNG over time. At some point, this can render regasified LNG unacceptable into transmission and distribution lines sometimes due to its aging or not meeting consumer's specification (British Petroleum & International Gas Union, 2011).

2.2.1.2.Boil-off during ships unloading mode

The ship unloading mode is a period whereby the LNG ship cargo is moored to the jetty to unload LNG through arms and pipeline unto receiving terminal storage tank. The main sources of BOG released during ships unloading process are vapour return to the ship tanker, ship's pump heat propagation into LNG, heat ingress through LNG rundown lines and associated equipment, high ship's operating pressure compared to storage tank, jetty cooling down in case it is not continuous, and mixing the existing LNG stock with freshly unloaded one of different quality (Dobrota et al., 2013). According to Benito (2009), due to the return of vapour from the LNG storage tank to the LNG carrier while unloading the ship cargo, BOG generation can be as much as 8 to 10 times the BOG generation during holding operational mode. Under normal circumstance, if the BOG is returned to the ship cargo from storage tank during unloading to fill the ullage, no BOG will be release to atmosphere either from ship or receiving terminal with such balance system (Dobrota et al., 2013). The heat ingress into pipelines depends on the length of pipeline though pipelines are well insulated, for a pipeline less than a kilometer, a 5% of total BOG can be generated while for seven kilometers pipeline, approximately 45% of total BOG can be generated (British Petroleum & International Gas Union, 2011). Depending on the ship capacity, the pump energy varies. The ship pump energy used during unloading almost all change into heat due to turbulence and friction

which eventually get absorbed by LNG. To adjust with such heat ingress, LNG auto-refrigerate by evaporating its small portion and can evaporate up to 20,000kg hourly (Sedlaczek, 2008).

2.2.1.3. Boil-off in storage tank during LNG holding mode

Holding mode is a period whereby the LNG is kept for a certain time in LNG storage tank, a period between loading and unloading of the storage tank (Sedlaczek, 2008). The main boil-off gas source during LNG holding operational mode are storage tanks and pipes due to heat leakage from environment surrounding the receiving terminal, and ambient pressure changes (Dobrota et al., 2013). Although the storage tanks and pipes are insulated to restrict heat ingress, heat ingresses inside the storage tank through the roof, wall, and bottom via convection, radiation and conduction and pipelines (British Petroleum & International Gas Union, 2011). Heat ingress through the tank due to large temperature difference between LNG and ambient environment (Dobrota et al., 2013). LNG storage tanks are well insulated to contain LNG from heat ingress and for daily BOG generation less than 0.05% of the tank capacity, however BOG generation can vary from 0.02 to 0.1% (British Petroleum & International Gas Union, 2011). A portion of LNG is continuously pumped and circulate into the rundown lines to keep it at cryogenic state. As LNG is recirculating, it absorbs heat from pumping, pipeline friction, and turbulent flow. Eventually, the absorbed heat causes further evaporation which adds BOG to the storage tank's. BOG quantity forms from LNG recirculation depends on rundown pipelines' length as well as pumps' power (British Petroleum & International Gas Union, 2011; Sedlaczek, 2008). As the BOR increases significantly inside LNG storage tank, atmospheric pressure drops and eventually the storage tank pressure as well as the LNG bubble point temperature decrease. The LNG temperature inside the tank decreases by 0.1^oC for each 0.01bar drop to equilibrate with this low pressure (Sedlaczek, 2008). This can only affect once the atmospheric pressure drop is rapid to significantly cause an increase in storage tank's boil-off rate. As the heat ingress into LNG, tank's vapour pressure increases. Therefore, to maintain safe pressure in the storage tank, BOG should be compressed out (Dobrota et al., 2013).

2.2.2. Boil-off gas recovery

The generated BOG quantity released out is recovered from storage tank via the use of compressors and transmitted towards one of various use (Sedlaczek, 2008).

2.2.3. Boil-off gas use

Various use of BOG recovered at receiving terminal are returning to ship's tank, fuel, recondensed into LNG, feeding BOG into natural gas distribution network, reliquefied and stored, and flare (Sedlaczek, 2008).

2.2.3.1. Returning to ship's tank

During LNG ship cargo unloading period, the ullage space is continuously formulated as the LNG is pumped out to the receiving terminal tank via unloading arms and rundown lines. The BOG formed and filled into the storage tank is continually filled into tanker ship by return blower to avoid vacuum creation inside the ship. This process can last for 12 to 18 hours depending on the ship cargo capacity and the unloading flowrate (Dobrota et al., 2013). Unlike the unloading arm and pipelines which are maintained cold, the return line is not maintained cryogenic. Hence, the returning BOG is firstly cooled before being filled into ship cargo (Sedlaczek, 2008). During the start of unloading, the BOG returned temperature can be almost ambient temperature and required to be cooled to -1400C and below. This is done by desuperheater via putting BOG in contact with LNG (Tarakad, 2000).

2.2.3.2. Boil-off gas use as fuel

The gas discharged from the BOG compressor is rich in methane since lighter components such as methane and nitrogen are preferentially evaporated (British Petroleum & International Gas Union, 2011). It is a suitable to be used as fuel. For a receiving terminal require with SCV in case there is no seawater or restricted by regulation, a substantial amount of fuel is needed and compressed BOG can be used. The discharged compressed BOG is suitable than vaporized LNG for it is cheap, do not require to be depressurized and a prior heating before being used as fuel like vaporized LNG. For a large send-out capacity, a vaporised LNG gas is required to supplement the discharged BOG from compressor due to extensive fuel needed (Tarakad, 2000).

2.2.3.3. Recondensing into LNG

LNG after being pumped out by submerged LP pump from storage tank, the LNG pressure rises as well as the LNG temperature faintly. Since the LNG is subcooled, it can absorb gas and keep it in liquid form. A recondenser use this LNG property to recondense the discharged BOG from compressor unto liquid. It is an economically advantageous option to recondense BOG into LNG. At a recondenser operating pressure ranging from 6 to 8 barg, a kilogram of send-out LNG from

submerged LP pump can attain a 0.1 kg of discharged BOG from BOG compressor. This could be enough to recondense the holding mode BOG generation and almost all BOG generation during ship unloading operation mode if the send-out capacity is high. For an unexpected turndown or shutdown of send-out at a receiving terminal due to a certain circumstance, the LNG send-out cannot be enough to absorb all discharged compressed BOG and an alternative option must be designed instead of flaring BOG (Tarakad, 2000). However, the vaporised LNG send-out fluctuate due to demand, operational issues, market conditions, environmental regulations, storage capacity, safety, maintenance, and disruptions of natural gas supply chain (British Petroleum & International Gas Union, 2011; Geman & Ohana, 2009; IGU, 2024; Mokhatab et al., 2014; Pindyck, 2004).

2.2.3.4. Compressing to gas distribution network feed

Although it is expensive to compress gas to high pressure, BOG can be compressed into gas distribution network when there is no or less fuel demand such as for SCV, no internal BOG gas demand, and no or very low send-out. Therefore, recondensation become so low, and the remaining BOG use option is to pressurize it and send into pipeline distribution instead of flaring or venting by high pressure compressor to handle the least BOG possible like BOG generation during holding operational mode (Tarakad, 2000).

2.2.3.5. Liquefying and storing into LNG storage tank

Under certain circumstances such as large heat ingress and large rapid pressure changes or when the connection to gas distribution pipeline is currently not working or with no internal fuel demand, large BOG volume can be generated. To handle this extensive BOG generation in these scenarios, BOG can be recovered, liquefied via gas expander cycles through turbo expander means and stored back to the storage tank (Mokhatab et al., 2014).

2.2.3.6. Flaring

Although it is not acceptable as a continuous basis due to economic and environmental concerns, flaring become the last only possible option. Under certain unexpected circumstances such plant disruption, Flare can be used to dispose BOG for safety reasons under emergencies occasions (Tarakad, 2000).

2.3.CNG

CNG is a natural gas is compressed form, non-toxic supercritical fluid, a mixture of hydrocarbon gases and vapours dominated mainly by methane gas used, stored, sold, transported and distributed

via CNG system (Smitherman et al., 2013; Speight, 2019). Compressed natural gas is a fossil alternative fuel with large energy content for vehicle, heating, and electricity generation. Its composition varies from a place to another (Rehnlund, 2008). It is one of the promising eco-fuels though it is challenging to harness it from its raw form, but it is cheap, environmentally friendly, safe to handle, and its resource is available. CNG performance is relatively low compare to conventional fuel but its low emissions serve as an enhancement toward automotive sector (Ashok & Nanthagopal, 2018). CNG plant to be developed, the raw gas supply must not be beyond 7bcm/year and not less than 1bcm/year, and the distance between plant and consumers should not exceed 2000 km (Mokhatab et al., 2014). Natural gas is compressed into CNG and stored at 200 to 250 bars not more than 260 bar at ambient temperature. For vehicles, CNG fuel is filled into CNG designated vehicle tanks at 200 bars (Milojević et al., 2012). For a natural gas to be used as a reliable fuel, a knock resistance is required to dedicate natural gas to high compression ratio and high turbocharger boost of an engine. This knock resistance is manifested in methane number (MN) of a certain natural gas. The least methane number in natural gas is 65 and the minimum acceptable MN for CNG as an automotive fuel quality is also 65 according to drafted European standards. However, most of the natural gas supply approximately 99.8% provide MN above 70, and natural gas fuel should provide at least MN of 70 as minimum from automotive point of view (Kramer et al., 2017). For Chinese physical and chemical indicator of natural gas fuel, combustible concentration should be in range between 5 to 15%, self-ignition point range between 630 to 730⁰C, specific gravity relative to air of 0.65, and octane number of 130 (Rehnlund, 2008). Since it has this high-octane number, CNG is not liable to knocking than gasoline and its compression ratio is 12.5:1 higher to boost operating efficiency (Milojević et al., 2012). The CNG powered vehicle emits 0.1 particulate matter gram pre mile and emissions reactivity of 500mg /mile which is relatively small compared to other vehicle-fuels due to its high methane content (Finlayson-Pitts & Pitts Jr., 2000). According to Aslam et al. (2006), the typical CNG combustive properties are MON of 120, molar mass of 16.04, carbon weight fraction of 75% mass, stoichiometric air/fuel ratio of 16.79 and mixture density of 1.24, lower heating value of 47.377 MJ/kg and stoichiometric lower heating value of 2.77 MJ/kg, flammability range between 5 and 15, and spontaneous ignition temperature of 645⁰C. According to M. I. Khan et al. (2015), physicochemical CNG properties value for octane number range from 120 to 130, molar mass of 17.3, stoichiometric air/fuel mass of 17.2 and mixture density of 1.25, lower heating value of 47.5 MJ/kg and stoichiometric lower

heating value of 2.62 MJ/kg, energy of combustion of 24.6 MJ/m³, flammability in air range from 4.3 to 15.2% vol in air, speed of propagation of 0.41m/s, adiabatic flame temperature of 1890⁰C, auto-ignition temperature of 540⁰C, and Wobbe index between 51 and 58 MJ/m³. Pandit (2017) said that CNG properties values are 540⁰C for auto ignition temperature, -180⁰C for flashing point, and specific gravity of 0.65. These properties vary from a composition to another since CNG composition depends on the natural gas source and vary from a place to another. According to Kouroussis & Karimi (2006), CNG is mainly made of methane with octane number of 120 and more, energy content ranges from 33,000 to 44,000 BTU/gallon, and with energy ratio of 3.94:1 compared to gasoline. Graham et al. (1998) suggested that natural gas composition should be containing methane with minimum 90%, Ethane of 4% as the maximum, propane not more than 1.7%, butane and heavier not more than 0.7%, carbon dioxide and nitrogen not more than 3%, hydrogen less or equal to 0.1%, carbon monoxide less or equal to 0.1% and oxygen not more than 0.5%.

CHAPTER III

RESEARCH MATERIAL AND METHODOLOGY

This chapter is devoted to presenting the research materials and methods adopted to address the research objectives to achieve research goals. It includes operation conditions, designed receiving terminal, heat leakage, and BOG management used in this research.

3.1. Research material

3.1.1. Software

A numerical simulation model has been made and used to simulate the receiving terminal and BOG management with the inserted conditions and assumptions.

In this study, modelling and simulation focused on receiving terminal operations mainly for BOG generation and management for efficient use of natural resources. The numerical simulation employed is Aspen HYSYS V11 while the heat leakage in pipelines was evaluated using Begges and Brill (1979) correlation embedded in simulator. Aspen HYSYS is a widely used simulator to simulate chemical processes from unit operations to full plant scale. It provides opportunity to do chemical engineering calculation by employing mass and energy balance, vapour-liquid equilibrium, mass and heat transfer, chemical kinetics, fractionation, as well as pressure drops (Naji et al., 2019b).

Therefore, aspen HYSYS were employed to simulate the LNG receiving terminal and BOG conversion into CNG.

3.1.2. Equation of state

To simulate the model of LNG receiving terminal, Peng-Robinson cubic equation of state embedded in simulator were used as a thermodynamic fluid package property.

Peng-Robinson equation of state is among the most accurate and tuned better to liquid densities (Poling et al., 2008). It can handle fluids properties calculations during production, transportation and processing of hydrocarbons with associated mixture. Peng-Robinson equation incurs a good vapour pressure, molar volume, volumetric behaviour, upper retrograde regions, upper dew points, vapor-liquid equilibrium, critical properties, water content, and hydrates predictions (Robinson et al., 1977).

Therefore, Peng-Robinson equation of state was selected for its suitability to the model.

3.1.3. Operation conditions

The initial operating conditions and characteristics of the input data used have been summarised in this section. The approach of the used LNG with its characteristics, weather conditions, and receiving terminal operational modes used have been detailed.

3.1.3.1. LNG Composition

LNG composition varies from a natural gas source to another, and it is hard to depict the constant composition to refer to. Therefore, the composition of LNG used in this work was obtained from Querol et al. (2010) and shown in table 3 below.

Table 3. LNG composition and initial storage temperature used.

Component	Lean LNG (%)	Medium LNG (%)	Rich LNG (%)
Methane	98.6	92.3	85.87
ethane	1.18	5	8.4
propane	0.1	1.5	3
butane	0.02	0.6	1.2
pentane	0	0.1	0.23
Nitrogen	0.1	0.5	1.3
Storage temperature ($^{\circ}\text{C}$)	-160	-160.7	-163.1

The LNG composition and storage temperature were used as the initial storage at the receiving terminal and as the unloaded LNG from ship cargo to the LNG receiving terminal storage tank.

3.1.3.2. Weather conditions

To predict the rate of BOG generation, it is necessary to forecast the weather conditions at the LNG receiving terminal because these influence heat ingress into LNG pipelines and storage tank. Weather conditions which influence heat leakage are mainly ambient temperature and pressure, solar radiation, and soil temperature. In this study, the ambient pressure was neglected and the soil temperature assumed constant. The ambient temperature and solar radiations used were depicted from real data of Maputo weather conditions from 26th may to 13th June 2024. The depicted period is a transition period from rainy season between October and April to dry season between June and September (Gomes et al., 2014). The Maputo ambient temperature data in this period have been

depicted from AccuWeather and solar radiation from Tutiempo network. The collected ambient temperature and solar radiation data can be found in annexes.

The mean annual soil temperature globally is range from -0.7 to 3.6°C depending on air temperature. Maputo annual soil temperature ranges from 2 to 8°C and vary from 4 to 6°C in the depicted months of May and June (Lembrechts et al., 2022). Therefore, a constant soil temperature of 5°C were used in this study.

Maputo region had a very changing annual maximum wind speed. From 1973 to 2010, the large maximum wind speed was 32.5 m/s in 2001, and the least maximum wind speed was 12.2 m/s in 2010 (Xiong et al., 2014). According to Badger et al. (2024), the mean wind speed at 100m in Maputo varies from 5 to 6.4 m/s. Mozambican mean wind speed can be found in annexes. Since in pipeline heat transfer calculations, the wind speed is necessary for it is the medium of heat transfer towards pipelines, 5 m/s was used as wind speed at receiving terminal because pipelines are near to the ground with many wind obstacles.

3.1.3.3. Operational mode

The designed receiving terminal operation has been three repeatable operation mode, LNG regasification, ships unloading, and holding mode. Each mode has been studied independently but starting with the last parameters of the previous mode. The study has started with LNG regasification mode, followed by ships unloading, and ended up with holding mode.

3.1.3.3.1. LNG regasification mode

During this mode, the receiving terminal was only subjected to the regasification of stored LNG. The operation that was taking place are the LNG regasification, BOG recovery and conversion. The heat leakage was solely into the LNG storage tank through its roof, wall, and bottom as shown in figure 4 below.

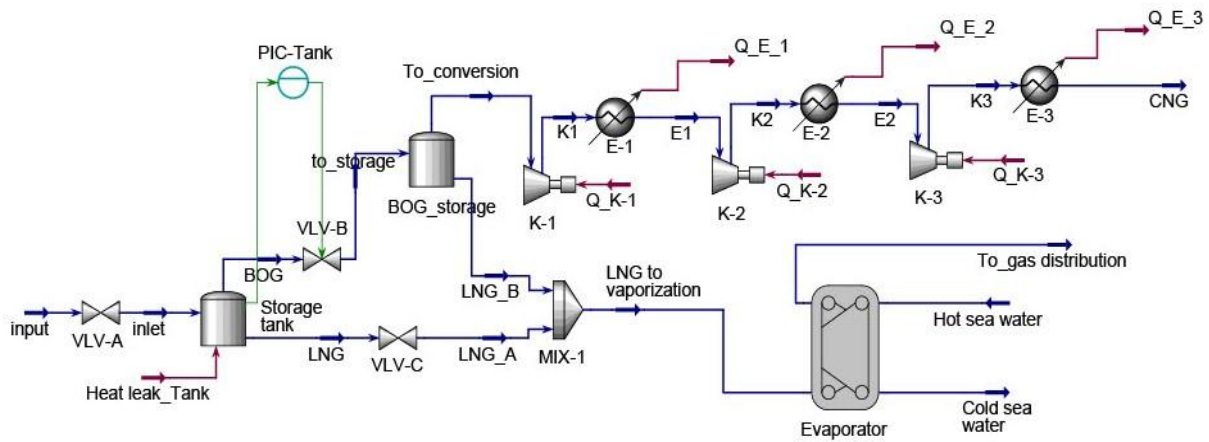


Figure 4. Simulated LNG regasification flowchart.

3.1.3.3.2. Ships unloading mode

Ships unloading operation mode was solely the LNG unloading from ships via unloading arms and rundown lines and storing to the storage tank as shown in figure 5 below. During this mode, the operation that was taking place are ships unloading, LNG storing, BOG recovery, return to the ship to maintain the tanker pressure and conversion. The heat leakage was subjected to ship pumps, pipelines, and storage tank.

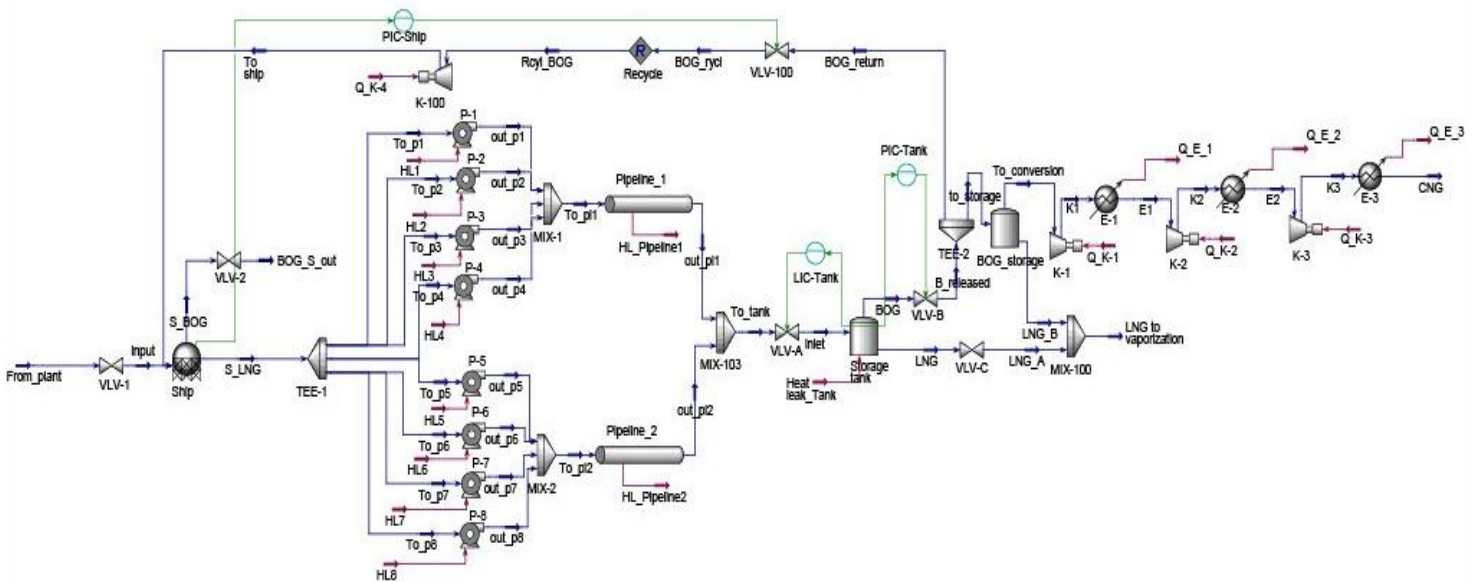


Figure 5. Simulated ships unloading mode flowchart.

3.1.3.3.3. Holding mode

During LNG holding mode, LNG was kept stationary stored inside the storage tank for a period of 24 hours as detailed in figure 6. BOG recovery and compression systems were solely operating. The heat ingress considered was into the storage tank.

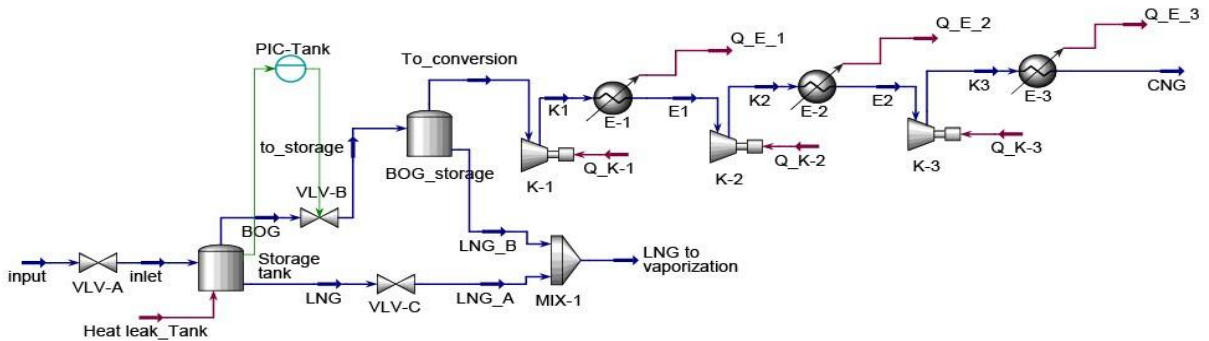


Figure 6. Simulated LNG holding mode flowchart.

For each LNG compositional type depicted, all the operation modes were simulated with each mode occurring independently after the end of another.

3.1.4. Designed Receiving terminal

Although the receiving terminal has been designed for this work, not all aspects of the LNG receiving terminal were detailed herein. For this study, the detailed aspects were, ships capacity at the jetty, unloading arms, pipelines, storage tank, and terminal vaporised LNG send-out capacity based on existing LNG receiving terminals.

3.1.4.1. Ship

LNG receiving terminals are designed for specific range of ship carriers they can accommodate based on capacity. The study suggested the used capacity with its pumping capacity. However, the ship carrier was assumed to supply the constant LNG composition during unloading hence no heat ingress was subjected into LNG ship carrier that can alter the LNG composition.

3.1.4.1.1. Ship Capacity

Currently, the LNG ship capacity varies from 1,000m³ to approximately 260,000m³ with a single to four tanks per ship base one their capacity (Mokhatab et al., 2014). The ship with 150,000m³

and 4 tanks capacity has been used for this work. It was designed to have the height of 32m, and the following fabric and insulation.

Table 4. LNG ship carrier fabric, insulation and their thickness.

	Material	Thermal conductivity (W/m.K)	Thickness (cm)
Inner layer	9% Ni steel	18.3	5
insulation	Polyurethane	0.025	30

3.1.4.1.2. Ship pumps

Coyle & Patel (2005) suggested that LNG cargo pumps capacity range from 1350 to 2000 m³/h with 150 to 240 m head. However, HYUNDAI-JC CARTER-SNECMA LNG marine pump can deliver an LNG at 1400 to 2000 m³/h flowrate with 135 to 190m range of head rise at different motor output power (Hyundai, 2007). Eight ship unloading pumps has been used in the study with two pumps in each ship tank. For all LNG compositional types simulated, each pump was assigned the 1400m³/h capacity with 138 m head and efficiency of 0.75.

3.1.4.2. Unloading arm

To transfer the LNG from ship cargo tanks to pipelines towards the storage tank, an articulated pipe system or unloading arms are necessary. For this study, four unloading arms connected at the top of ship cargo tanks have been used with a single unloading arm to each tank.

3.1.4.3. Rundown lines

Pipeline has been used to transfer gas since 500 BCE in China. There are four pipelines for gas transport, gathering with 4 to 12 inches diameter, transmission with 16 to 56 inches diameter and 15 to 120 bar operating pressure, distribution with 2 to 28 inches diameter and up to 14 bar operating pressure, and service pipelines with less than 0.2 inches diameter and less than 0.5 bar operating pressure (Hafner & Luciani, 2022). At a receiving terminal, the material fabric and insulation for pipeline are 36% Ni steel insulated with fumed silica panels, aerogel blankets or polyurethane foam, 316L stainless steel, 9% Ni steel insulated with vacuum PIP with bulkheads, nanogel annular fill or blankets, and API X52 carbon steel insulated by vacuum PIP with bellows. The insulation thickness can range from less than an inch to tens of inches and each insulator has its own thermal conductivity (Phalen et al., 2007; Shammazov & Karyakina, 2023). The length of

pipeline from the jetty to the storage tank either subsea or surface settled depends on the distance from unloading arms to the storage tank and length can range from 100m to tens of kilometres (Backhaus & Friedrichs, 1980; Lu et al., 2018). LNG is transferred from unloading arms to the storage tank through pipeline. Depending on a certain receiving terminal, number of pipelines, material fabric, the dimension, length, and pipe insulation vary as the receiving terminal is designed. Mainly pipe dimension, length and insulation determine how much BOG can be generated for a certain environmental condition. Three pipelines used in this work are made of mild steel with 30 and 30.1 inches inner and outer diameter respectively, insulated by urethane foam of 0.025m thickness and 0.018W/m. K thermal conductivity. Two pipelines were used as the unloading line for LNG and the remaining one as a BOG return loading to the ship during LNG unloading. The effect of solar radiation in pipeline heat ingress were omitted, heat ingress was subjected to ambient temperature changes and a constant air speed of 5m/s.

3.1.4.4. Storage tank

An above-ground full containment storage tank with capacity of 200,000m³ has been used in simulation and designed based on existing receiving terminal storage tanks as shown in table 5 below with its fabrics and sizes. It was designed to have 40m height and 79.79m diameter with all connection at the roof. The tank was simulated to maintain the cryogenic temperature and pressure not more than 117Kpa for safety concern.

Table 5. LNG storage tank material, thermal conductivity, thickness, and absorptivity.

Section	Material	Thermal conductivity (W/m.K)	Thickness (m)	Absorptivity (-)
Wall	9% Ni steel	18.3	0.02	0.8
	Glass wool	0.0329	0.15	0.8
	Perlite	0.026	0.9	0.3
	Concrete	1	0.525	0.6
Roof	Aluminium	235	0.003	0.075
	9% Ni steel	18.3	0.02	0.8
	Glass wool	0.0329	0.15	0.8
	Perlite	0.026	0.9	0.3
	Concrete	1	0.3	0.6
	Steel liner	45	0.005	0.45
	Air cavity			0.01
Bottom	9% Ni steel a	18.3	0.02	-

Load bearing glass wool a	0.03	0.5	-
Load bearing glass wool b	0.03	0.5	-
9% Ni steel b (Sub-floor)	18.3	0.02	-
Carbon steel liner	45	0.001	-
Plywood	0.012	0.13	-
Sand layer	0.15	0.005	-
Concrete slab heater	1	2	-

3.1.4.4.1. Roof

A suspended domed roof was used with inner aluminium layer supporting glass wool and perlite insulations with an outer concrete cover.

3.1.4.4.2. Wall

The primary role of the wall is to provide structural resistance and LNG insulation from external heat ingress. The 9% Ni steel primarily is in contact with LNG, followed by extensive perlite insulation, and sealed by a bulk concrete wall externally.

3.1.4.4.3. Bottom

A 9% Ni steel internally start as a primary seal of the LNG, followed by thicker glass fiber as an insulator sealed by another 9% Ni steel plate, and a footing cover of concrete seal as the external layer. There is a constant heating underneath the tank to avoid soil water heating, a constant 5⁰C was used as the constant soil temperature in this study.

3.1.4.5. Send-out Capacity

According to Kim et al. (2010), the designed Samcheok LNG receiving terminal of 12 tanks with 200,000m³ each, the gasification capacity was designed to be 2340 ton/h. For this study, the designed LNG receiving terminal with a single tank simulates was designed to vaporise 200,000kg of LNG per hour and send-out to distribution lines.

3.2. Research methodology

This section focuses on research methodology to evaluate heat ingress into storage tank, pipes and pumps, to manage BOG recovered, safety and control measure taken, and LNG, BOG and CNG properties.

3.2.1. Heat ingress

Heat ingress in storage tank, pipes and pumps have been calculated via the simulator and manually before being inserted into simulator.

3.2.1.1. Heat ingress into storage tank

Heat leakage inside the storage tank ingress through the tank roof, wall, and bottom. Heat leakage in each section of the tank has been analysed independently hourly to get the actual heat that leak through the tank insulation from hourly climate conditions. Sum of the heat ingress in all three sections were insulated into a tank to find the actual BOG generation hourly as in equation (1).

$$Q_{Tank} = Q_{roof} + Q_{wall} + Q_{bottom} \quad [W] \quad (1)$$

The total hourly heat ingress was calculated and inserted into the storage tank in all LNG receiving terminal operation modes.

To obtain the actual heat ingress into the LNG, the thermal resistance of each material in all three sections of the tank were calculated using equation (2).

$$Thermal\ resistance\ (R_T) = \frac{Thickness\ of\ material\ (d)}{Material\ thermal\ conductivity\ (k)} \quad \left[\frac{m^2 K}{W} \right] \quad (2)$$

The BOG layer inside the tank above LNG imply the thermal resistance while the heat ingress from the roof and wall at its layer side. Therefore, vapour thermal resistance was calculated.

To get BOG thermal resistance, a measure of how quick heat spreads into the BOG or BOG thermal diffusivity was calculated using equation (3) below.

$$\alpha = \frac{k}{BOG\ Specific\ heat\ capacity\ (c) \times BOG\ density\ (\rho)} \quad \left[\frac{m^2}{s} \right] \quad (3)$$

Whereby α stands for thermal diffusivity of BOG.

The BOG thermal resistance (R_{BOG}) was calculated by using the following equation (4).

$$R_{BOG} = \frac{1}{BOG\ convective\ heat\ transfer\ coefficient\ (h) \times area} + \frac{1.595}{0.026 \times area} \quad \left[\frac{m^2 K}{W} \right] \quad (4)$$

Whereby, the BOG convective heat transfer coefficient (h) was calculated by using the following equation (5).

$$h = \frac{k_{BOG} \times \text{tank characteristic length } (L)}{BOG \text{ Nusselt number } (Nu)} \quad \left[\frac{W}{K} \right] \quad (5)$$

The characteristic length of the tank and BOG Nusselt number (Nu) were calculated by using the following equation (6) and (7).

$$Nu = 0.13 \times \left(\frac{\text{Prandtl number } (Pr) \times \text{Grashof number } (Gr)}{1 + \left(\frac{0.622}{\text{Prandtl number } (Pr)} \right)^{\frac{9}{16}}} \right)^{\frac{1}{3}} \quad [-] \quad (6)$$

$$\text{Tank characteristic length } (L) = \frac{\text{Tank volume } (V)}{\text{Tank area } (A)} \quad [m] \quad (7)$$

The dimensionless Prandtl number (Pr) and Grashof number (Gr) was calculated by using the following equation (8) and (9).

$$Pr = \frac{\text{Kinematic viscosity } (v)}{\alpha} \quad [-] \quad (8)$$

$$Gr = \frac{\text{gravity acceleration } (g) \times \text{BOG thermal expansion } (\beta) \times (T_{BOG} - T_{\infty}) \times L^3}{\nu^2} \quad [-] \quad (9)$$

3.2.1.1.1. Heat input through the roof

The heat ingress through the roof calculations has include the tank material, ambient air and the topmost BOG layer thermal resistance (TR_R) to get the actual heat leaked as shown in equation (10).

$$TR_R = R_{aluminium} + R_{glass\ wool} + R_{9\% \ Ni\ steel} + R_{perlite} + R_{concrete} + R_{steel\ liner} + R_{air\ cavity} + R_{BOG} + R_{ambient\ air} \quad \left[\frac{m^2 K}{W} \right] \quad (10)$$

Where R signify the thermal resistance for the respective material and medium the heat passed through to reach LNG.

As the total thermal resistance at roof section was available, the heat transfer coefficient was calculated as well through the following equation (11).

$$\text{Roof heat transfer coefficient} = \frac{1}{\text{Thermal resistance}_{\text{Total at roof}}} \left[\frac{W}{m^2K} \right] \quad (11)$$

Then, the heat ingress through the roof was calculated by using the equation (12) below.

$$Q_{\text{Roof}} = Q_{\text{ambient temperature}} + Q_{\text{solar radiation}} \quad [W] \quad (12)$$

Where $Q_{\text{ambient temperature}}$ (Q_{atr}) and $Q_{\text{solar radiation}}$ (Q_{srr}) are heat ingress from ambient temperature and solar radiation through the roof and BOG layer respectively. These heats have been calculated by using the following equation (13) and (14).

$$Q_{\text{atr}} = \text{Roof heat transfer coefficient} \times \text{tank area} \times (T_{\text{tank}} - T_{\infty}) \quad [W] \quad (13)$$

Where the T_{tank} is the temperature in tank.

$$Q_{\text{srr}} = \text{Roof absorptivity} \times \text{solar radiation} \times \text{area}_{\text{tank dome}} \quad [W] \quad (14)$$

Whereby the roof absorptivity was calculated by using the following equation (15).

Roof absorptivity

$$= \frac{\sum[(\text{Medium absorptivity}_i \times \text{roof medium thickness}_j) + (\text{BOG absorptivity} \times \text{BOG layer thickness})]}{\sum \text{roof medium absorptivity} + \text{BOG absorptivity}} \quad [-] \quad (15)$$

3.2.1.1.2. Heat input through the wall

The heat ingress through the wall calculations has include the tank material, and ambient air to get the actual heat leaked.

$$TR_W = R_{9\% \text{ Ni steel}} + R_{\text{glass wool}} + R_{\text{perlite}} + R_{\text{concrete}} + R_{\text{ambient air}} \quad \left[\frac{m^2K}{W} \right] \quad (16)$$

As the total thermal resistance at wall section (TR_W) was available using equation (16), the wall heat transfer coefficient (HTC_W) was calculated as well through the following equation (17).

$$HTC_W = \frac{1}{\text{Thermal resistance}_{\text{Total at wall}}} \left[\frac{W}{m^2K} \right] \quad (17)$$

Then, the heat ingress through the wall was calculated by using the equation (18) below.

$$Q_{\text{wall}} = Q_{\text{ambient temperature}} + Q_{\text{solar radiation}} \quad [W] \quad (18)$$

Where $Q_{\text{ambient temperature}}$ (Q_{atw}) and $Q_{\text{solar radiation}}$ (Q_{srw}) are heat ingress from ambient temperature and solar radiation through the wall layers. These heats have been calculated by using the following equation (19) and (20).

$$Q_{atw} = HTC_W \times \text{tank wall area} \times (T_{\text{tank}} - T_{\infty}) \quad [W] \quad (19)$$

$$Q_{srw} = \text{Wall absorptivity} \times \text{solar radiation} \times \text{area}_{\text{wall}} \quad [W] \quad (20)$$

Whereby the wall absorptivity (WA) was calculated by using the following equation (21).

$$WA = \frac{\sum(\text{Medium absorptivity}_i \times \text{roof medium thickness}_j)}{\sum \text{wall medium absorptivity}} \quad [-] \quad (21)$$

3.2.1.1.3. Heat input through the bottom

The heat ingress through the bottom calculations has include the tank materials to get the actual heat leaked.

$$TR_B = R_{9\% \text{ Ni steel } a} + R_{\text{glass wool } a} + R_{\text{carbon steel}} + R_{\text{concrete}} + R_{\text{ambient air}} \\ + R_{9\% \text{ Ni steel } b} + R_{\text{glass wool } b} + R_{\text{plywood}} + R_{\text{sand}} \quad \left[\frac{m^2 K}{W} \right] \quad (22)$$

As the total thermal resistance at bottom (TR_B) section was available using in equation (22), the heat transfer coefficient at the bottom (HTC_B) was calculated as well through the following equation (23).

$$HTC_B = \frac{1}{\text{Thermal resistance}_{\text{Total at bottom}}} \quad \left[\frac{W}{m^2 K} \right] \quad (23)$$

Then, the heat ingress through the bottom was calculated by using the equation (24) below.

$$Q_{\text{bottom}} = HTC_B \times \text{tank bottom area} \times (T_{\text{tank}} - T_{\text{bottom}}) \quad [W] \quad (24)$$

Where the T_{bottom} is the temperature at the bottom of the tank.

3.2.1.2. Heat ingress into pipes

During unloading and recirculation of LNG to cool down the unloading arm and pipeline, ambient heat ingress into pipeline. The study did not the heat ingress during recirculation for it can be also done by primary unloading ship BOG to cool rundown lines and unloading arms. Also, the heat ingress from solar radiation have been neglected for it is not significant due to duration of the unloading and the continuous LNG movement while it is being unloaded. To account properly the heat leakage into pipelines, the pipeline fabric and insulation with their thermal conductivity and dimension, hourly ambient temperature, settling medium, and wind speed have been provided in designed receiving terminal section and insulated in simulator to calculate actual heat ingress.

3.2.1.3. Heat ingress into pumps

Ship pumps and storage tank LP pump do leak part of the pumping energy into LNG during unloading and recirculation of LNG into unloading arms and pipelines. Since the LNG recirculation have been omitted in the study, only the heat transferred into LNG by ship pumps during LNG unloading have been calculated and inserted into the simulator to provide BOG generation. The pumps' power were calculated by using this equation (25) below for all LNG.

$$Q_{pump} = \frac{\bar{m}_{pumping} \times g \times H}{3600} \left(\frac{1}{\eta} - 1 \right) \quad [W] \quad (25)$$

Where the Q_{pump} is the power used by the pump, $\bar{m}_{pumping}$ is the pump capacity, g is the gravity acceleration, and η is the pump efficiency.

The pumping capacity has been given by the following equation (26).

$$\bar{m}_{pumping} = LNG \text{ density} \times \text{volumetric pump capacity} \quad [kg/h] \quad (26)$$

The gravity acceleration taken was 9.81 m/s, density was calculated into simulator, and other coefficient and pump capacity was provided in designed receiving terminal section.

To maintain the pressure and temperature in ship tanks, the volume of the LNG being unloaded must always be equal to BOG being returned from LNG storage tank. This BOG is excluded from the BOG recovered for it must be returned to the ship.

3.2.2. BOG management

The BOG management is different as the operational modes are.

During LNG regasification mode, the BOG generated inside the tank was continually replacing the LNG sent out for regasification. In case of BOG excess generation due to large heat ingress, the BOG was kept inside the tank until the tank pressure reaches 117 kPa and released out of the tank to maintain safety of the tank.

During ships unloading mode, the BOG generated in pumping and piping system, and storage tank were partially kept in the storage tank and partially returned to the ship to maintain temperature and pressure at the ship. In case of BOG excess generation due to large heat ingress, the BOG was kept inside the tank until the tank pressure reaches 117 kPa and released out of the tank to maintain safety of the tank.

During LNG holding mode, BOG generated inside the tank was kept inside the storage tank until the pressure inside the tank built-up and reach the 117 kPa. Then, the BOG was progressively released out of the storage tank to avoid overpressure for safety of the facilities, people and environment.

3.2.2.1. BOG recovery

BOG released out of the storage tanks in each mode for all LNG were kept in another storage tank. BOG generated was continually getting recovered into the storage tank before converting it into CNG to avoid the compressor to run in empty pump throughput for BOG excess release is not a continuous process. Thereby, the compressor was safe from sudden stop and damage.

3.2.2.2. BOG compression into CNG

The recovered BOG stored into the tank was continually compressed into CNG. The process was done using multistage compressor with three stages of compressors and coolers. The compressors operated in reciprocating operating mode with 6.055 compression ratio for each compressor and cooler dynamically changed the cooling rate to achieve the ambient temperature of 25⁰C.

3.2.3. Safety and control

This study also covered the safety and control of the process. Safety and control of the process differed from one operation mode to another.

During LNG regasification mode, a pressure controller was used in storage tank to dynamically regulate the pressure inside the storage tank. The pressure was regulated to the set point of 117 kPa by opening and closing a valve (VLV-B) to release BOG excess out to the BOG storage tank (BOG_storage) and avoiding tank pressure from getting lower than one atmospheric pressure. Therefore, the safety of LNG storage tank was ensured.

During ships unloading mode, three controllers have been employed to ensure the safety of the process. A pressure controller was used to keep the ship pressure constant by dynamically opening and closing valve (VLV-100) returning BOG into ship to replace the unloading LNG hence avoiding vacuum in ship. This was done to maintain pressure and temperature inside the ship. Another pressure controller to control pressure inside the LNG storage tank was also employed. This pressure controller served to open and close dynamically the valve (VLV-B) to release or hold BOG inside the storage tank to avoid tank pressure from being over 117 kPa or below 1

atmospheric pressure. The released BOG was partially returned to the ship and stored into BOG storage tank. In the study, a level controller has been used avoid tank overfilling above 95% of the storage tank capacity by closing the valve (VLV-A) when the tank is at the 95% of its capacity.

During LNG holding mode, a pressure controller ensured safety pressure inside the tank by dynamically opening and closing the valve (VLV-B) to release or hold BOG inside the tank. This was done to avoid the tank pressure from being out of the range between 1 atmospheric pressure and 117 kPa.

3.2.4. LNG, BOG and CNG properties

The LNG, BOG and CNG properties changes has been analysed in this study. The LNG and BOG composition and properties s have been depicted from simulator and analysed by using excel. CNG composition and properties has been depicted from simulation result except stoichiometric air to fuel ratio in mass per mass and volume per volume, and specific gravity relative to air analysed by using CAT® Methane number calculator, methane number by Wärtsilä methane number calculator through inserted CNG composition, Wobbe index, and octane number were calculated by using the following equation (27) and (28).

$$Wobbe\ index = \frac{CNG\ higher\ heating\ value\ \left[\frac{MJ}{Nm^3}\right]}{CNG\ specific\ gravity\ [-]} \quad \left[\frac{MJ}{Nm^3}\right] \quad (27)$$

and

$$Motor\ octane\ number\ (MON) = (8 \times methane\ number) + 25 \quad [-] \quad (28)$$

Although the real MON can be provided by the experiment, the above rough estimation provides an estimation of MON for the study because this study was based on simulation rather than experiment.

CHAPTER IV

RESULTS AND DISCUSSION

This chapter undergoes the results of the LNG receiving terminal model, LNG and BOG property changes, recoverable BOG, boil-off gas management, resulted CNG properties and energy analysis.

4.1. Heat ingress

According to the three different LNG composition and Maputo weather conditions for the specified period depicted from literature, heat leaks in different parts of the receiving terminal was calculated and its independent associated LNG and BOG volume and mass have also computed. The depicted time is a transition from hot to cold season.

4.1.1. Heat ingress to the LNG storage tank

According to the designed LNG receiving tank from the above chapter, the heat leaks in the tank from three different section namely the roof, wall, and bottom and different LNG composition were computed with the associated volume and mass of LNG and BOG as weather condition changes.

Heat leaks were evaluated within three different simulation model modes: receiving tank LNG regasification, ship unloading, and LNG receiving tank holding mode. As described in previous chapter, this transition time is considered to have moderate wind speed, moderate and low temperature to depict the moderate to low BOG production.

4.1.1.1. LNG regasification

During this mode, the LNG is pumped from the storage tank at the receiving terminal to regasification plant before being sent to the end customers through pipe distribution lines.

Lean, medium, and rich LNG are predominantly consisting of methane (i.e. >95 , >90 , and ≥ 85 but below 90% of the LNG respectively), nitrogen content between 0.1 and 1.3 % with higher as the LNG is richer and traces of heavier hydrocarbons such as ethane, propane and butane as prescribed from previous chapter. As they contain lighter components at different amount, they resisted different times before the release of excess BOG to maintain safe pressure inside storage tank during LNG regasification mode. Lean, medium, and rich LNG kept holding BOG inside the tank for 29 hours, 44 hours, and 5 hours respectively before BOG formation increased pressure beyond

117 kPa as noticeable in figure 7, 8, and 9 below. After 295, 186 and 175 hours, the excess BOG continuously gets released from lean, medium, and rich LNG storage tank but with a diminishing trend and a hump up during daytime to the hottest time of a day.

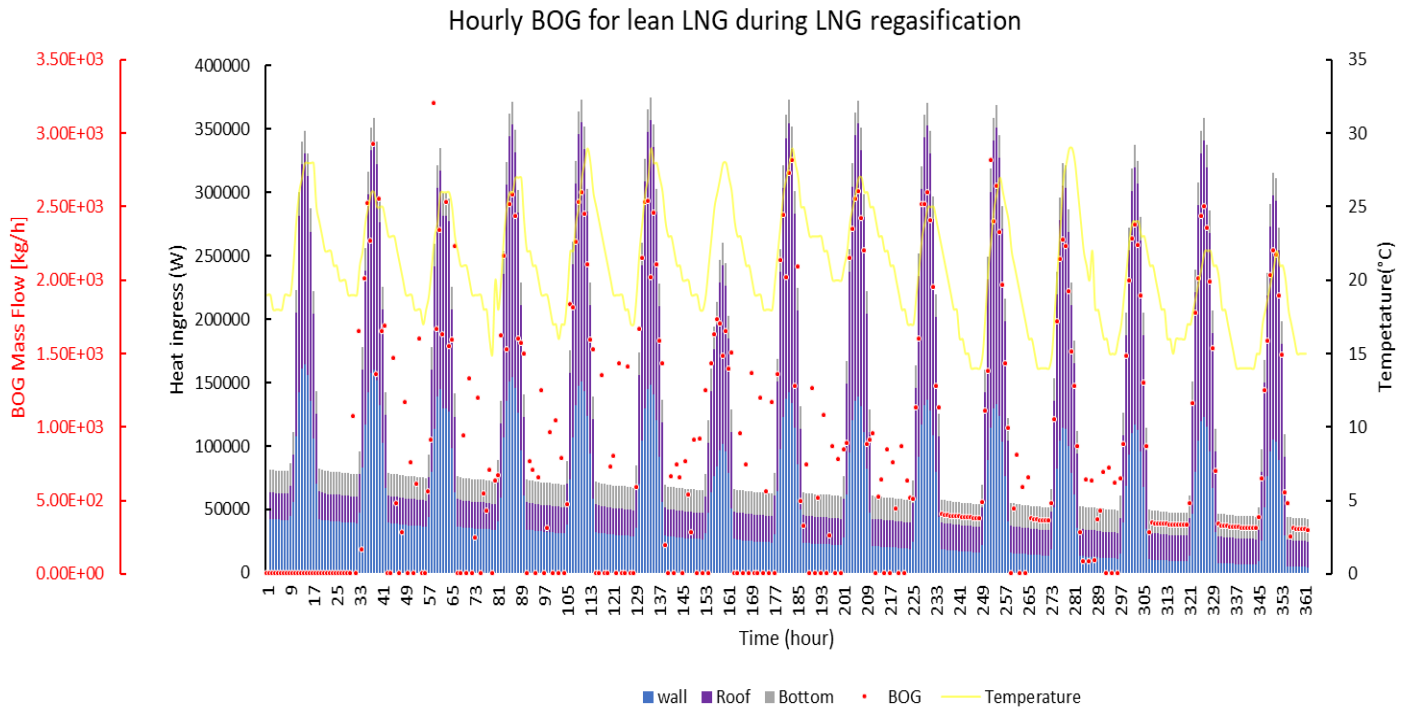


Figure 7. Hourly BOG excess formation from lean LNG during LNG regasification from receiving terminal tank.

During LNG regasification from the storage tank at the LNG receiving terminal, the heat ingress decrease progressively as the weather transition time goes with sudden hump during the day. The lean, medium, and rich LNG storage tank can withstand 361, 383, and 406 hours respectively constantly supplying the specified mass of LNG to regasification hourly.

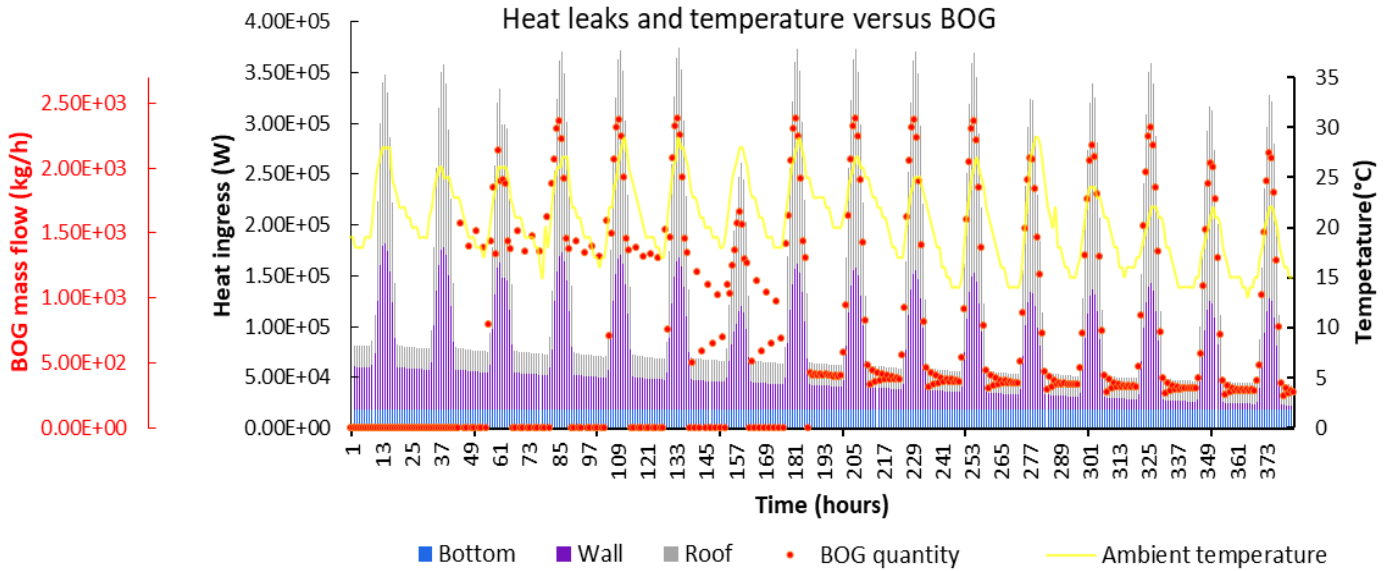


Figure 8. Hourly BOG excess formation from medium LNG during LNG regasification from receiving terminal tank.

During the transition time from hot to cold season, the temperature decreases gradually with sudden hump during day hours. The sudden hump during daytime causes more heat ingress in LNG storage tank so as the more BOG formation during daytime. The more BOG formation, the more unsafe to keep it in tank since it raises the pressure beyond safe pressure. Thus, the BOG is released to avoid accident, and the high excess BOG is released at the high heat ingress of a daytime while lowest BOG release occurs during night hour or without solar radiation as it is seen in figure 7, 8, and 9. Heat leaking in the storage tank decreases gradually as the season changes. Such decrease in heat ingress is different in the section parts of the tank. Whereby, the heat leaks through the wall decreases more than heat through the roof and bottom. This is due to the three facts: the surrounding ambient temperature, solar radiation, and the LNG level in the tank. The more the solar radiation and ambient temperature, the more heat capable of leaking through the tank wall. LNG level in the tank affects the contact surface to the wall, the more the quantity of LNG in the tank, the higher LNG level and large surface prone to heat ingress through tank wall. These three affects in parallel, the more the solar radiation, the more ambient temperature will be and with high level of LNG in the tank; the more heat will ingress in LNG inside the tank through the wall as it can be seen during the start of regasification in figure 7, 8, and 9.

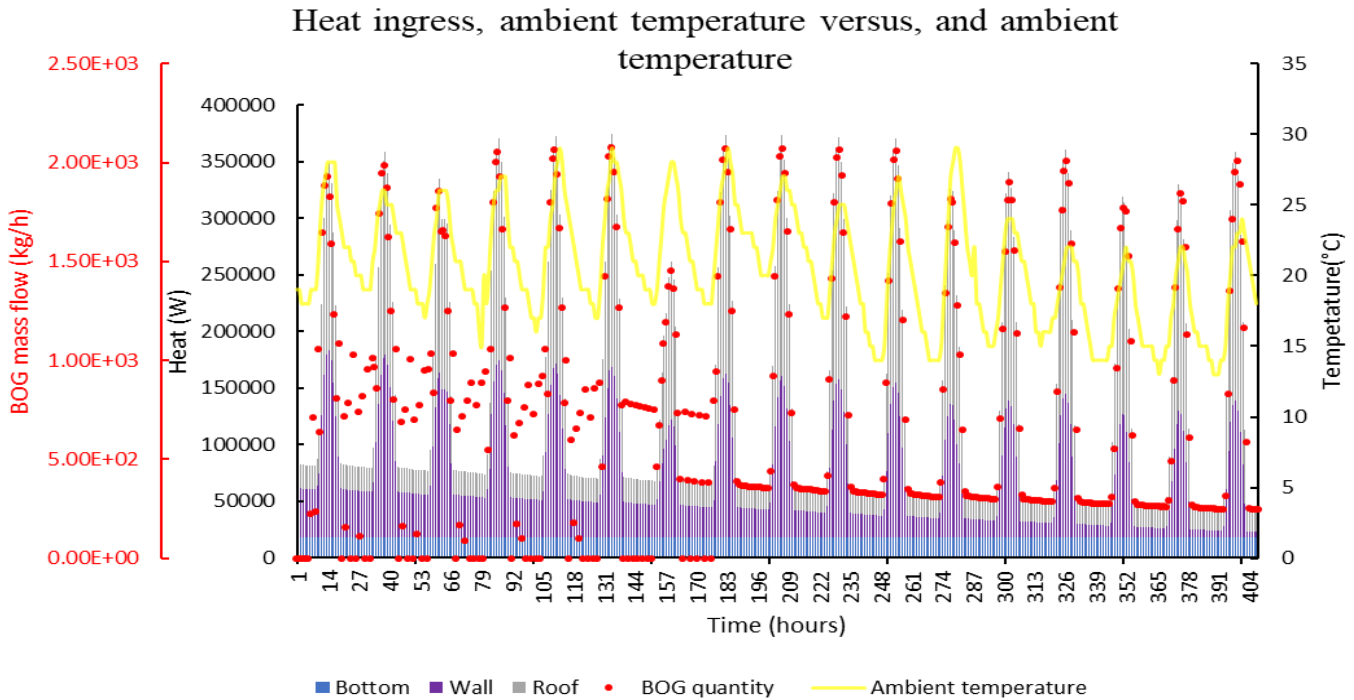


Figure 9. Hourly BOG excess formation from rich LNG during LNG regasification from receiving terminal tank.

The heat leaks through the roof to LNG suddenly increases during the day. This due to the facts of ambient temperature, solar radiation and the LNG level. The more the ambient temperature and solar radiation, the sudden increase of the heat leaks through the roof. The LNG level determines how much leaked heat can reach the LNG, when the LNG level is high, the more heat will get to it for the layer of gas is low but as the LNG level decreases in tank, the wider gas layer that the leaked heat has to pass through to reach the LNG. Therefore, even if there might be high solar radiation and ambient temperature, the less they will gasify the LNG stored as it can be seen in the previous figures at the late hours from 200 hours, 229 hours, and 176 hours to the last time for lean, medium, and rich LNG. In contrast, the higher the LNG level inside the tank, the more heat necessary to vaporize the stored LNG for it is in thermal equilibrium as it can be seen in first 50, 49, and 40 hours with low BOG production at high ambient temperature and solar radiation for lean, medium, and rich LNG respectively as noticeable in figure 7, 8, and 9. The bottom of the tank was kept at the constant temperature and contribute the almost constant heat ingress to LNG. The heat leaks through tank bottom in only affected by how the LNG temperature in the tank changes as in figure 10 it can be seen. LNG temperature changes slightly so does the bottom heat

leaks. The more the LNG temperature increases due to heat ingress, the less the bottom heat ingress due to the fact the heat transfer base on temperature difference. Therefore, as the tank bottom temperature was kept constant at 5 °C and the LNG temperature was increasing while the heat transfer continually decreased so as the heat ingress through the tank bottom.

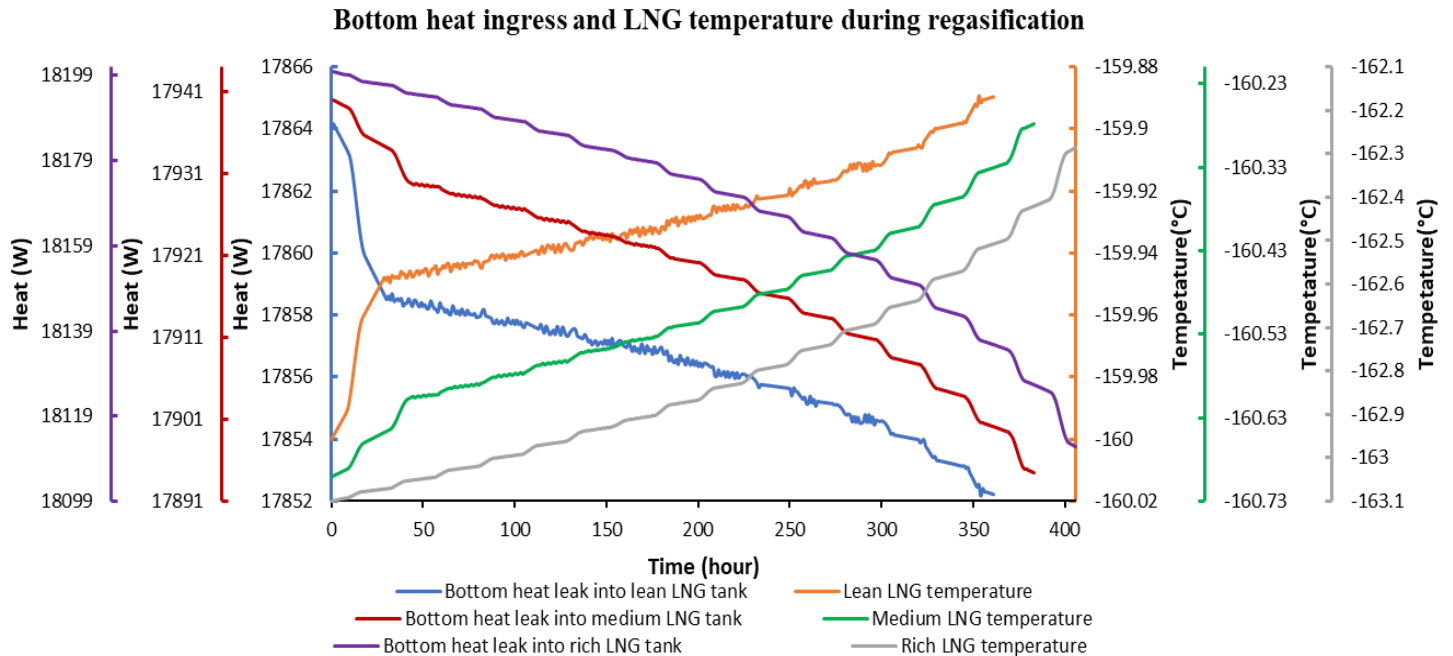


Figure 10. Relationship of bottom heat leaks and the LNG temperature changes during LNG regasification.

During periods without solar radiation, sudden noisy changes in lean, medium and barely in rich LNG temperature occur as a results of intermittent BOG excess release and thus heat ingress through the tank bottom noisily changes. After the BOG excess release at solar radiation absence time the LNG temperature slightly increase for the BOG continues to form but kept in tank before the unsafe pressure point is reached. Before the reach of excess BOG, the first 29 hours, 44 hours, and 5 hours of lean, medium, and rich LNG regasification, the heat ingress through storage tank bottom decrease rapidly for the LNG temperature rises rapidly. As the BOG excess release starts, the heat leak change moderately decreases with intermittent changes like noise until 295 and 176 hours for lean and medium LNG while rich LNG display no intermittent changes after regasification begins. This continuous BOG excess formation was due to built-up LNG temperature higher than boiling temperature and continually rising slowly. Thus, this continuous BOG formation slightly increases the LNG temperature and reduce bottom heat ingress intermittently towards intermittent changes. After these hours to the end of LNG regasification,

the heat leaks decrease more with moderate decreasing slope at night and high decreasing slope during the day due to continuous excess BOG formation release so as lean LNG temperature increase.

4.1.1.2. Ship unloading or receiving terminal storage tank filling

During this process, LNG is carried out from the vessels by ship pumps through two pipes and stored in the receiving terminal storage tank. Each LNG compositional type has simulated and supposed that this process take place after lowest possible LNG level is reached in storage tank at each respective LNG.

Storage tank filling started at 1:00’ on 10th June, 2024, after the reaching of approximately 10% of tank volume of lean LNG in storage tank. The storage tank filling lasted for approximately 15 hours and a half for all LNGs with low amount remaining amount filled in less than a half of the last hour. Small portion of LNG evaporate along the pipes and pumps, while the remaining entered into the storage tank, experiencing heat leakage that led to further evaporation. Excess BOG formation due to heat leakage has been studied as detailed in figure 11.

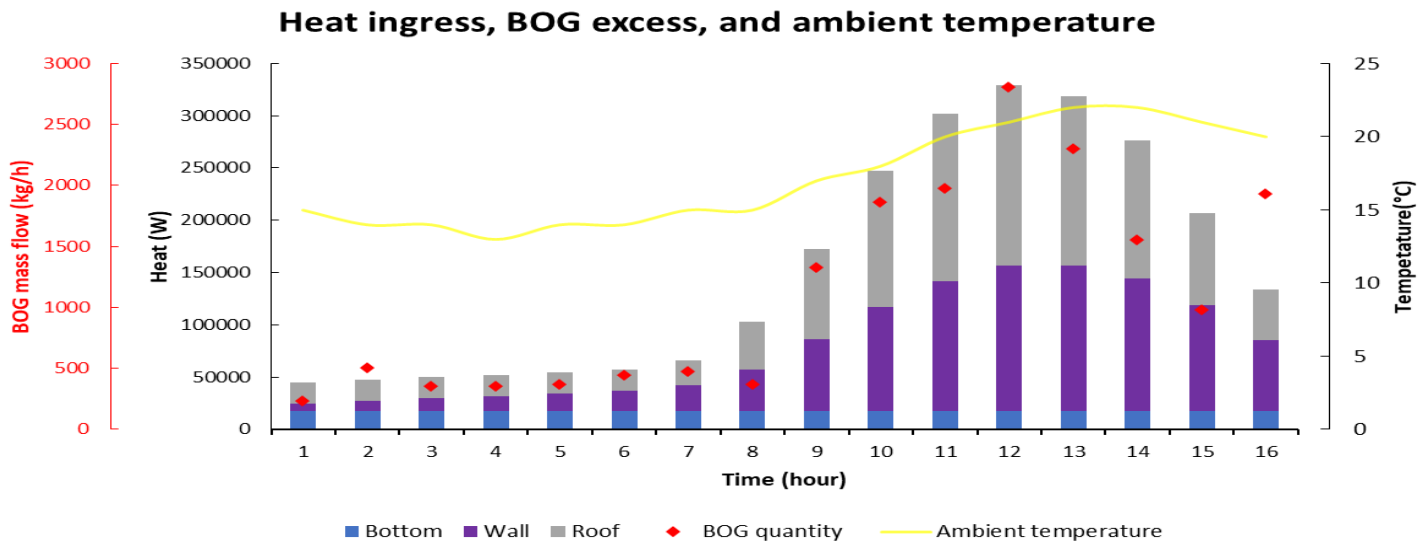


Figure 11. Hourly BOG excess released from lean LNG during LNG storage tank filling at receiving terminal.

A subsequent filling process began at 11:00’ PM on the same day with medium LNG, again lasting 15 hour and almost a half to reach approximately 95% of the tank volume. Similar LNG evaporation and heat leakage occurred with findings elaborated in figure 12.

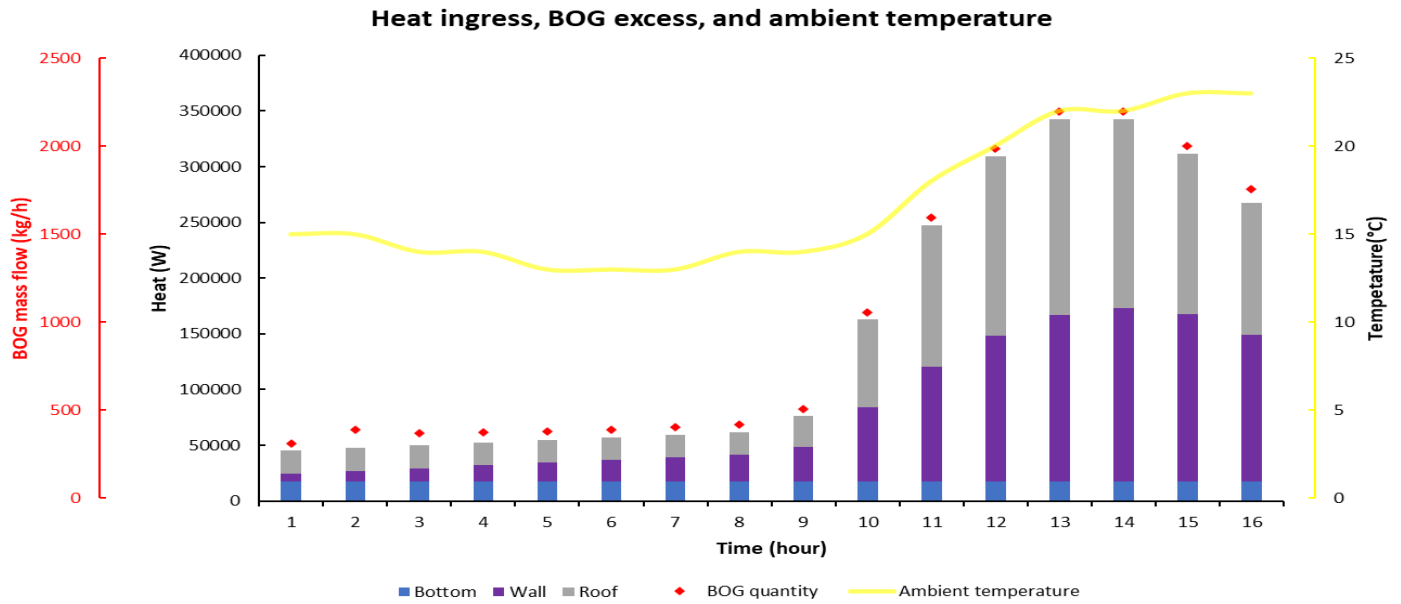


Figure 12. Hourly BOG excess released from medium LNG during LNG storage tank filling at receiving terminal.

Finally, another filling started at 10:00' PM on 11th June 2024, with rich LNG repeating the 15 hours and almost a half duration and experiencing similar evaporation and heat leakage as detailed in figure 13.

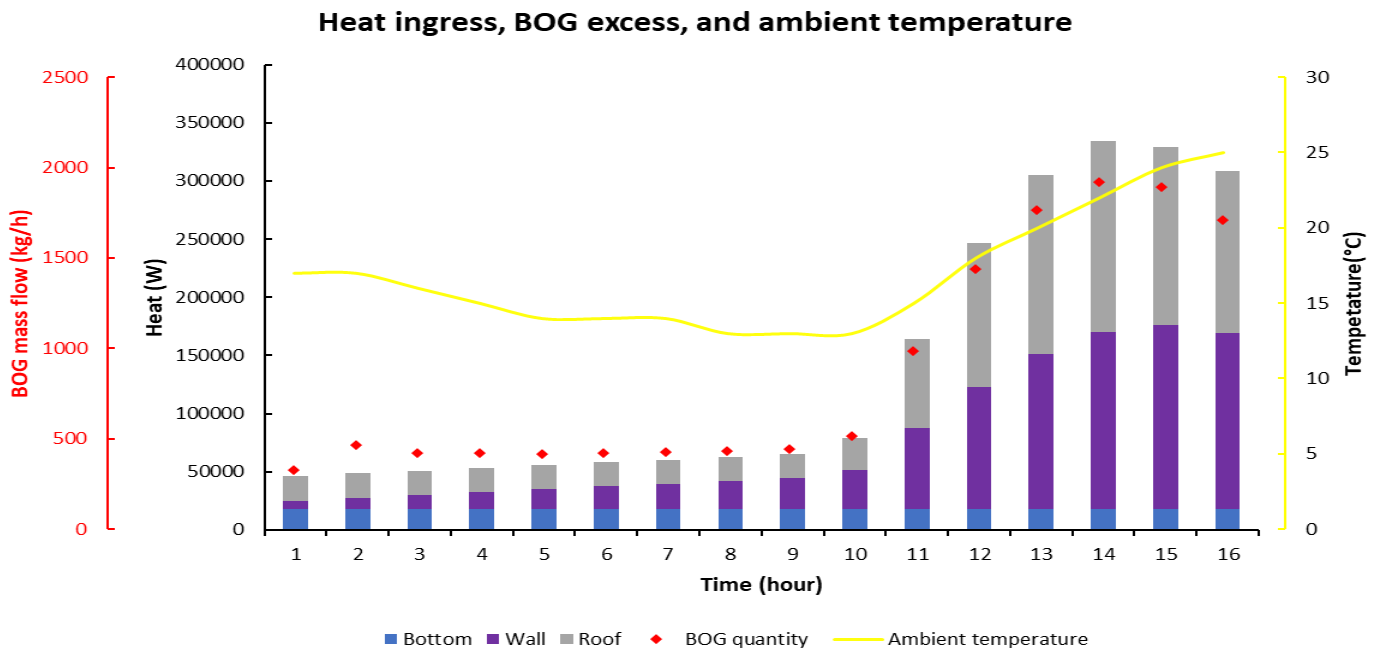


Figure 13. Hourly BOG excess released from rich LNG during LNG storage tank filling at receiving terminal.

The storage tank filling from vessels was simulated to start 1:00' AM to 4:00' PM on 10th June 2024, based on the weather condition of that day, right after the end of lean stored LNG regasification time. It was simulated to start again at 11:00' PM on 10th June, continuing to 2:00' PM on 11th June 2024, after the end of the medium LNG stored regasification time, and once more from 10:00' PM on 11th June 2024, after the end of the rich LNG stored regasification time, based on gathered weather conditions data.

During the first six hours of lean LNG tank filling, heat ingress increased slowly, then rapidly, and gradually decreased after twelve hours, as shown in figure 11. This heat leakage varied across different tank sections.

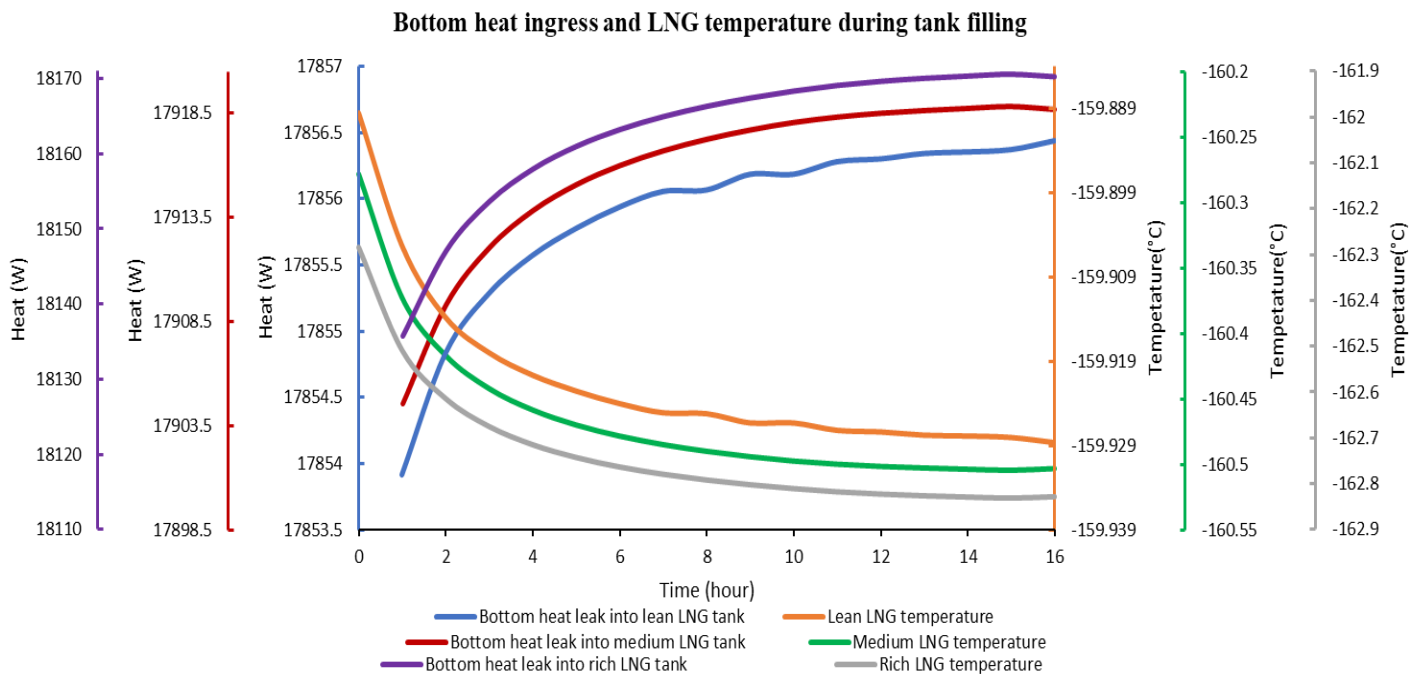


Figure 14. Relationship of bottom heat ingress and LNG temperature change.

The heat ingress through the tank bottom, as seen in figure 14, increased as the LNG temperature decreased due to the large amount of colder LNG unloaded from the ship. The greater the LNG temperature decrease, the more heat leaked from the tank bottom, as the heat transfer depends on the temperature difference between the tank bottom and the LNG. During the first seven hours of lean LNG filling, bottom heat ingress inside the tank increased rapidly because the remaining LNG

was slightly hotter, and the introduction of colder LNG further decreased the overall temperature, thereby increasing bottom heat ingress. After seven hours, the bottom heat ingress increased slowly as the LNG temperature decreased gradually until the end of the filling process. For medium LNG tank filling, during the first eight hours, heat ingress increased slowly at first, then rapidly, and started to decrease after fourteen hours, as noted in figure 12. This trend is similar, with the heat ingress through the tank bottom (figure 14) increasing as the LNG temperature decreases. During the first eight hours, bottom heat ingress increased rapidly due to the leftover LNG being slightly hotter. After ten hours, the bottom heat ingress increased slowly as the LNG temperature gradually equalized with the incoming LNG temperature. For rich LNG tank filling, during the first nine hours, heat ingress followed a similar pattern, increasing slowly initially, then rapidly, and starting to decrease after fourteen hours, as observed in figure 13. The heat ingress through the tank bottom (figure 14) increased with the decreasing LNG temperature. During the first ten hours, bottom heat ingress increased rapidly due to the hotter leftover LNG, with heat ingress increasing slowly after twelve hours as the LNG temperature stabilized.

The heat leaks through the walls of lean, medium, and rich LNG tanks are influenced by three main factors: ambient temperature, solar radiation, and the height of the LNG column inside the tank. These factors work together, and as shown in figures 11, 12, and 13, heat ingress through the wall increases with rising ambient temperatures, creating a noticeable hump during the day when temperatures are higher and lowering at night when temperatures drop and there's no solar radiation. Solar radiation significantly accelerates heat leakage, especially from the seventh to the end of tank filling, with the highest heat leakage and BOG excess formation occurring at peak solar radiation hours (12:00 to 13:00 on June 10, 11, and 12, 2024). The height of the LNG column inside the tank also determines the extent of heat leakage from the tank wall to the LNG. This can be observed during the first six to eight hours of tank filling, as seen in figures 11, 12, 13, 15, 16, and 17, where with no significant temperature change and no solar radiation, wall heat increases as the LNG column rises, implying that a larger LNG column inside the tank results in more LNG surface prone to heat ingress through the wall.

The heat leakage through the roofs of lean, medium, and rich LNG tanks is largely influenced by solar radiation and ambient temperature, and to a lesser extent by the height of the LNG column, with all factors affecting in parallel. During the filling of lean LNG, solar radiation starts at the

seventh hour and causes the previously constant roof heat ingress to rise rapidly, peaking between 12:00 and 13:00 on June 10, 2024, as seen in figures 11 and 15.

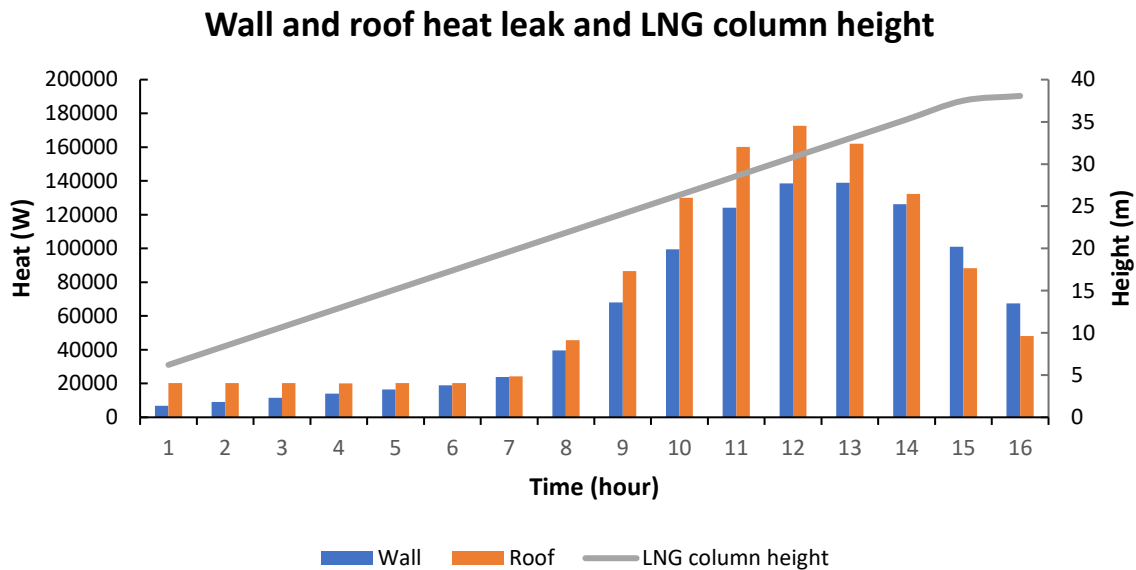


Figure 15. Relationship between tank wall and roof heat ingress and the height of lean LNG column.

Solar radiation has a greater influence on heat ingress than ambient temperature, with the highest heat ingress and BOG excess formation occurring during peak solar radiation times. As ambient temperature rises from 4:00 AM to 2:00 PM, the roof heat ingress increases due to the greater temperature difference facilitating heat transfer. Since the tank is filled with BOG at the top of the LNG, heat leakage through the roof passes through the BOG column to reach the LNG, with a larger BOG column reducing heat transfer to the LNG. During the filling of medium LNG, solar radiation starts at the eighth hour, with figures 12 and 16 showing similar patterns of roof heat ingress rising rapidly and peaking between 12:00 and 13:00 on June 10, 2024.

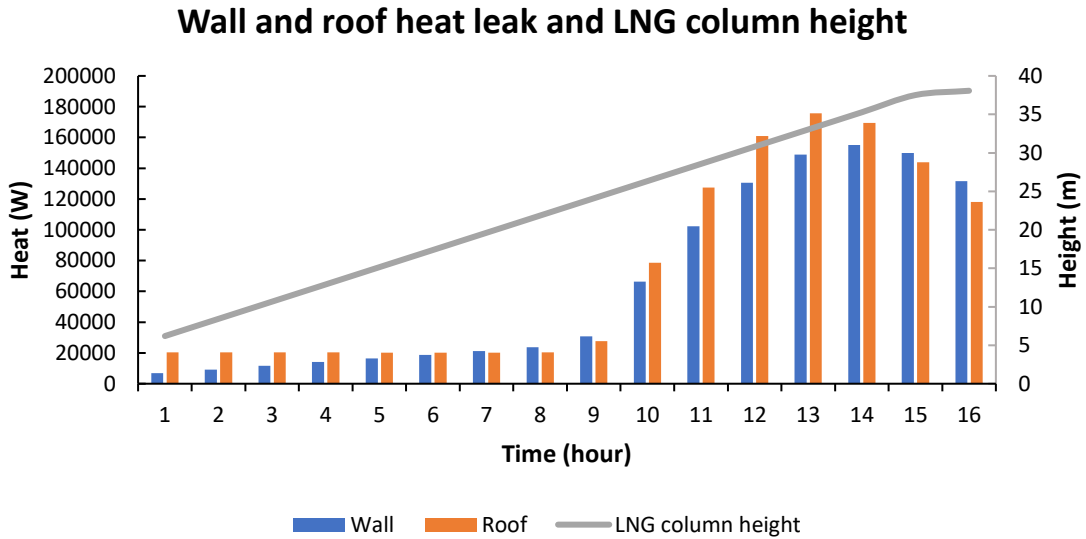


Figure 16. Relationship between tank wall and roof heat ingress and the height of medium LNG column.

The influence of solar radiation is more significant than ambient temperature. The highest heat ingress and BOG excess formation occur during peak solar radiation hours, and as ambient temperature rises from 1:00 AM to 2:00 PM, the roof heat ingress increases. For rich LNG tank filling, starting at the tenth hour, figures 13 and 17 illustrate the impact of solar radiation, with roof heat ingress rising rapidly and peaking between 12:00 and 13:00 on June 11, 2024. The pattern remains consistent, with solar radiation having a greater influence than ambient temperature, and heat transfer increasing with the temperature difference. A larger BOG column reduces the amount of heat reaching the LNG due to its thermal resistance.

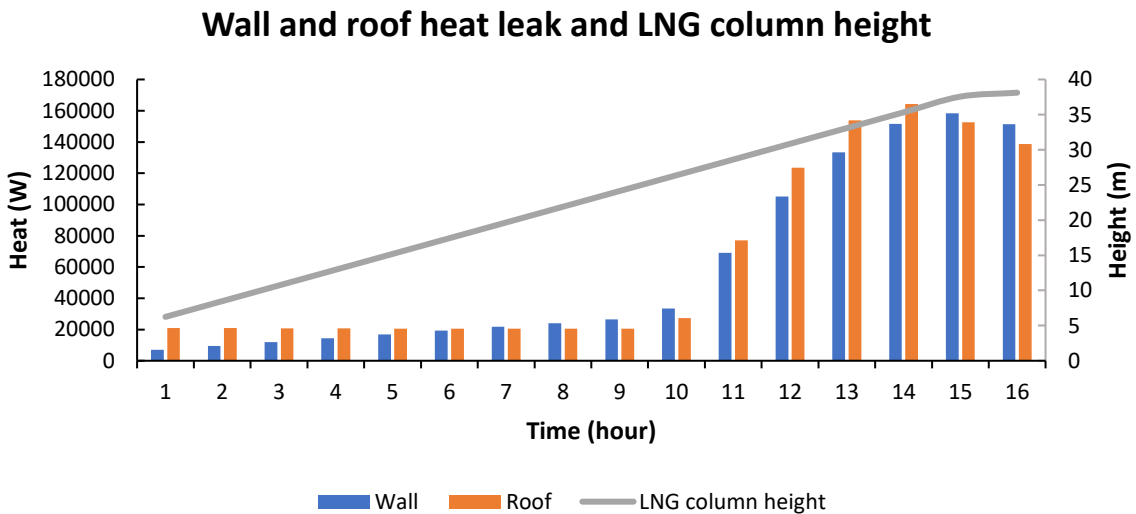


Figure 17. Relationship between tank wall and roof heat ingress and the height of rich LNG column.

4.1.1.3.Storage tank holding mode

The storage tank after being filled with LNG to the 95% of its volume, it has been simulated to be in holding mode without further filling and unloading to regasification plant for a day or twenty-four hours. Each LNG compositional type has been studied to unveil the heat ingress through the tank to LNG, its source, and impact on BOG excess.

The storage tanks filled with lean, medium, and rich LNG have been simulated in holding mode for 24 hours after being filled to approximately 95% of their volume capacity. For lean LNG, the simulation started from 5:00 PM on June 10, 2024, to 4:00 PM the following day (i.e., June 11, 2024). Heat ingress into stored lean LNG, originating from solar radiation and ambient temperature, propagated through the bottom, wall, and roof of the tank. The exact heat ingress and BOG excess resulting from such heat leakage were evaluated independently for each section of the tank, as seen in figure 18.

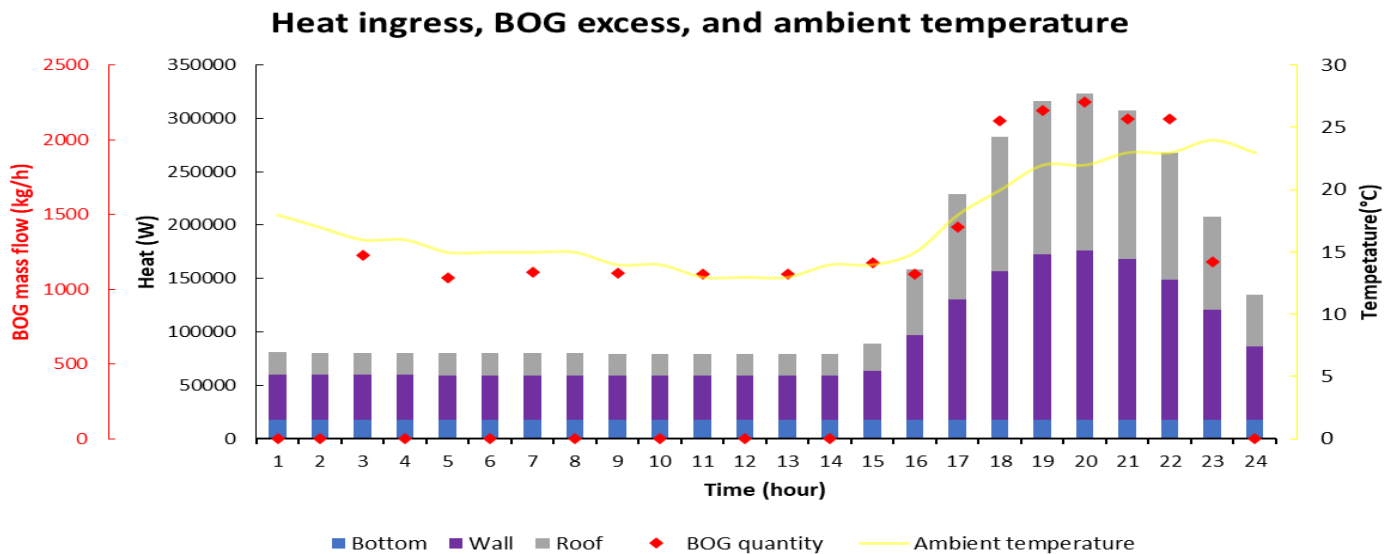


Figure 18. Relationship of heat, ambient temperature and hourly BOG excess released from receiving terminal lean LNG storage tank.

For medium LNG, the simulation began right after reaching 95% capacity, from 3:00 PM on June 11, 2024, to 2:00 PM the next day (i.e., June 12, 2024). Similar to lean LNG, heat ingress was

primarily due to solar radiation and ambient temperature, affecting the tank's bottom, wall, and roof, with evaluations shown in figure 19.

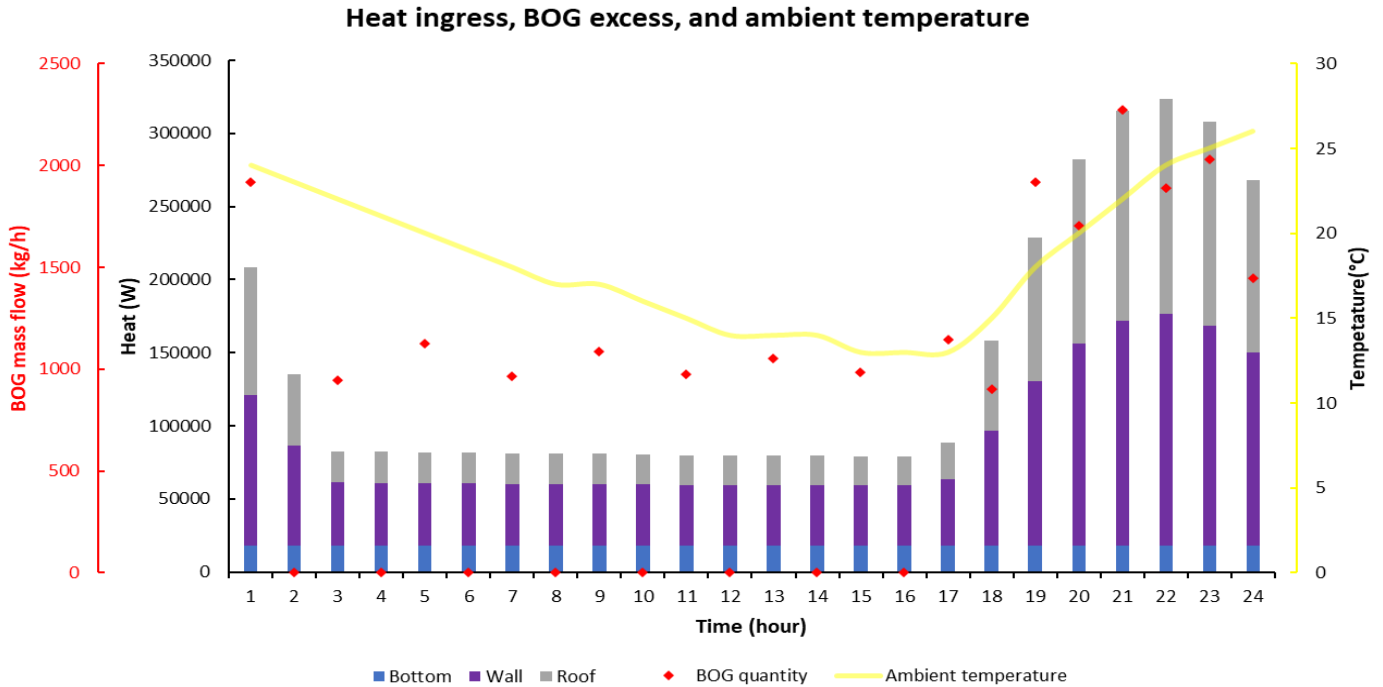


Figure 19. Relationship of heat, ambient temperature and hourly BOG excess released from receiving terminal medium LNG storage tank.

For rich LNG, the simulation covered from 2:00 PM on June 12, 2024, to 1:00 PM the following day (i.e., June 13, 2024), with heat ingress evaluated from all sources and each tank section independently. As with lean and medium LNG, solar radiation and ambient temperature were the primary sources of heat ingress, detailed in figure 20.

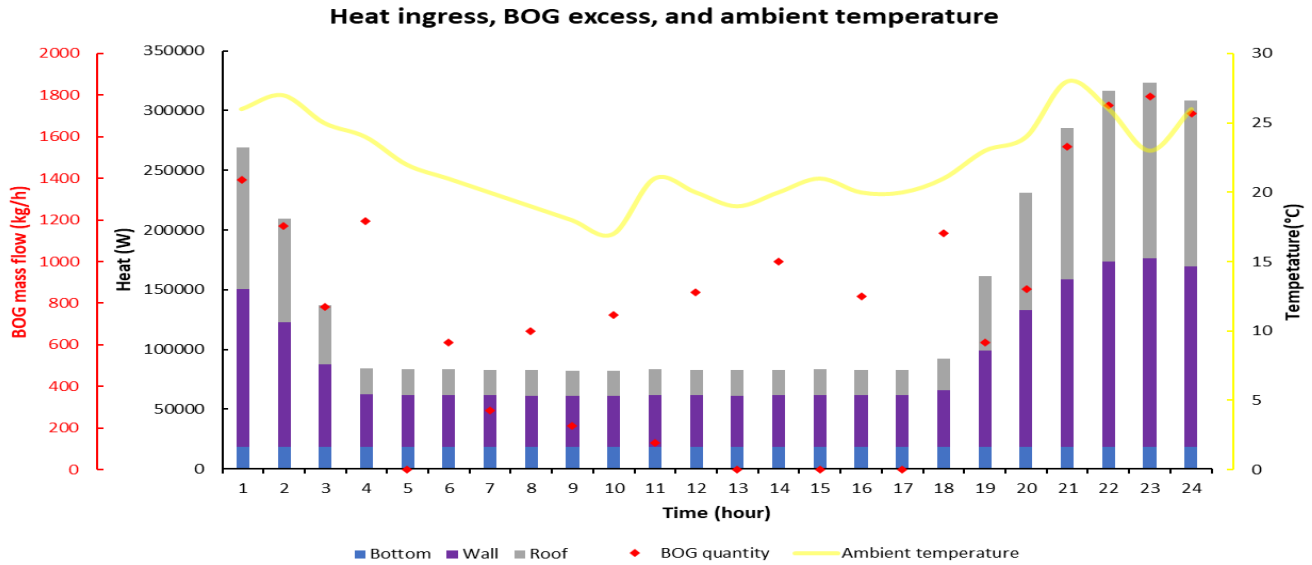


Figure 20. Relationship of heat, ambient temperature and hourly BOG excess released from receiving terminal rich LNG storage tank.

During the first fourteen hours of lean LNG storage tank holding mode, the heat ingress inside the tank remained relatively unchanged, affecting the bottom, wall, and roof, as shown in figure 18.

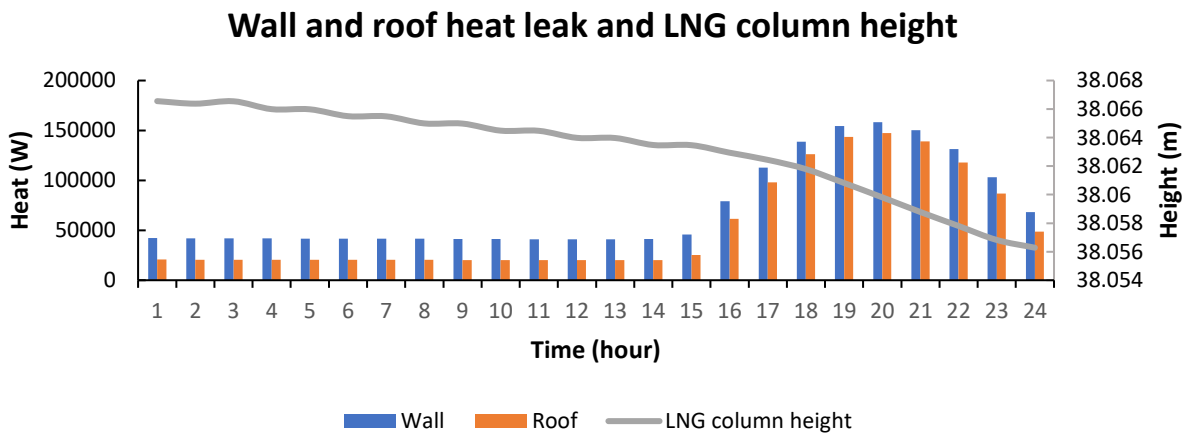


Figure 21. Relationship between tank wall and roof heat ingress and the height of lean LNG column.

During this period, ambient temperature initially decreased but began to rise at the thirteenth hour, with no solar radiation present. This suggests that significant heat ingress changes in the lean LNG tank are primarily due to solar radiation rather than ambient temperature fluctuations. This period is also marked by intermittent BOG excess releases, with one hour of release followed by an hour without, as the heat leakage without solar radiation was insufficient to consistently vaporize the

lean LNG. After fourteen hours without solar radiation, solar radiation intensity began rising at 7:00 AM and peaked at 1:00 PM, causing heat ingress through the wall and roof to rise and fall accordingly, while bottom heat ingress remained stable. The highest heat leakage and BOG release occurred during peak solar radiation (12:00 PM to 1:00 PM), rather than during the hottest hour (3:00 PM to 4:00 PM). This indicates that solar radiation, rather than ambient temperature, predominantly impacts BOG formation and heat leakage in the lean LNG storage tank. During the first two hours of medium LNG holding, both ambient temperature and solar radiation were decreasing (3:00 PM to 5:00 PM), leading to a significant drop in heat ingress, particularly through the wall and roof, and a reduction in BOG excess release, as shown in figure 19.

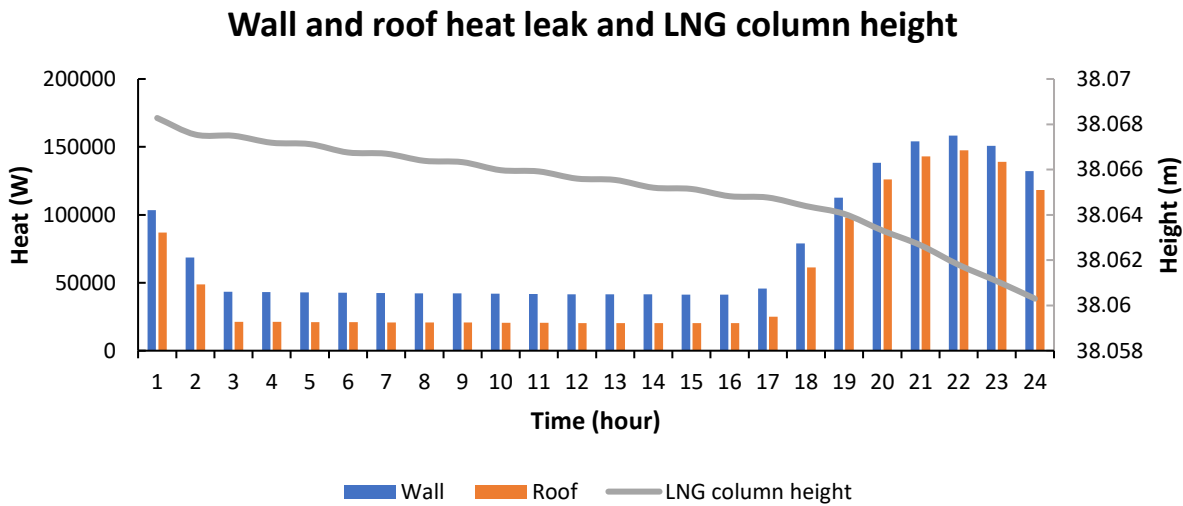


Figure 22. Relationship between tank wall and roof heat ingress and the height of medium LNG column.

From the third to sixteenth hour (5:00 PM to 7:00 AM), with no solar radiation and falling ambient temperature, heat ingress inside the tank remained consistent across all sections. This period also exhibited intermittent BOG excess release due to insufficient heat leakage without solar radiation. After sixteen hours, solar radiation began rising again at 7:00 AM, with peak intensity at 1:00 PM, causing heat ingress through the wall and roof to increase and then decrease, while bottom heat ingress remained unaffected. The highest heat leakage and BOG release occurred during peak solar radiation (12:00 PM to 1:00 PM), rather than during the hottest hour (2:00 PM to 3:00 PM). During the first three hours of rich LNG holding (2:00 PM to 5:00 PM), decreasing solar radiation resulted in a significant drop in heat ingress through the wall and roof, as well as a reduction in BOG excess release, as seen in figure 20.

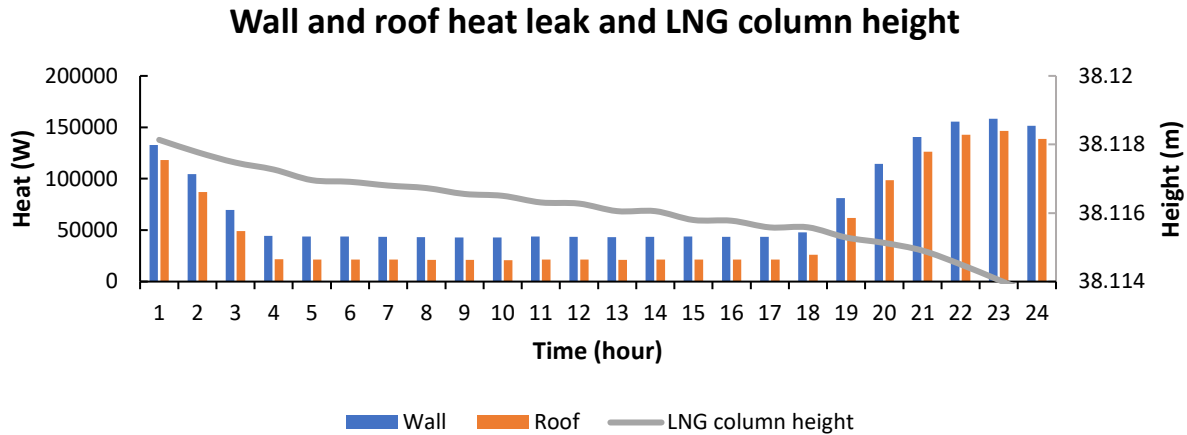


Figure 23. Relationship between tank wall and roof heat ingress and the height of rich LNG column.

From the fourth to seventeenth hour (5:00 PM to 7:00 AM), with intermittent ambient temperature changes and no solar radiation, heat ingress remained consistent across all sections. Intermittent BOG excess release occurred due to insufficient heat leakage without solar radiation. After seventeen hours, solar radiation began rising at 7:00 AM and peaked at 1:00 PM, causing heat ingress through the wall and roof to fluctuate, while bottom heat ingress remained stable. The highest heat leakage and BOG release occurred during peak solar radiation (12:00 PM to 1:00 PM), rather than during the hottest hour (10:00 AM to 11:00 AM). Thus, BOG excess formation and heat leakage in rich LNG storage tanks are also primarily influenced by solar radiation rather than ambient temperature.

As noticeable in figures 21, 22, and 23, the height of the LNG column inside the tank whether lean, medium, or rich lowly affects the heat ingress through the wall and the roof. During the holding mode, LNG slowly evaporates inside the storage tank, causing the LNG column to reduce. Intermittent BOG excess formation and release from the tank initially lead to a low decrease in the LNG column height, which rapidly reduces when there is no BOG excess release. This trend is due to LNG expanding when it accumulates significant heat, similar to water and milk, which expand and release large vapors when heated and shrink when cooled. When LNG accumulates enough heat, it expands and forms large BOG, increasing pressure and temperature inside the tank. Upon reaching a set pressure point, BOG excess is released to reduce pressure, which cools and slightly shrinks the LNG column. This cycle of heat ingress and LNG evaporation continues, with solar radiation playing a significant role in the process. The height of the LNG column impacts the

thermal resistance of the BOG layer, which slightly reduces heat ingress through the roof. As the LNG column height decreases, the contact area with the tank wall reduces, lowering the heat transfer. This dynamic interplay between heat ingress, LNG column height, and BOG formation leads to varying rates of evaporation and column height reduction, with the tank bottom temperature set to a constant 5°C influencing heat transfer due to temperature differences between LNG and the tank bottom. This phenomenon affects the overall heat ingress and LNG behavior inside the storage tank.

Given that the tank bottom is constantly maintained at 5°C, the heat ingress through the bottom of the tank depends on the temperature changes of the LNG, as heat transfer occurs due to the temperature difference between two bodies. The greater the temperature difference, the more significant the heat transfer, and vice versa.

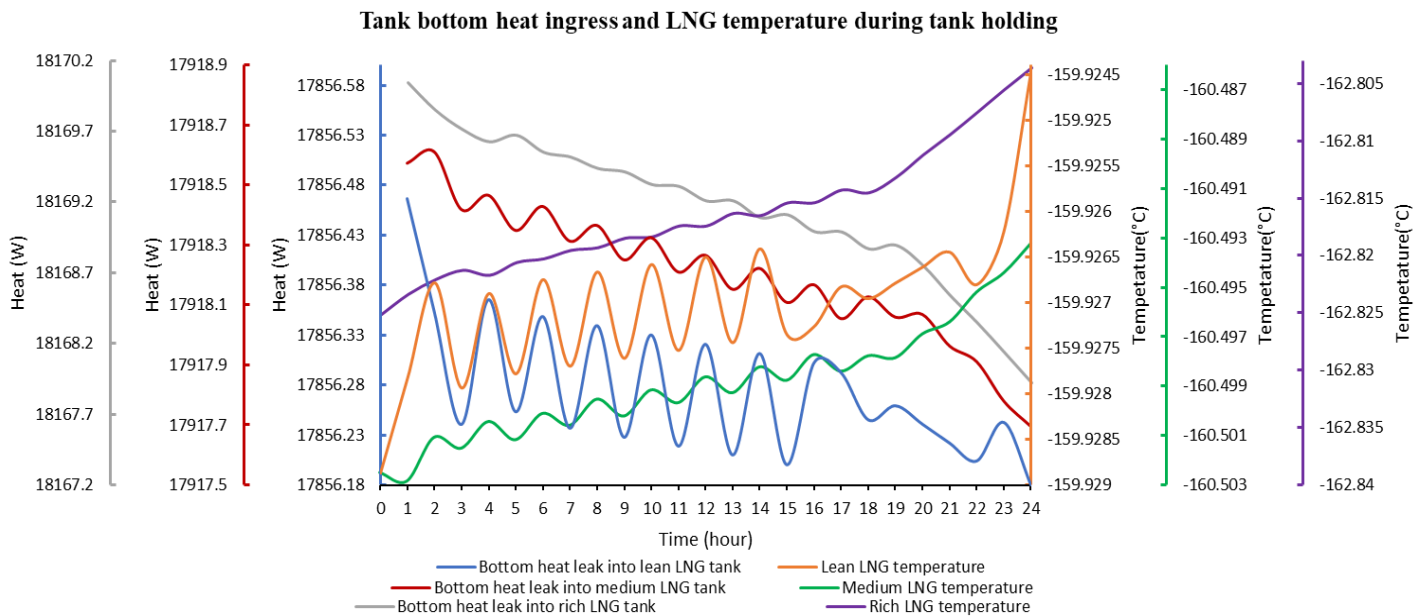


Figure 24. Relationship of tank bottom heat ingress and LNG temperature change.

For lean LNG, during the first fourteen hours, it cools down as BOG excess is released and its temperature rises in the absence of BOG release from the tank. This pattern implies that the cooler the lean LNG, the larger the temperature difference with the tank bottom, resulting in higher heat ingress, as seen in figure 24. Despite cooling through evaporation and BOG release, the lean LNG temperature generally trends upwards, failing to revert to its initial state. When solar radiation starts, the lean LNG temperature rises irreversibly due to rapid heat ingress, as depicted in figure

18, causing the LNG to cool through evaporation and BOG release. Consequently, heat ingress through the tank bottom decreases as the temperature difference between LNG and the tank bottom diminishes. At the 22nd hour, a significant drop in lean LNG temperature occurs due to a large BOG release, leading to higher heat ingress in the following hour as the increased temperature difference between LNG and the tank bottom, as shown in figure 24. Similarly, for medium LNG, during the first nineteen hours, it cools down as BOG is released, and its temperature rises in the absence of BOG release. The cooler the medium LNG, the larger the temperature difference with the tank bottom, resulting in higher heat ingress, as seen in figure 24. Despite cooling through evaporation and BOG release, the medium LNG temperature trends upwards, remaining uncooled to its initial state. With the onset of solar radiation at the seventeenth hour, the medium LNG temperature rises irreversibly due to rapid heat ingress, causing the LNG to cool through evaporation and BOG release. Consequently, heat ingress through the tank bottom decreases as the temperature difference between medium LNG and the tank bottom diminishes. For rich LNG, during periods without solar radiation from the fourth to the seventeenth hour, it cools down as BOG is released, and its temperature rises in the absence of BOG release from the storage tank. The cooler the rich LNG, the larger the temperature difference with the tank bottom, resulting in higher heat ingress, as seen in figure 24. This leads to an intermittent series of temperature changes and heat ingress through the tank bottom. Despite cooling through evaporation and BOG release, the rich LNG temperature trends upwards, failing to cool to its initial state. During solar radiation periods within the first three hours and from the eighteenth hour onwards, the rich LNG temperature rises irreversibly due to rapid heat ingress, causing the LNG to cool through evaporation and BOG release. Consequently, heat ingress through the tank bottom decreases as the temperature difference between rich LNG and the tank bottom diminishes, revealing that bottom heat ingress inside the rich LNG storage tank is directly induced by changes in the rich LNG temperature. Therefore, it is revealed that the heat ingress and BOR into LNG storage tank depends on the weather conditions, LNG level in tank and not all heat leakage goes to the LNG alone but also the top BOG layer as M. S. Khan et al. (2020) has found.

4.1.2. Heat ingress in piping and pumping

Heat leakage through LNG pumping and piping were analysed for the above specified period during the ship unloading or LNG storage tank filling at the receiving terminal to assess the impacts of ambient temperature for all LNG compositional types studied. The ship unloading period for all

the scenarios was simulated with gathered weather conditions of June, 2024, a transitional time from summer to winter in Maputo. As prescribed in the previous chapter, the two run-down lines (loading and unloading pipeline) used are 2km long mild steel, having an inner and outer diameter of 30 inch and 30.1 inch respectively, a urethane foam insulation with thickness of 0.025m and a thermal conductivity of 0.018 W/m.K each. Eight cargo pumps were used in simulation and calculation of heat leakage through LNG pumping, each has pumping flow rate of 1400m³/h, a pump head of 137.96m, 137.99m, and 130.03m for lean, medium, and rich LNG respectively and with efficiency of 0.75.

4.1.2.1. Pumping

As it has been prescribed in previous chapter, the assumption was made that the heat leakage in pump do not get affected by the ambient temperature and solar radiation for pumps are assumed to be submerged into vessel tanks. Hourly, heat leakage through pumps and it was found to be equal for each pump pumping the same flow rate for each compositional LNG type head. For all LNGs, the first fifteen hours of filling have the same heat leakage while the remaining time, heat ingress has reduced since low amount was pumped as remaining to reach 95% volume of the storage tank. As it is detailed in the table 6, the total heat leakage through the pumps during ships unloading is 9113580.68W, 9669720.77W, and 10196772.59W for lean, medium and rich LNG respectively.

Table 6. Hourly heat ingress into LNGs from the pumps and pumped LNG volume.

Time	Lean		Medium		Rich	
	Pumped LNG (m ³ /h)	Heat (W)	Pumped LNG (m ³ /h)	Heat (W)	Pumped LNG (m ³ /h)	Heat (W)
1	11202.47	597611.85	11200.19	634080.05	11200.04	668640.83
2	11202.47	597611.85	11200.19	634080.05	11200.04	668640.83
3	11202.47	597611.85	11200.19	634080.05	11200.04	668640.83
4	11202.47	597611.85	11200.19	634080.05	11200.04	668640.83
5	11202.47	597611.85	11200.19	634080.05	11200.04	668640.83
6	11202.47	597611.85	11200.19	634080.05	11200.04	668640.83
7	11202.47	597611.85	11200.19	634080.05	11200.04	668640.83
8	11202.47	597611.85	11200.19	634080.05	11200.04	668640.83
9	11202.47	597611.85	11200.19	634080.05	11200.04	668640.83
10	11202.47	597611.85	11200.19	634080.05	11200.04	668640.83
11	11202.47	597611.85	11200.19	634080.05	11200.04	668640.83

12	11202.47	597611.85	11200.19	634080.05	11200.04	668640.83
13	11202.47	597611.85	11200.19	634080.05	11200.04	668640.83
14	11202.47	597611.85	11200.19	634080.05	11200.04	668640.83
15	11202.47	597611.85	11200.19	634080.05	11200.04	668640.83
16	2800.616	149402.96	2800.048	158520.01	2800.01	167160.21
Total		9113580.68	9669720.77		10196772.59	

4.1.2.2. Piping

The run-down pipelines have been simulated with assumption that the solar radiation did not impact, suspended in air near to the ground and constant wind velocity of 5m/s. The impact ambient temperature and wind velocity to heat ingress inside pipeline for all LNGs. LNG from ship pumps were collected to pass through two pipelines before being loaded into storage tank.

The storage tank filling with lean LNG was simulated to start at 1:00 AM and continue until 4:00 PM on 10th June, 2024. Subsequently, the storage tank filling with medium LNG was simulated to begin at 11:00 PM on 10th June, 2024, and end at 2:00 PM on 11th June, 2024. Finally, the storage tank filling with medium LNG was simulated to start at 10:00 PM on 11th June, 2024, and conclude at 1:00 PM on 12th June, 2024.

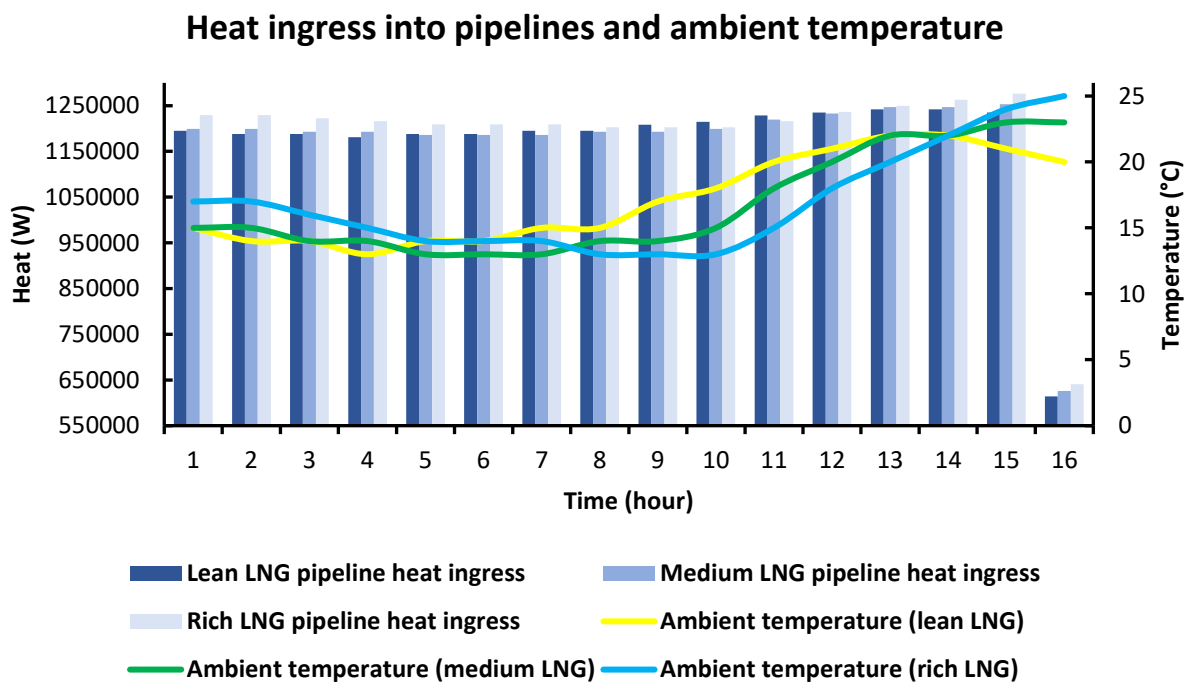


Figure 25. Relationship between heat ingress into run-down pipelines and ambient temperature.

As noticeable in figure 25, the filling of the lean LNG storage tank started with the ambient temperature slowly decreasing and began to rise at the fifth hour (5:00 AM), then started to drop again at the fifteenth hour (3:00 PM) until the last hour. As the ambient temperature dropped, the heat ingress inside the pipes containing lean LNG slightly decreased, and as it increased, the heat leakage also slightly increased. The heat leakage at the last hour was minimal because the remaining lean LNG was very small, filling the storage tank to 95% of its volume. Similarly, the filling of the medium LNG storage tank began with the ambient temperature slowly dropping and starting to rise at the eighth hour (5:00 AM) until the end of loading. The ambient temperature's changes slightly affected the heat ingress and heat leakage in the pipes containing medium LNG. The heat leakage at the last hour was minimal despite the high temperature, as the remaining medium LNG was small, filling the tank to 95% of its volume. For rich LNG, the filling started with the ambient temperature slowly dropping and beginning to rise at the eleventh hour (8:00 AM, 12th June, 2024) until the end of loading. The ambient temperature changes slightly impacted the heat ingress and leakage in the pipes containing rich LNG. The heat leakage at the last hour was minimal despite the high temperature, as the remaining rich LNG was small, filling the tank to 95% of its volume. Therefore, the ambient temperature changes slightly affected the heat ingress into the LNG passing through the pipeline hourly.

Although the pipelines are sealed, it was found that the heat continually ingress through them as Phalen et al. (2007) stated during the analysis of updated LNG pipeline.

4.1.2.3. Total heat leakage into pumping and piping

The boil-off gas form as a results of heat ingress into the piping and pumping were evaluated and analysed for each LNG compositional type, it has been found that the amount of BOG contribution to BOG formation from LNG pumping and piping depends on the hourly heat ingress at each LNG.

As more heat leaks into the LNG piping and pumping systems from the cargo vessel to the storage tank at the receiving terminal, BOG formation increases, and vice versa, as noticeable in figure 26. The primary heat leakage occurs through the pipes, which rely on the ambient temperature, while during pumping, it depends on the LNG volume put through and the pump head, except for the last hour. During the last hour, the pumped and piped LNG whether lean, medium, or rich is small, resulting in minimal heat leakage during pumping and piping.

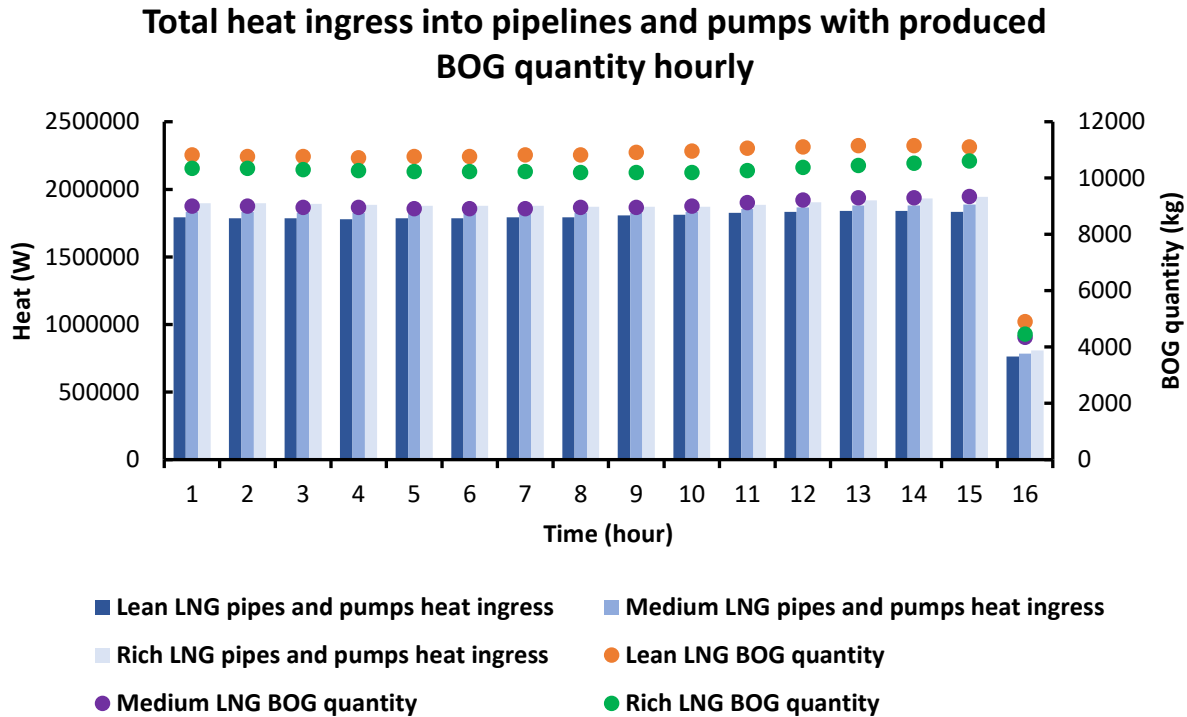


Figure 26. Relationship between BOG formation and heat ingress through piping and pumping of the LNG.

Therefore, during pumping and piping of LNG from the ship to the storage tank at the receiving terminal, heat ingress through pumps due to pump mechanisms and through pipelines due to ambient temperature they are exposed to lead to BOG formation. The BOG formation as well as the heat ingress into piping and pumping differ for each LNG for their compositional and properties' differences. Even though there is no BIG difference in the heat ingress, the BOG quantity from lean LNG is higher than the two remaining and the least amount is from medium LNG.

As Sedlaczek (2008) found, most of the pump's heat turns into heat that leak into the LNG and with addition of BOG generated from the pipelines, unloading operations generate almost 10 times of BOG than tank.

4.2. LNG and BOG properties changes

The LNG properties changes as a portion of it change into vapour form as a result of heat ingress. As the LNG properties change over time, the emitted BOG change over time for it is being produced from different LNG. Changes of LNG and BOG properties have been evaluated and analysed differently for each LNG compositional type in each mode at the receiving terminal.

4.2.1. Composition

Composition of LNG is change over time as it vaporises due to heat ingress inside different parts of the receiving terminal for each LNG component vaporise differently. The lighter components tend to vaporise earlier and easily compare to heavier components. Therefore, the LNG composition changes. BOG also change because of compositional change of the LNG. Timely, the BOG formation depends on the LNG composition, the lighter components in LNG. The lighter components will firstly evaporate as a result of heat leakage towards LNG.

4.2.1.1. LNG regasification mode

Lean LNG changes differently in each mode: LNG gasification, storage tank filling, and ship unloading, and these changes have been evaluated along with the resulting BOG variations. Similarly, medium LNG and rich LNG each exhibit distinct changes in their respective modes of LNG gasification, storage tank filling, and ship unloading, with corresponding evaluations of the resulting BOG changes.

During regasification, the storage tank was initially simulated to constitute 95% of its volume with LNG and 5% with BOG, with the composition in equilibrium as shown in Table 7. For lean, medium, and rich LNG regasification, the tank initially held LNG and BOG.

Table 7. Initial LNG and BOG composition inside storage tank during LNG regasification.

Components	Initial composition (mole fraction)					
	Lean		Medium		Rich	
	LNG	BOG	LNG	BOG	LNG	BOG
Methane	0.986	0.977	0.923	0.87319	0.8587	0.67287
Ethane	1.18E-02	2.62E-05	5.00E-02	8.95E-05	8.40E-02	9.35E-05
Propane	1.00E-03	2.45E-08	1.50E-02	2.68E-07	3.00E-02	2.76E-07
n-Butane	2.00E-04	6.04E-11	6.00E-03	1.20E-09	1.20E-02	1.03E-09
n-Pentane	0	0	0.001	2.50E-12	0.0023	2.10E-12
Nitrogen	1.00E-03	0.023	5.00E-03	1.27E-01	1.30E-02	3.27E-01

As noticeable in figures 27, 28, and 29, the composition of LNG during regasification initially does not change significantly due to the absence of BOG excess formation and release. For lean LNG, this stability lasts for the first 29 hours, for medium LNG, it lasts for the first 44 hours, and for rich LNG, it lasts for the first 5 hours. After these periods, the compositions of lean, medium,

and rich LNGs start to change significantly, with a progressive increase in compositional changes as regasification continues until the end of each LNG's regasification process.

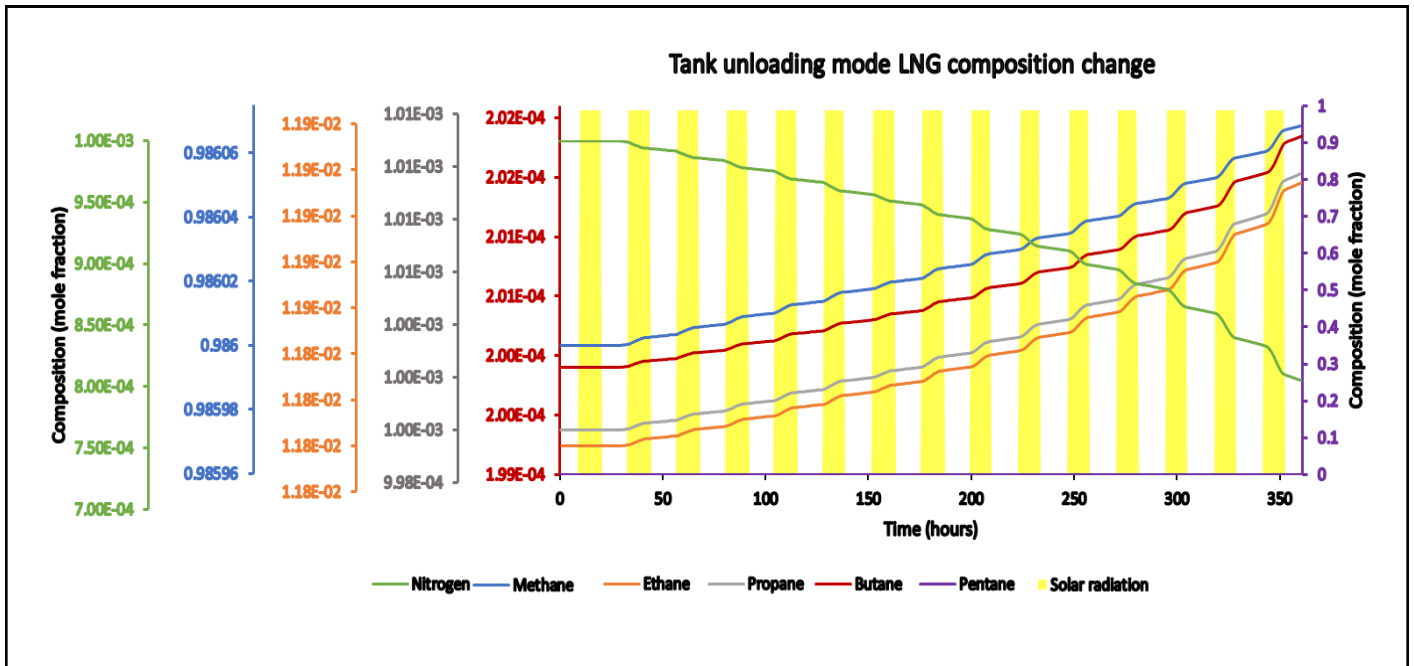


Figure 27. Lean LNG compositional change during LNG regasification.

As observable from figures 27, 28, and 29, the most significant increases and decreases in LNG components occur during daytime with the presence of solar radiation, while gentler changes occur during periods without solar radiation. For lean LNG, the nitrogen content reduces while other components increase, as nitrogen is the lightest constituent and evaporates first and more extensively than other components. This leads to a higher fraction of methane, ethane, propane, and butane in lean LNG. Similarly, for medium LNG, nitrogen content decreases while the molar fractions of hydrocarbons increase, following the same pattern of nitrogen evaporating first. This results in increased fractions of methane, ethane, propane, butane, and pentane in medium LNG.

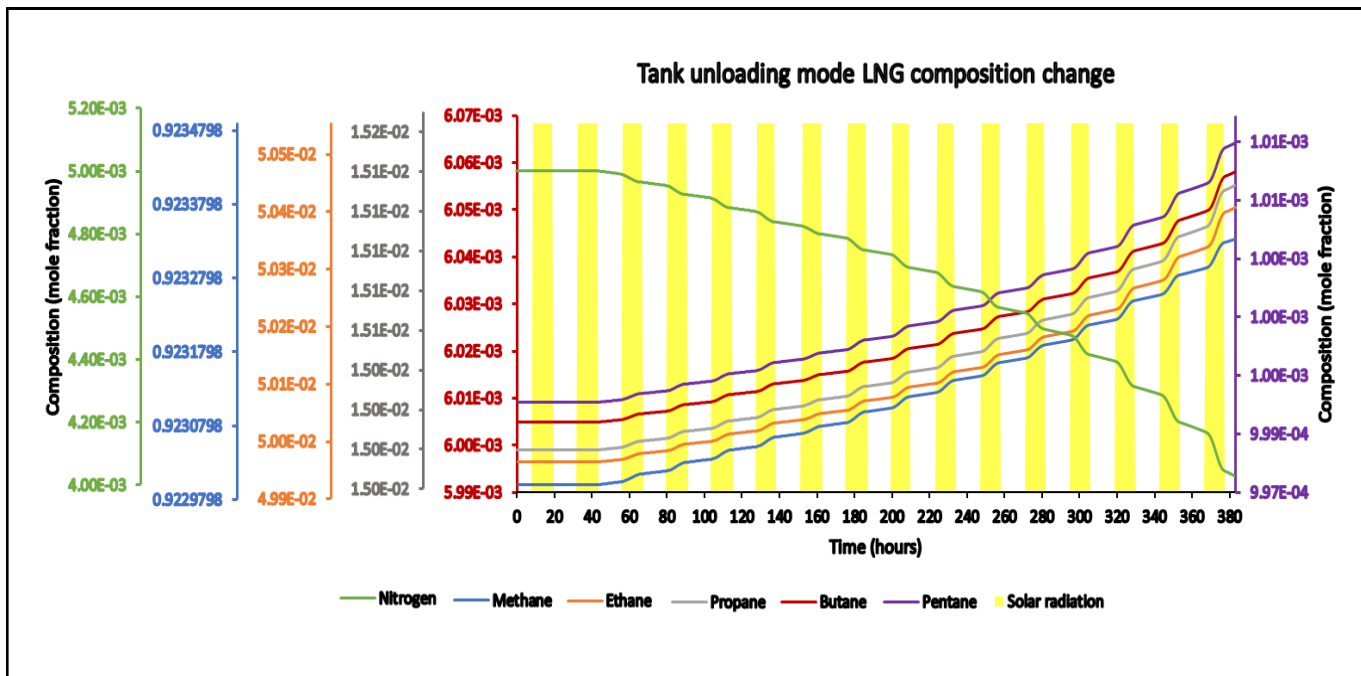


Figure 28. Medium LNG compositional change during LNG regasification.

For rich LNG, the nitrogen content also reduces, leading to increased hydrocarbon fractions, including methane, ethane, propane, butane, and pentane. These changes in each LNG component continue until the end of the regasification process, with nitrogen depleting and other components' fractions increasing.

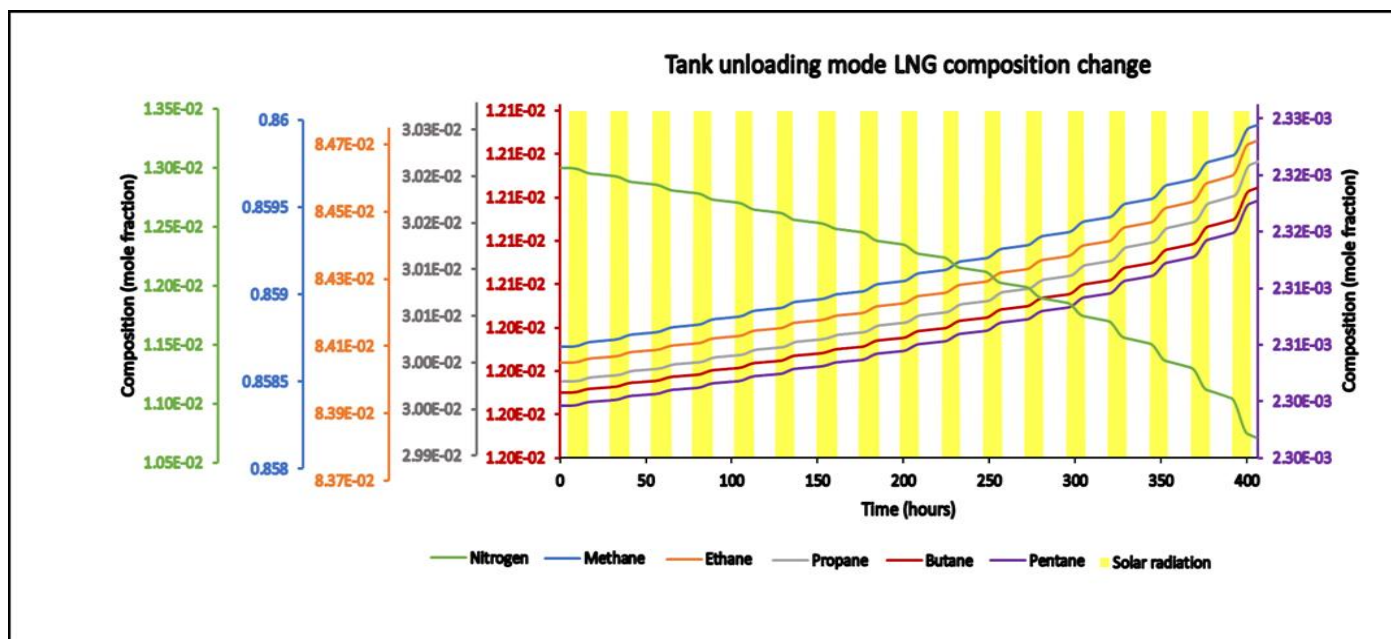


Figure 29. Rich LNG compositional change during LNG regasification.

During the first 29 hours of lean LNG regasification, methane and nitrogen BOG components change gently, while ethane, propane, and butane rise rapidly, as shown in figure 27. During this period, no BOG excess is released from the storage tank, causing BOG to accumulate inside the tank. Nitrogen, being the lightest, evaporates more initially and decreases in the evaporated BOG over time as it diminishes from lean LNG. Methane, the second lightest component, evaporates progressively more as time passes and nitrogen depletes. The heavier components ethane, propane, and butane increase rapidly during this BOG accumulation period as they are not released from the tank. Similarly, during the first 44 hours of medium LNG regasification, methane and nitrogen BOG components change gently, while ethane, propane, butane, and pentane rise rapidly, as shown in figure 28. No BOG excess is released during this period, causing BOG to accumulate inside the tank. Nitrogen evaporates more initially and decreases in evaporated BOG over time as it diminishes from medium LNG. Methane evaporates progressively more as nitrogen depletes, while the heavier components ethane, propane, butane, and pentane increase rapidly, with a sudden peak at the 39th hour due to high heat leakage after mid-day on 27th May, 2024, from intense solar radiation. For rich LNG, during the first 5 hours of regasification, methane and nitrogen BOG components change gently, while ethane, propane, butane, and pentane rise rapidly, as shown in figure 29. During this period, no BOG excess is released, causing BOG to accumulate inside the tank. Nitrogen evaporates more initially and decreases in evaporated BOG over time as it diminishes from stored rich LNG. Methane evaporates progressively more as nitrogen depletes, while the heavier components ethane, propane, butane, and pentane increase rapidly as they are not released from the tank.

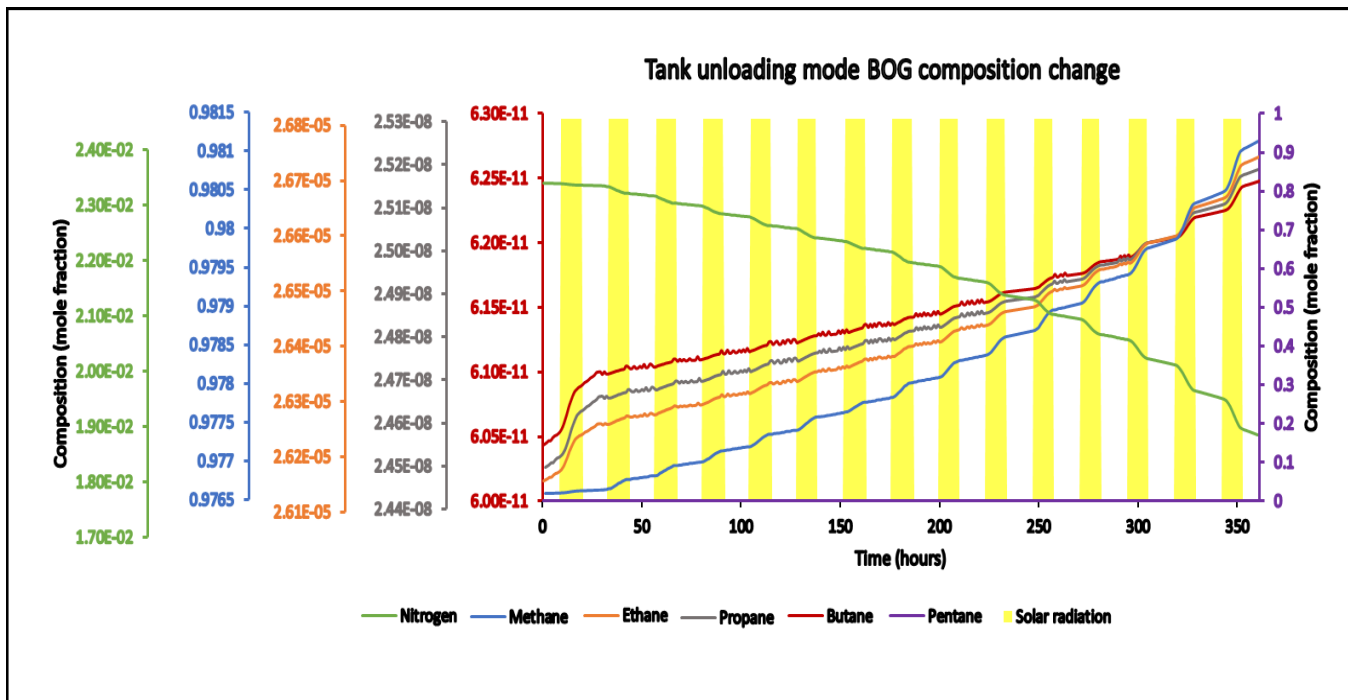


Figure 30. BOG composition changes during lean LNG regasification.

During the regasification process, methane, ethane, propane, and butane components progressively increase in hourly BOG formation while nitrogen decreases due to its depletion from LNG. The depletion of nitrogen and the increase of other BOG components are more noticeable during periods of solar radiation (daytime) and occur more gently without solar radiation. As observable in figures 30, 31, and 32, the slopes of the lighter components are higher than those of the heavier BOG components, indicating that lighter components increase more in hourly BOG formation. During periods of no solar radiation, heavier components (ethane, propane, and butane) display intermittent increases and decreases, with more sudden changes the heavier the component. This is because heavier components evaporate very low and take time to increase again with low heat ingress without solar radiation. After 300 hours of lean LNG regasification, 200 hours of medium LNG regasification, and 200 hours of rich LNG regasification, the hourly BOG components, except nitrogen, increase rapidly due to heat buildup in LNG, which progressively raises its temperature.

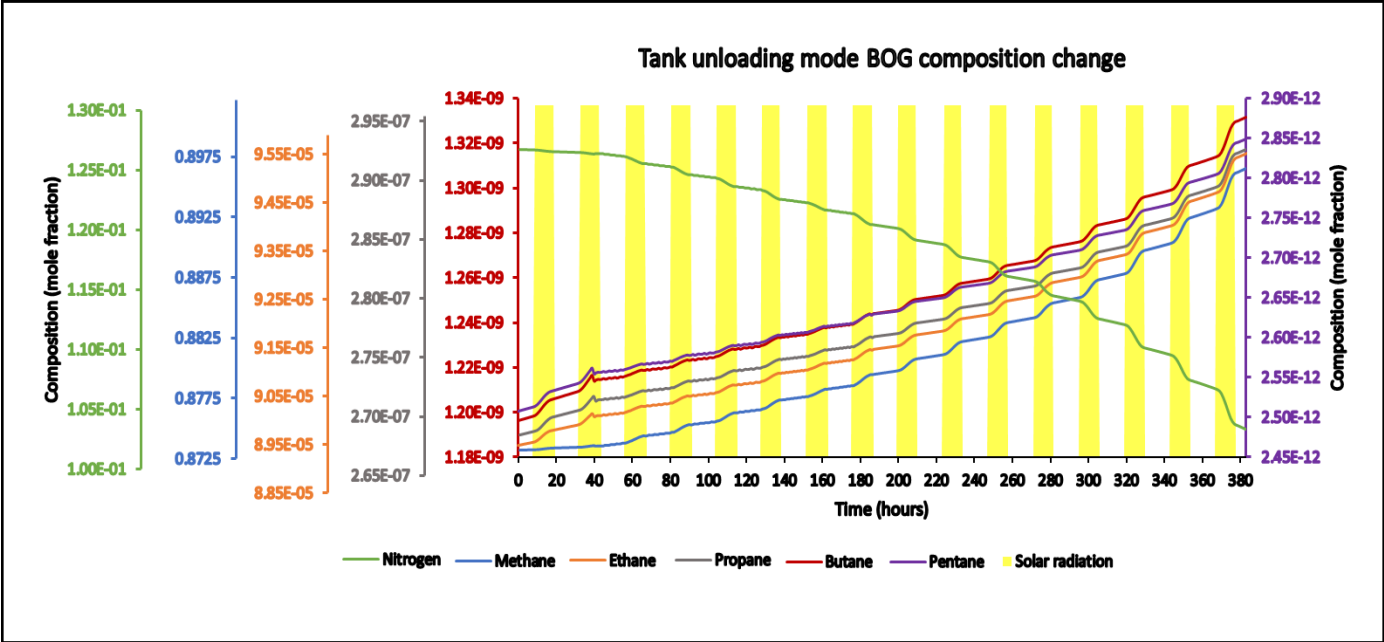


Figure 31. BOG composition changes during medium LNG regasification.

This rapid increase is more pronounced during periods of solar radiation and gentler without solar radiation but without intermittent rises and falls of heavier components. Nitrogen depletion also rises more during periods of solar radiation and gently decreases without it.

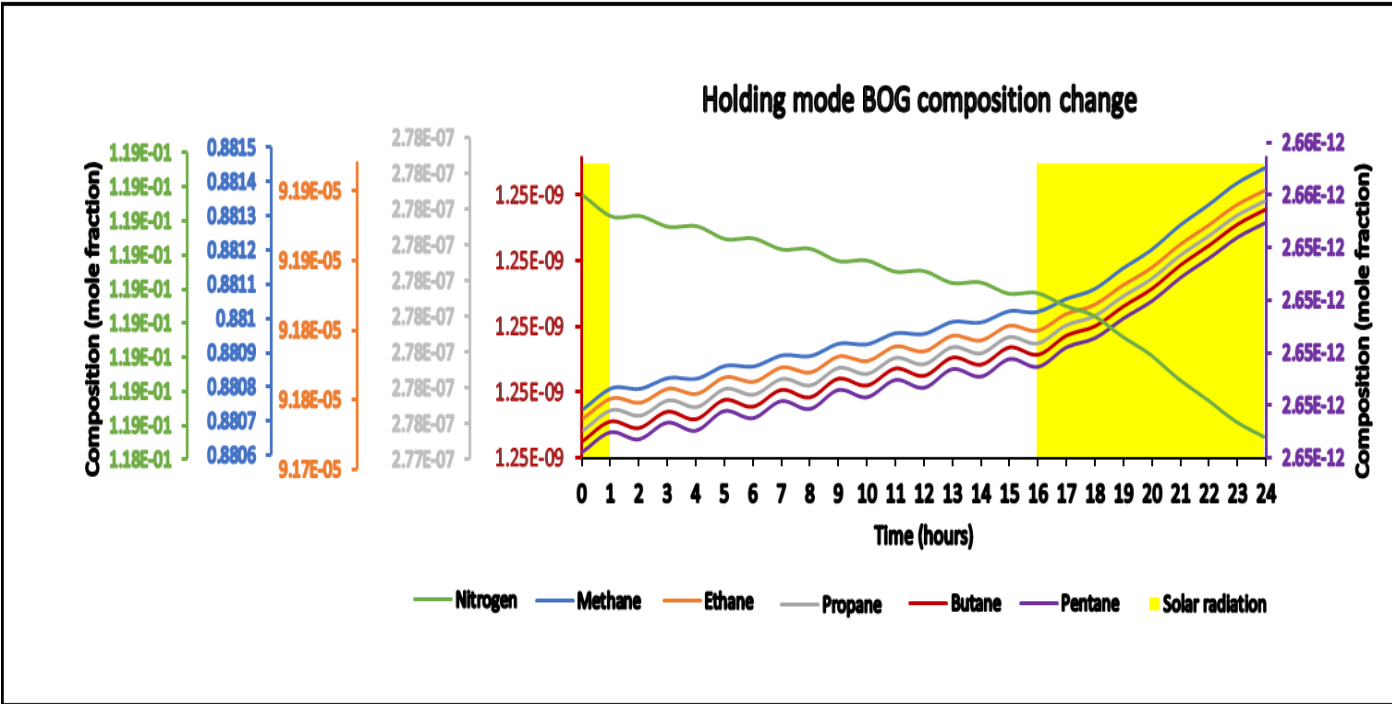


Figure 32. BOG composition changes during rich LNG regasification.

After each regasification process, the storage tank LNG and BOG compositions change to the compositions shown in table 8 before tank filling.

4.2.1.2. Ship unloading or storage tank filling mode

During ship unloading, the storage tank was simulated to initially contain lean LNG (occupying 10% of the storage tank volume) and BOG (occupying 90% of the storage tank volume) in equilibrium with the following composition. This simulation setup was similarly applied to medium LNG and rich LNG, where each type of LNG constituted 10% of the storage tank volume and BOG made up 90%, with their compositions in equilibrium accordingly.

Table 8. Initial LNG and BOG composition inside storage tank during ship unloading.

Components	Initial composition (mole fraction)					
	Lean		Medium		Rich	
	LNG	BOG	LNG	BOG	LNG	BOG
Methane	0.98607	0.98112	0.9234	0.89654	0.85998	0.7205
Ethane	1.19E-02	2.67E-05	5.04E-02	9.54E-05	0.0847	0.00011
Propane	1.01E-03	2.52E-08	1.51E-02	2.92E-07	0.0302	3.30E-07
n-Butane	2.02E-04	6.25E-11	6.05E-03	1.33E-09	0.0121	1.30E-09
n-Pentane	0	0	0.00101	2.90E-12	0.00232	2.70E-12
Nitrogen	8.05E-04	1.89E-02	4.03E-03	1.03E-01	0.0107	0.27939

As observable from figures 31, 32, and 33, the loading of LNG into the storage tank began with some leftover LNG of the composition shown in table 8. This leftover LNG was poor in nitrogen but rich in hydrocarbons because a significant portion of nitrogen had evaporated compared to other hydrocarbons during the regasification process. As the ship was unloaded towards the receiving terminal storage tank, the LNG in the storage tank began to be enriched in nitrogen since the incoming LNG from the ship had a larger mole fraction of nitrogen compared to the leftover LNG, as shown in table 9. Consequently, during the first few hours of tank filling three hours for lean and medium LNG, and two hours for rich LNG the molar fractions of hydrocarbons decreased rapidly as the LNG in the tank became enriched with nitrogen. This does not mean that hydrocarbons were not being loaded; rather, the rising mole fraction of nitrogen inside the tank caused a decrease in the molar fraction of hydrocarbons, and the incoming LNG's hydrocarbon

mole fraction was lower than that of the leftover hydrocarbons in the tank, as noticeable in table 9.

Table 9. Ship unloaded lean LNG composition.

Components	Loaded LNG (mole fraction)		
	lean	medium	rich
Methane	0.986	0.923	0.8587
Ethane	0.0118	0.05	0.084
Propane	0.001	0.015	0.03
n-Butane	0.0002	0.006	0.012
n-Pentane	0	0.001	0.0023
Nitrogen	0.001	0.005	0.013

From the third to the twelfth filling hours during the solar radiation period, the nitrogen enrichment inside the storage tank gently decreases as the nitrogen mole fraction inside the tank approaches that of the incoming unloaded LNG from the ship. This occurs for both lean and medium LNG, with the hydrocarbon mole fractions also aligning closer to the incoming LNG hydrocarbons' composition. Similarly, after the second to the eleventh filling hours during the solar radiation period, the nitrogen enrichment inside the storage tank for rich LNG gently decreases, with the nitrogen mole fraction inside the tank getting closer to that of the incoming unloaded rich LNG. Consequently, the hydrocarbon mole fractions also get closer to the composition of the incoming rich LNG hydrocarbons.

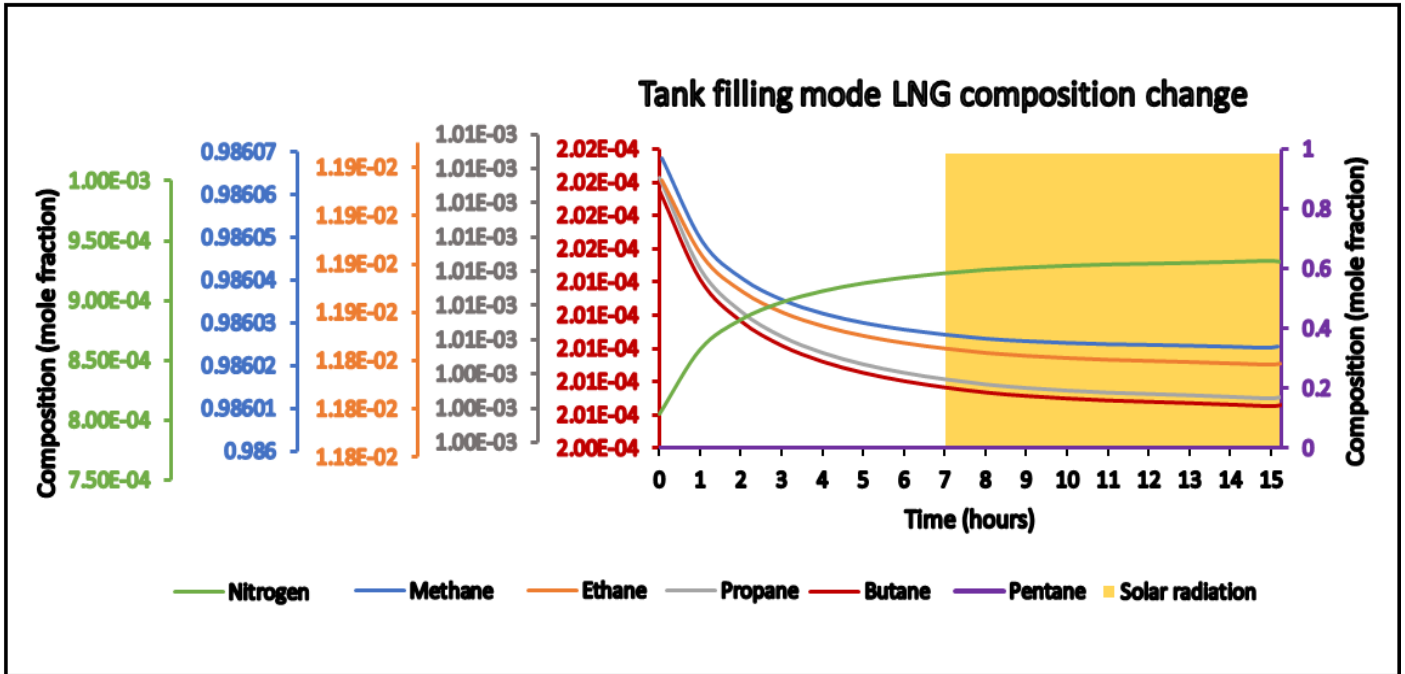


Figure 33. Lean LNG compositional change during storage tank loading.

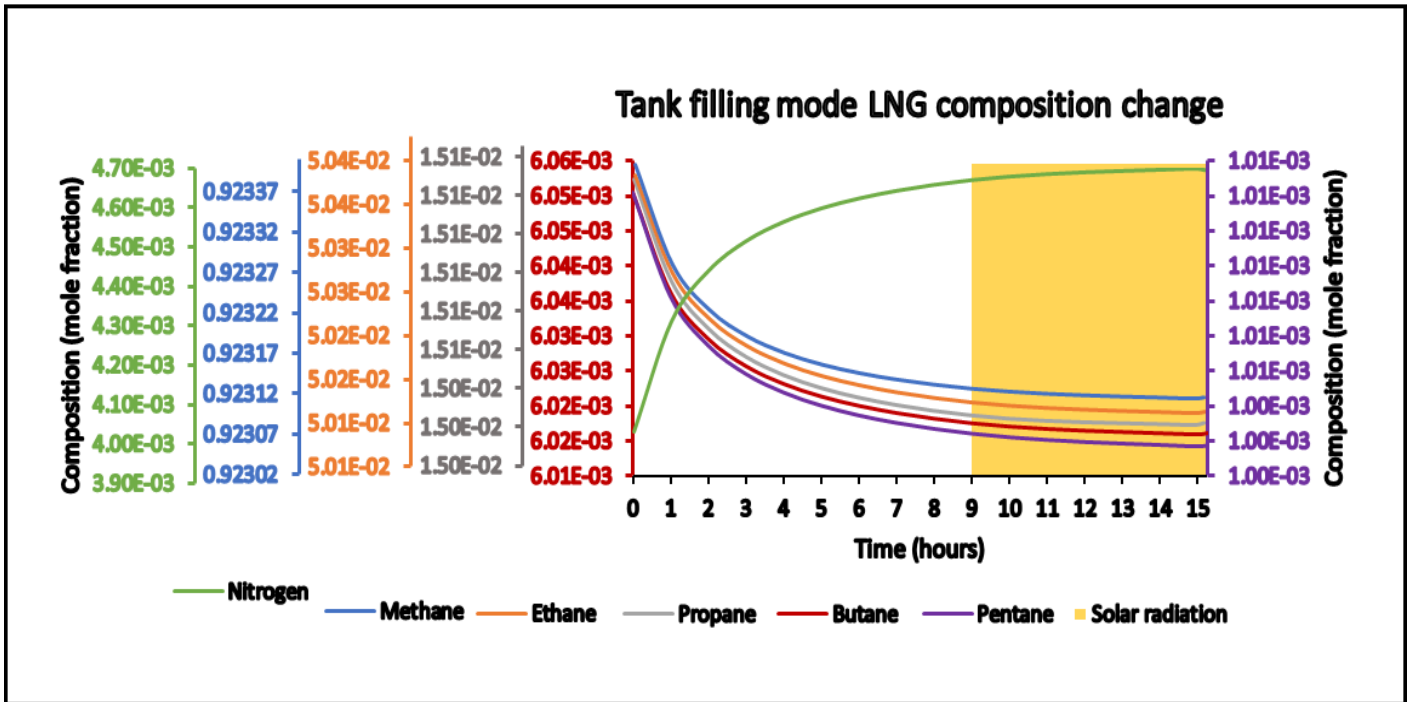


Figure 34. Medium LNG compositional change during storage tank loading.

After twelve hours of LNG filling during periods of solar radiation, the LNG composition inside the storage tank barely changes as it approaches the composition of the incoming LNG from the

ship. This applies to lean LNG, medium LNG, and rich LNG. As observable in figures 33, 34, and 35, once the LNG composition inside the tank gets closer to the incoming LNG composition, it remains relatively stable for the remainder of the tank filling process during the presence of solar radiation.

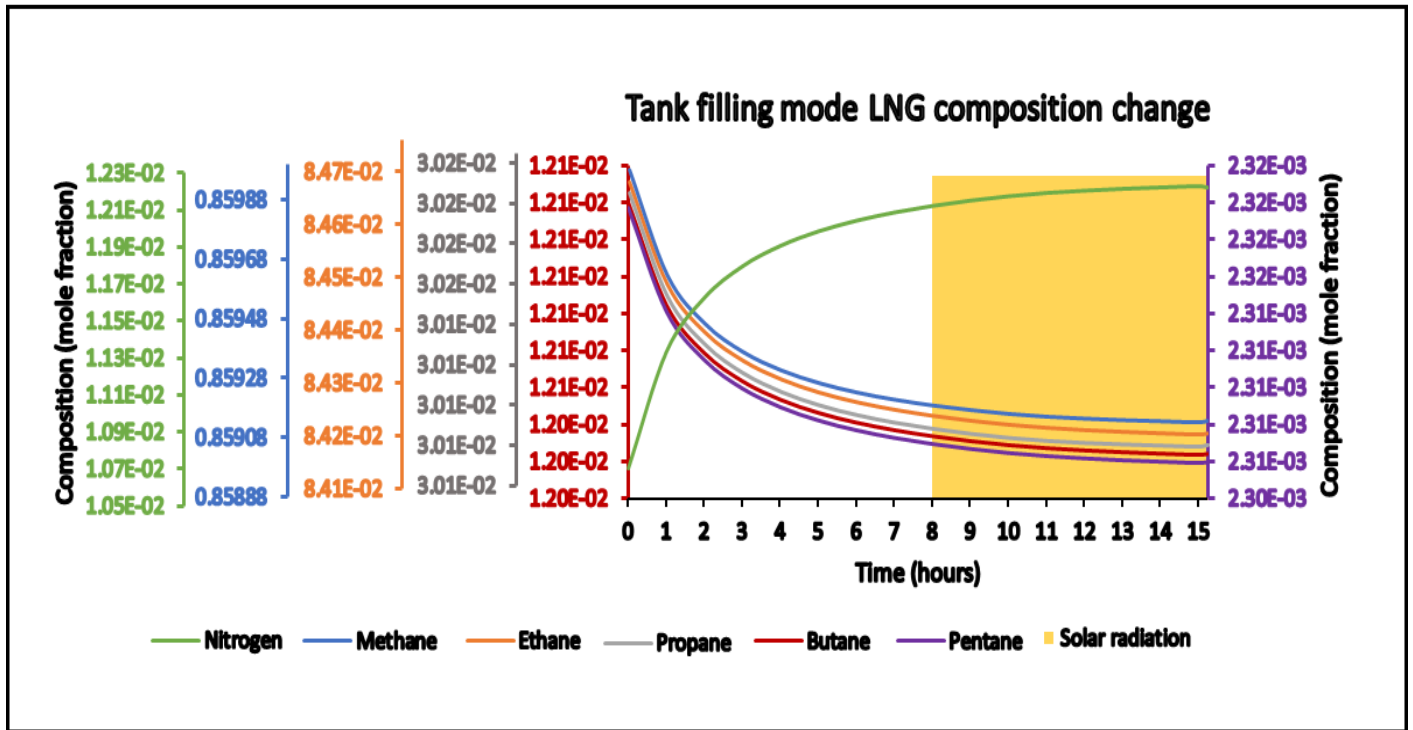


Figure 35. Rich LNG compositional change during storage tank loading.

During ship unloading, the volume previously occupied by BOG inside the storage tank progressively gets replaced by the incoming LNG (lean, medium, or rich), causing an increase in BOG as part of the unloaded LNG turns to vapor and a small portion of the existing LNG also vaporizes. This increase in BOG is due to heat ingress into the pumps, pipelines, and storage tank. As a result, the storage tank releases BOG to avoid overpressure. Part of the released BOG is returned to replace the incoming LNG from the ship to maintain pressure and temperature, while another part is recovered to be converted into CNG. This process applies to lean, medium, and rich LNG during their respective ship unloading operations.

Hourly, the BOG composition inside the tank changes due to the mixture of incoming BOG with unloaded LNG (lean, medium, or rich) from pumps and pipes, leftover BOG inside the storage, and BOG formation during loading. As noticeable in figures 36, 37, and 38, the BOG inside the

tank gets enriched in nitrogen after the end of regasification, as it was previously depleted in both LNG and BOG. This enrichment is accompanied by a rapid decrease in hydrocarbons in BOG, as nitrogen, being the lightest component, evaporates more. This process occurs similarly for lean, medium, and rich LNG, with nitrogen enrichment and hydrocarbon depletion observable in each case.

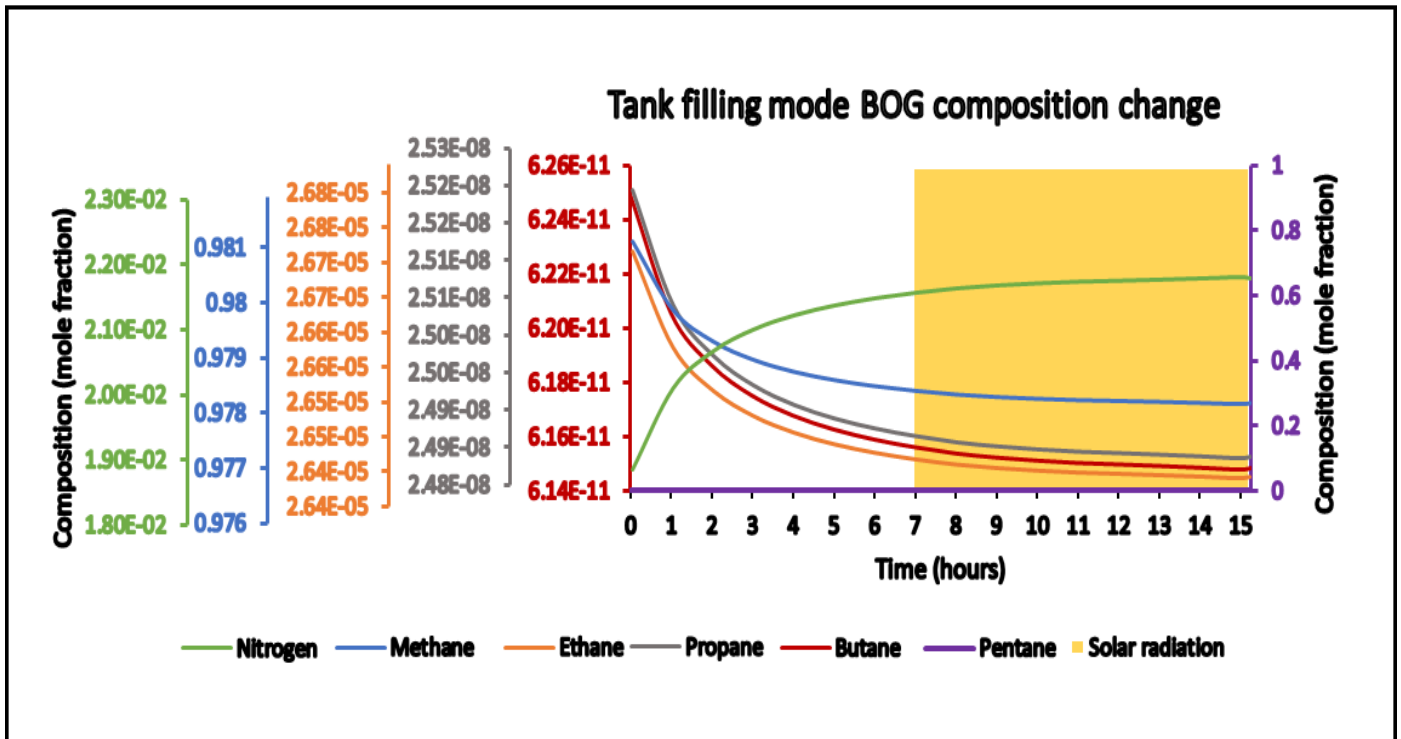


Figure 36. BOG composition changes during lean LNG storage tank loading.

From the third to the twelfth ship unloading hours whereby solar radiation started from the seventh hour for lean LNG filling, the ninth hour for medium LNG filling, and the eighth hour for rich LNG filling the BOG composition changes gently as the incoming and stored LNG compositions align. Consequently, nitrogen gently increases in BOG while hydrocarbon compositions decrease slowly. From the twelfth hour to the last filling period, the BOG composition inside the storage tank barely changes because the incoming and filled LNG compositions are similar, resulting in BOG compositions getting closer and the BOG volume decreasing towards 5% of the tank volume, as noticeable in figures 34, 35, and 36.

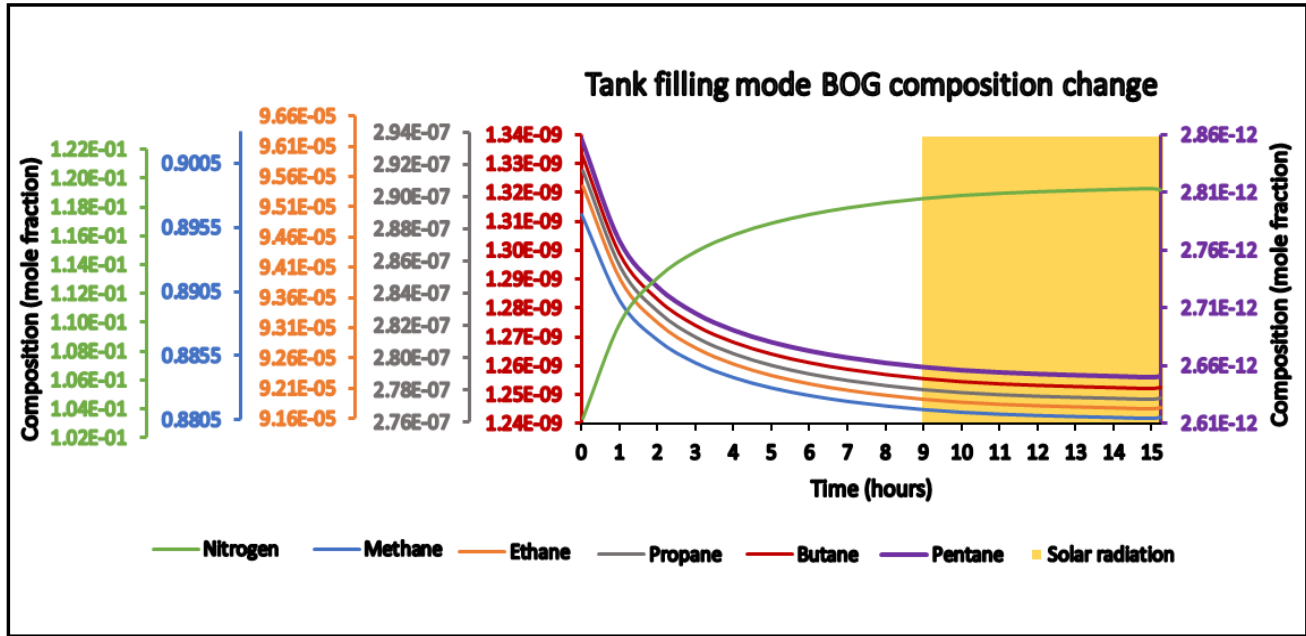


Figure 37. BOG composition changes during medium LNG storage tank loading.

Initially, from ship unloading to the third hour for lean and medium LNG, and to the second hour for rich LNG, the BOG composition changes rapidly with a drop in hydrocarbons and an increase in nitrogen content. As the process continues, the BOG composition stabilizes, with methane molar fraction dropping slightly compared to other hydrocarbons, as it is the second lightest component after nitrogen and progressively evaporates more than the remaining hydrocarbons.

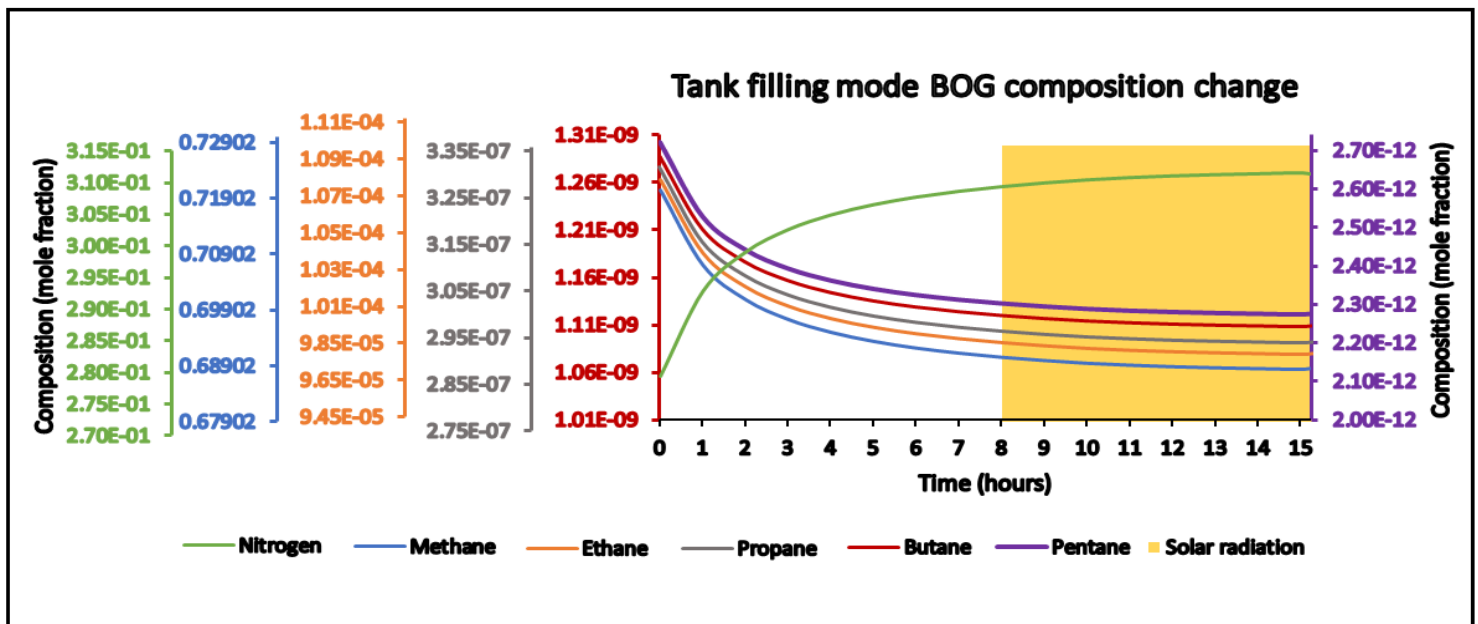


Figure 38. BOG composition changes during storage tank loading with rich LNG.

At the end of filling the storage tank with lean, medium, or rich LNG, the tank was filled to approximately 95% with LNG and 5% with BOG, achieving equilibrium with the compositions listed in table 10.

Table 10. Final LNG and BOG composition inside storage tank after ship unloading.

Components	Final composition (mole fraction)					
	Lean		Medium		Rich	
	LNG	BOG	LNG	BOG	LNG	BOG
Methane	0.98602	0.97818	0.9234	0.89654	0.85998	0.7205
Ethane	1.18E-02	2.64E-05	5.04E-02	9.54E-05	0.0847	0.00011
Propane	1.00E-03	2.48E-08	1.51E-02	2.92E-07	0.0302	3.30E-07
n-Butane	2.01E-04	6.15E-11	6.05E-03	1.33E-09	0.0121	1.30E-09
n-Pentane	0	0	0.00101	2.90E-12	0.00232	2.70E-12
Nitrogen	9.33E-04	2.18E-02	4.03E-03	1.03E-01	0.0107	0.27939

The lean LNG filling took 15.2497 hours, the medium LNG filling took 15.2496 hours, and the rich LNG filling took 15.2492 hours for the storage tank to reach 95% of its capacity.

4.2.1.3. LNG storage tank holding mode

After the storage tank was filled up to 95% with LNG and BOG reduced to 5% of the storage tank volume, achieving the specified compositions listed in table 10, each type of LNG lean, medium, and rich was simulated to be stored in the tank for twenty-four hours. This simulation involved maintaining the lean, medium, and rich LNG storage tanks with their respective compositions for a full day.

As observable in figures 39, 40, and 41, during the initial storage tank holding modes for lean, medium, and rich LNG, the LNG composition inside the tanks changed depending on the presence of solar radiation.

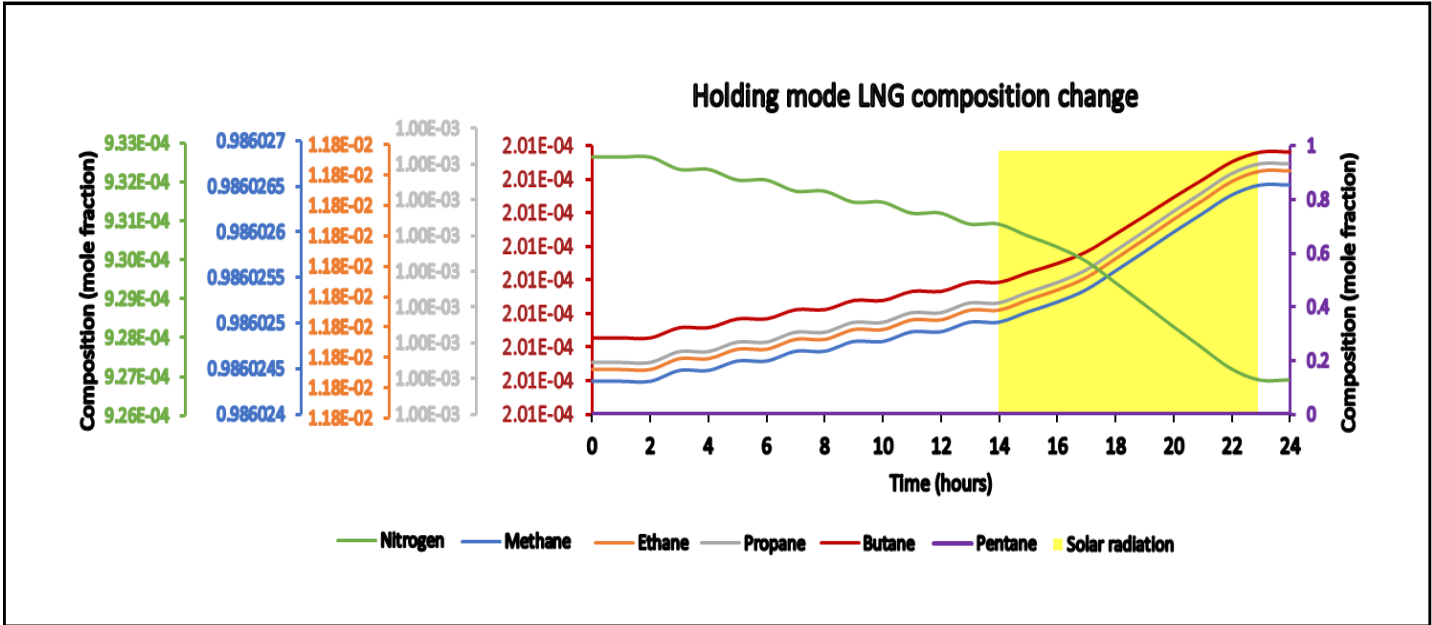


Figure 39. Lean LNG compositional change during storage tank holding mode.

For lean LNG, in the first two hours with no solar radiation, the composition did not change due to insufficient heat ingress. From then until the fourteenth hour, a sequence of compositional changes followed by nearly no changes occurred due to periodic BOG excess releases caused by nitrogen evaporation.

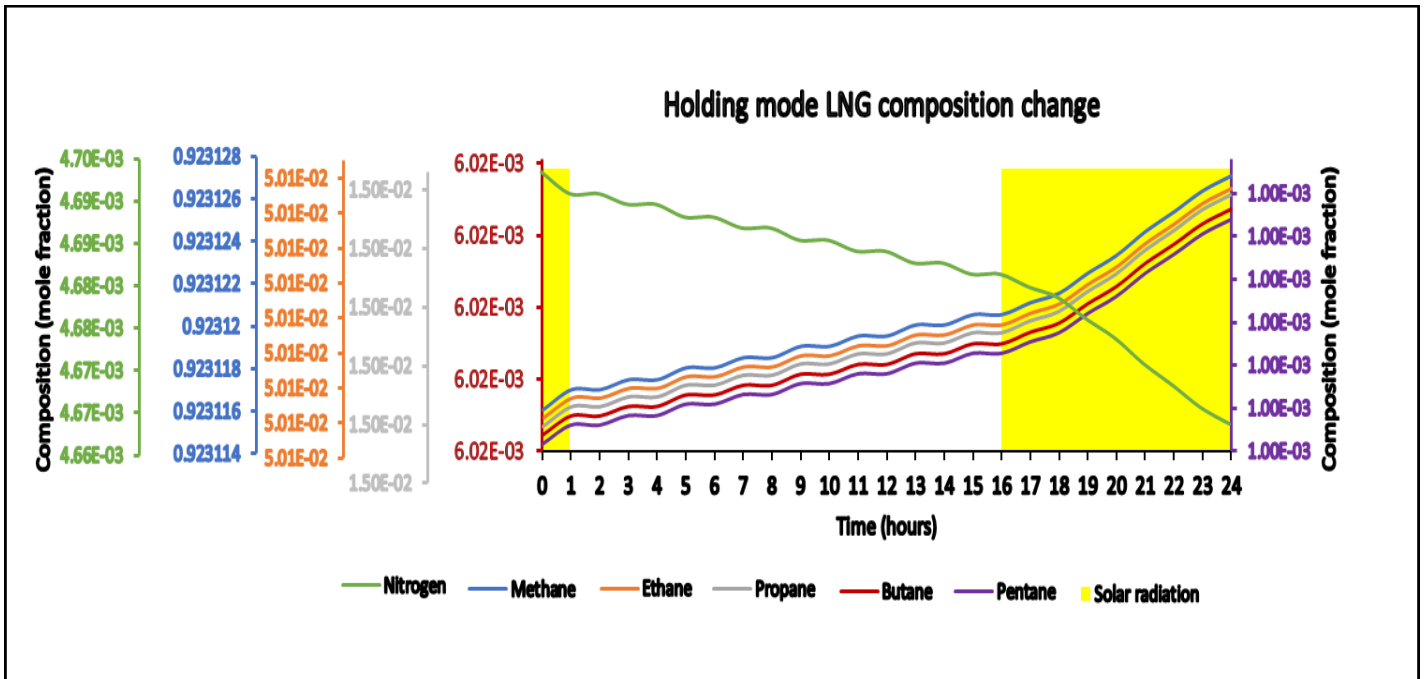


Figure 40. Medium LNG compositional change during storage tank holding mode.

For medium LNG, with solar radiation present in the first hour, the composition changed rapidly due to sufficient heat ingress, followed by a similar sequence until the sixteenth hour.

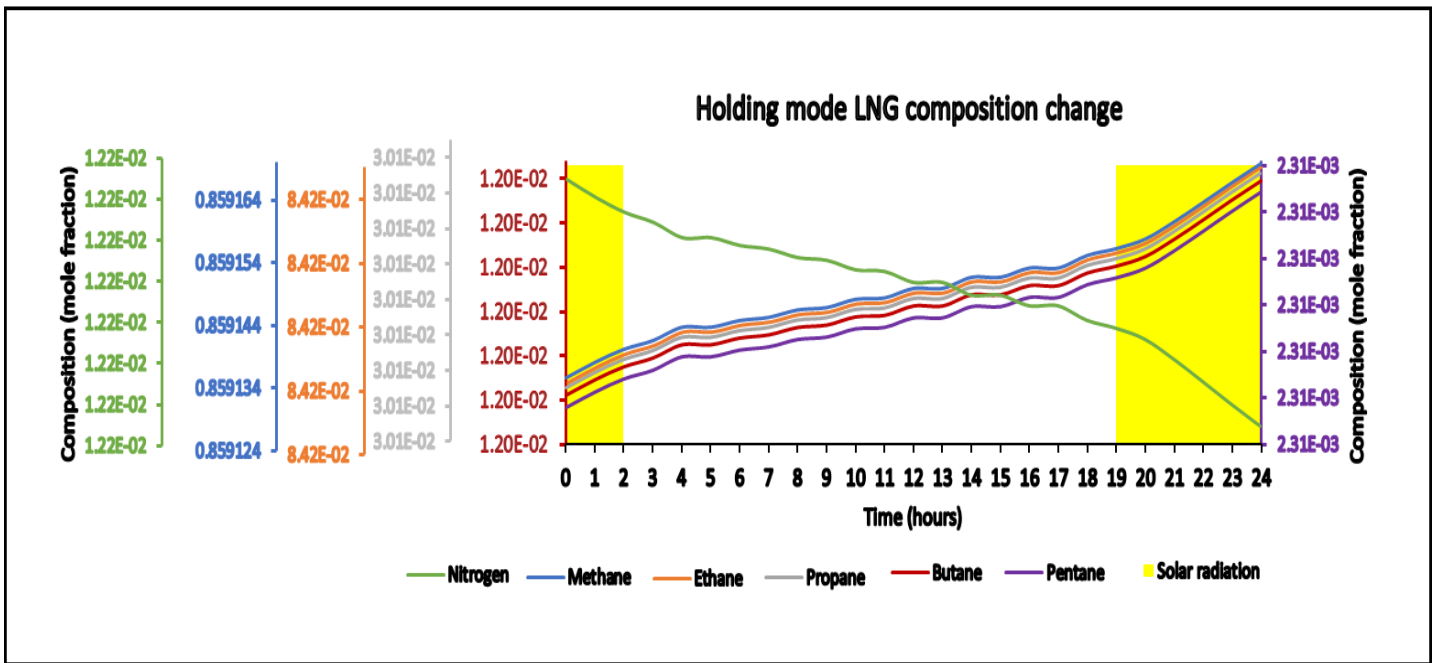


Figure 41. Rich LNG compositional change during storage tank holding mode.

For rich LNG, the composition changed rapidly in the first two hours with solar radiation, continuing until the fourth hour. From the sixth to the twelfth hour, hydrocarbons rose and nitrogen depleted due to heat ingress, followed by a similar sequence until the nineteenth hour with no solar radiation. In all cases, the release of BOG excess led to a drop in nitrogen and an increase in hydrocarbon molar fractions, while periods with no BOG excess formation resulted in nearly constant compositions.

From the fourteenth to the twenty-third hours of the lean LNG holding mode, the composition rapidly changes due to solar radiation, which increases heat ingress and forms BOG excess hourly. The compositional changes rise and fall gently, then steeply at the peak solar radiation hour (18th hour), and become gentle again as solar radiation decreases, leading to nitrogen depletion and a rise in hydrocarbons. From the end of the twenty-third hour onward, with no solar radiation, the LNG composition barely changes. Similarly, for medium LNG from the sixteenth to the twenty-fourth hours, the composition rapidly changes with solar radiation causing BOG excess, following a similar pattern, peaking at the 21st hour. Nitrogen depletes and hydrocarbons rise gently, steeply,

and gently again. For rich LNG from the nineteenth to the twenty-fourth hours, the composition rapidly changes with solar radiation, following a similar pattern, peaking at the 21st hour. The nitrogen depletes, and hydrocarbons rise gently, steeply, and gently again.

As observable in figures 42, 43, and 44, the BOG composition inside the storage tank changes significantly based on the presence of solar radiation during the holding mode for lean, medium, and rich LNG. In the first two hours of lean LNG storage without solar radiation, the BOG composition of methane and nitrogen did not change significantly due to insufficient heat ingress, while other hydrocarbons rose rapidly. From the third to the fourteenth hour, periods without solar radiation showed a sequence of BOG composition changes, with nitrogen and methane adjusting gently, while heavier hydrocarbons rose and fell intermittently, reflecting the heat ingress dynamics.

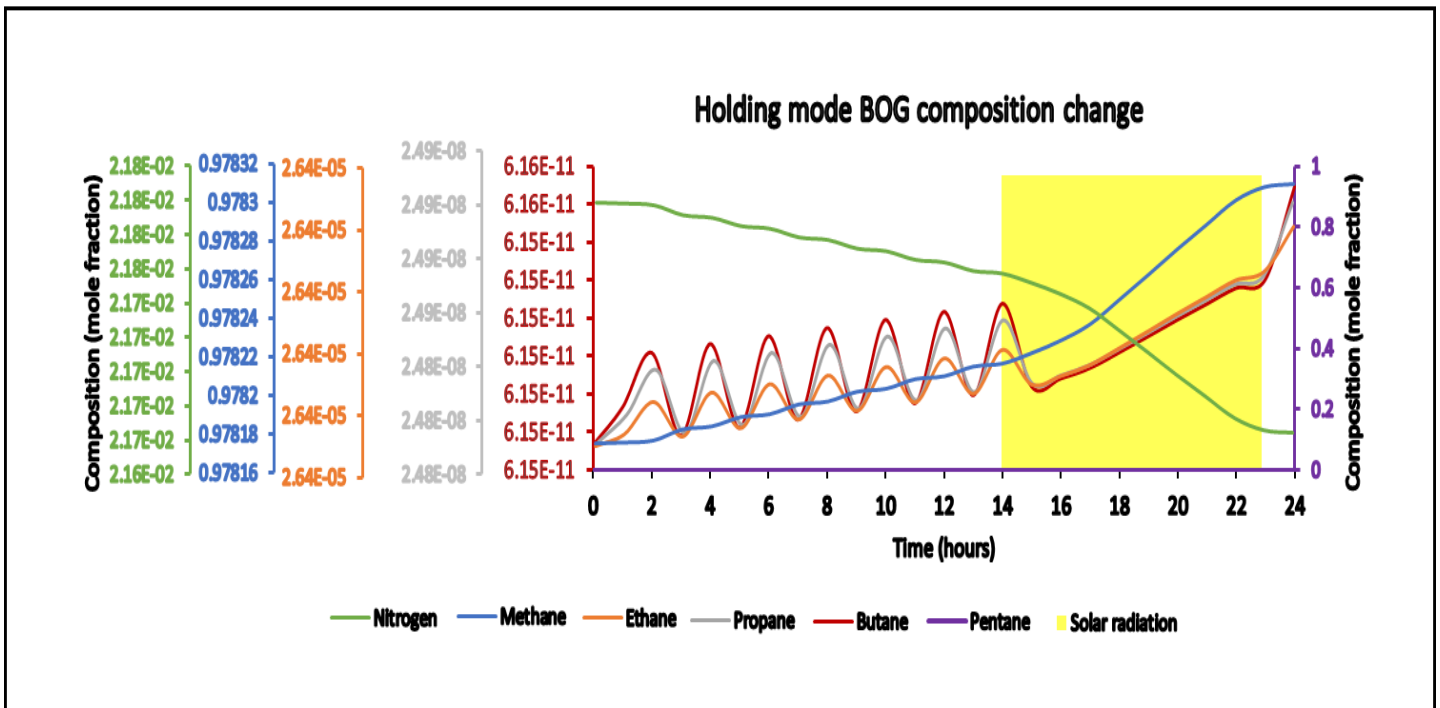


Figure 42. BOG composition changes during lean LNG storage tank holding mode.

For medium LNG, the first hour with solar radiation saw significant BOG composition changes due to BOG excess formation and release, followed by a sequence of gentle changes.

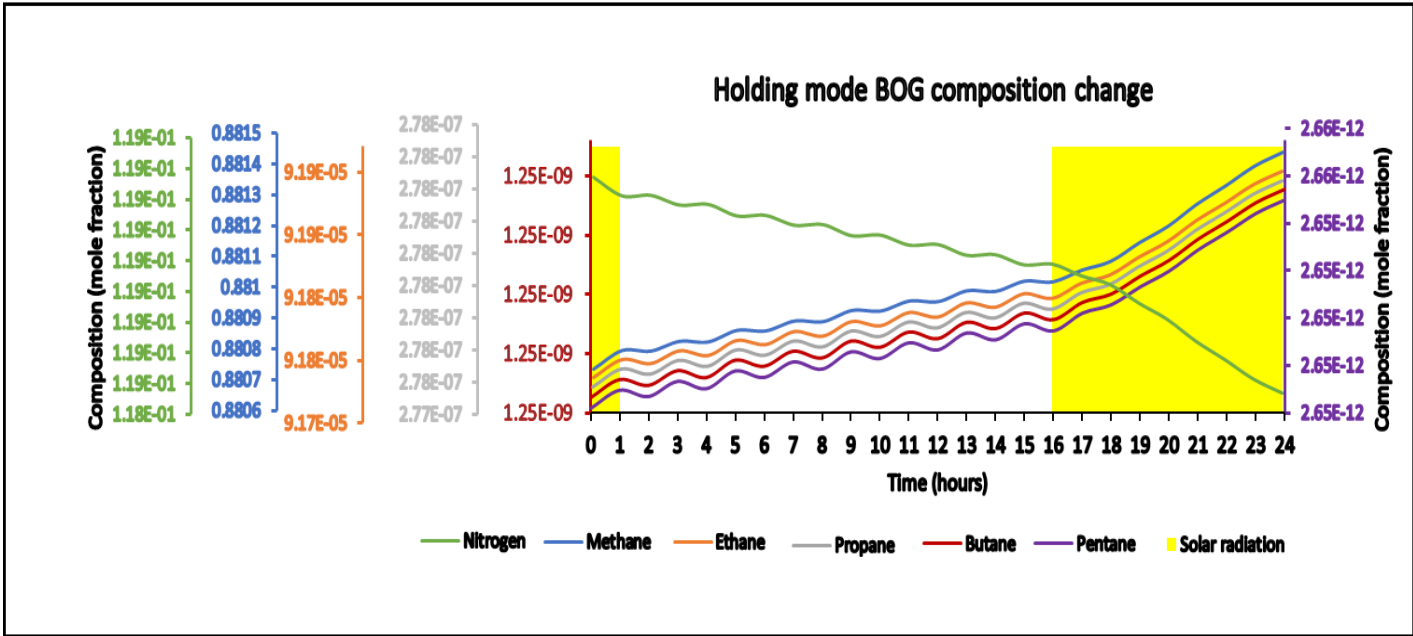


Figure 43. BOG composition changes during medium LNG storage tank holding mode.

Similar patterns were observed in rich LNG holding from the first four hours with solar radiation, continuing until the nineteenth hour. Throughout these periods, nitrogen gently decreased while hydrocarbons increased due to their respective evaporation characteristics. The release of BOG excess led to nitrogen drops and hydrocarbon increases, reflecting the dynamic balance of heat ingress and evaporation rates.

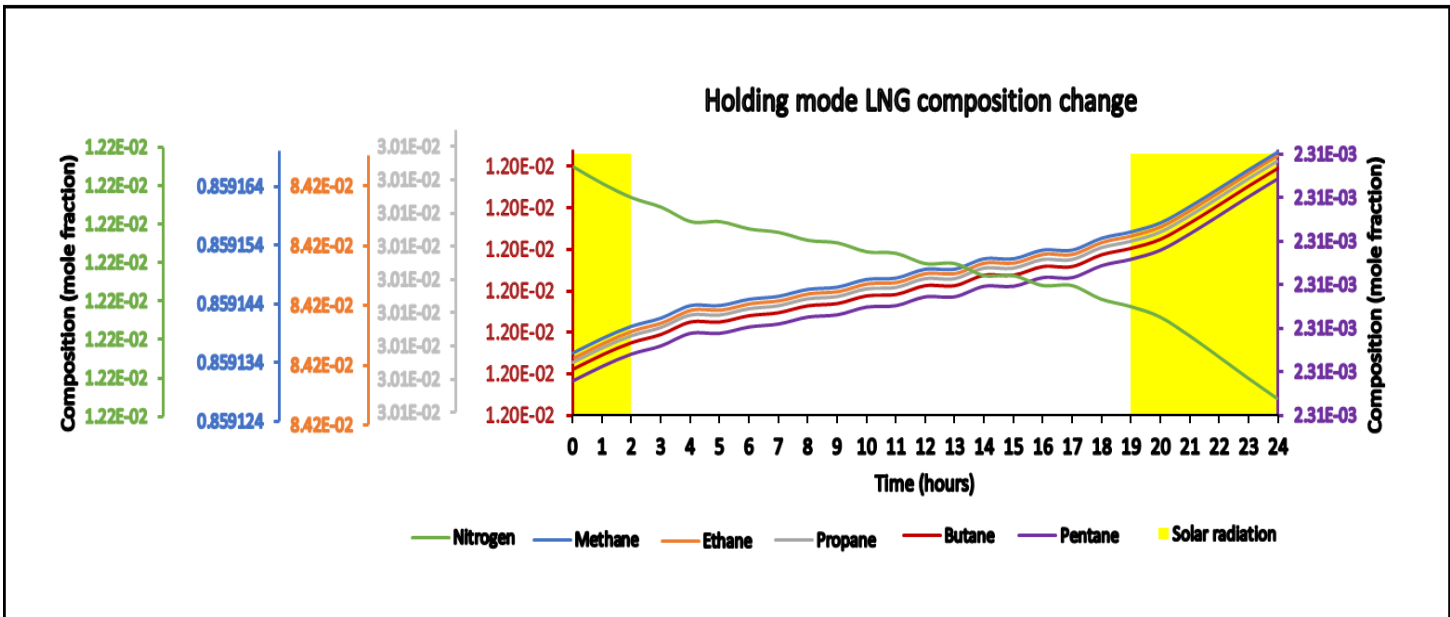


Figure 44. Rich LNG compositional change during storage tank holding mode.

From the fourteenth to the twenty-third hours of lean LNG holding mode inside the storage tank, the BOG composition rapidly changes with the presence of solar radiation due to increased heat ingress. Methane and nitrogen composition gradually change with solar radiation, peaking at the 18th hour, with nitrogen depleting and methane rising. Heavy hydrocarbons initially drop at the 15th hour before increasing until the twenty-second hour, then decreasing again as solar radiation fades from the 22nd to the twenty-third hour. Post-solar radiation, methane and nitrogen composition in BOG barely change, while heavy hydrocarbons rise. At the end of the day, LNG volume slightly decreases, BOG volume slightly increases, with LNG occupying approximately 95% and BOG 5% of the storage tank volume, as shown in table 11. Similarly, from the sixteenth to the twenty-fourth hours of medium LNG holding mode, BOG composition changes rapidly with solar radiation, peaking at the 21st hour. Nitrogen depletes and methane rises, with heavy hydrocarbons following a similar pattern. From the 23rd to the twenty-fourth hour, hydrocarbon compositions decrease with diminishing solar radiation. At the end of the day, LNG volume slightly decreases, BOG volume slightly increases, maintaining the same proportions. For rich LNG, from the nineteenth to the twenty-fourth hours, BOG composition changes rapidly with solar radiation, peaking at the 21st hour. Nitrogen depletes and methane rises, with heavy hydrocarbons following a similar pattern. Post 21st hour, hydrocarbon compositions slightly decrease. At the end of the day, LNG volume slightly decreases, BOG volume slightly increases, maintaining the same proportions as shown in table 11.

Table 11. Final LNG and BOG composition inside storage tank at the end of LNG holding mode.

Components	Final composition (mole fraction)					
	Lean		Medium		Rich	
	LNG	BOG	LNG	BOG	LNG	BOG
Methane	0.98603	0.97831	0.92313	0.88144	0.85917	0.68978
Ethane	1.18E-02	2.64E-05	5.01E-02	9.19E-05	0.08424	9.80E-05
Propane	1.00E-03	2.49E-08	1.50E-02	2.78E-07	0.03008	3.00E-07
n-Butane	2.01E-04	6.16E-11	6.02E-03	1.25E-09	0.01203	1.10E-09
n-Pentane	0	0	0.001	2.70E-12	0.00231	2.30E-12
Nitrogen	9.27E-04	2.17E-02	4.66E-03	1.18E-01	0.01216	0.31013

Therefore, heat ingress quantity largely most during the presence of solar radiation affects LNG and BOG compositional changes with independent changes as heavier a component is.

Therefore, the quantity of heat ingress, especially during the presence of solar radiation, significantly affects the compositional changes of LNG and BOG, with these changes varying independently based on the weight of each component. This effect is noticeable for lean, medium, and rich LNG, where the heavier components undergo distinct changes in composition. The lighter components reduced in LNG while increased in BOG. Nitrogen as the lightest rose in BOG to more than 30% from rich LNG which nearly coincided with Huang et al. (2022) findings of reaching up to more than 40%.

4.2.2. Molecular weight

The molecular weight of each LNG and BOG inside the receiving terminal storage tank at each mode has been studied for its change overtime.

4.2.2.1. LNG regasification

During LNG regasification, molecular weight changes of LNG and BOG inside the storage tank has been studied for each LNG namely lean, medium, and rich LNG.

At the start of regasification, lean, medium, and rich LNG each occupied 95% of the storage tank's volume, while BOG occupied the remaining 5%. The regasification of the 200,000 m³ tank lasted 361 hours for lean LNG, 383 hours for medium LNG, and 406 hours for rich LNG, with an LNG regasification capacity of 200,000 kg reconverted into gas hourly. During the regasification process, heat leakage inside the storage tank led to the evaporation of part of the LNG, affecting the natural composition and molecular weight of the initial LNG. The changes in composition and molecular weight resulted from the continuous evaporation and heat ingress during the regasification process.

The molecular weight of lean LNG decreases as some components turn into vapor due to heat leakage inside the storage tank, while the molar volume increases despite the depletion of lighter components. This molecular expansion from heat accumulation raises the lean LNG temperature from -160°C to -159.890°C. As lighter components evaporate, the remaining LNG swells to compensate for the temperature rise, as shown in table 12. For medium LNG, the molecular weight increases because lighter components vaporize, leaving heavier ones in the LNG. Heat accumulation also raises the medium LNG temperature from -160.7°C to -160.279°C, causing the remaining LNG to swell, as seen in table 12. Similarly, the molecular weight of rich LNG decreases with components turning to vapor due to heat leakage, and the molar volume increases despite the

depletion of lighter components. This raises the rich LNG temperature from -163.1°C to -162.280°C, with the remaining LNG swelling to compensate, as detailed in table 12.

Table 12. Initial and final molecular weight and volume of LNG during regasification.

	Lean LNG		Medium LNG		Rich LNG	
	Initial	Final	Initial	Final	Initial	Final
Molecular Weight (kg/ kgmole)	16.2569	16.2565	17.5335	17.5346	18.8524	18.846
Molar Volume (m ³ / kgmole)	0.03819	0.03821	0.03882	0.03888	0.0393	0.0394

The molecular weight of BOG inside the storage tank decreases gently during the initial hours of regasification for lean, medium, and rich LNG due to the evaporation of lighter components without the release of BOG excess. For lean LNG, this gentle decrease occurs in the first 29 hours, for medium LNG in the first 44 hours, and for rich LNG in the first 5 hours. As regasification continues, the depletion magnifies during periods of significant BOG excess release, especially during daytime with solar radiation, and moderately decreases during periods without solar radiation, as shown in figure 45. The evaporation of lighter components continually reduces the BOG molecular weight, and the release of BOG excess from the tank further decreases it, as lighter components enrich the BOG composition.

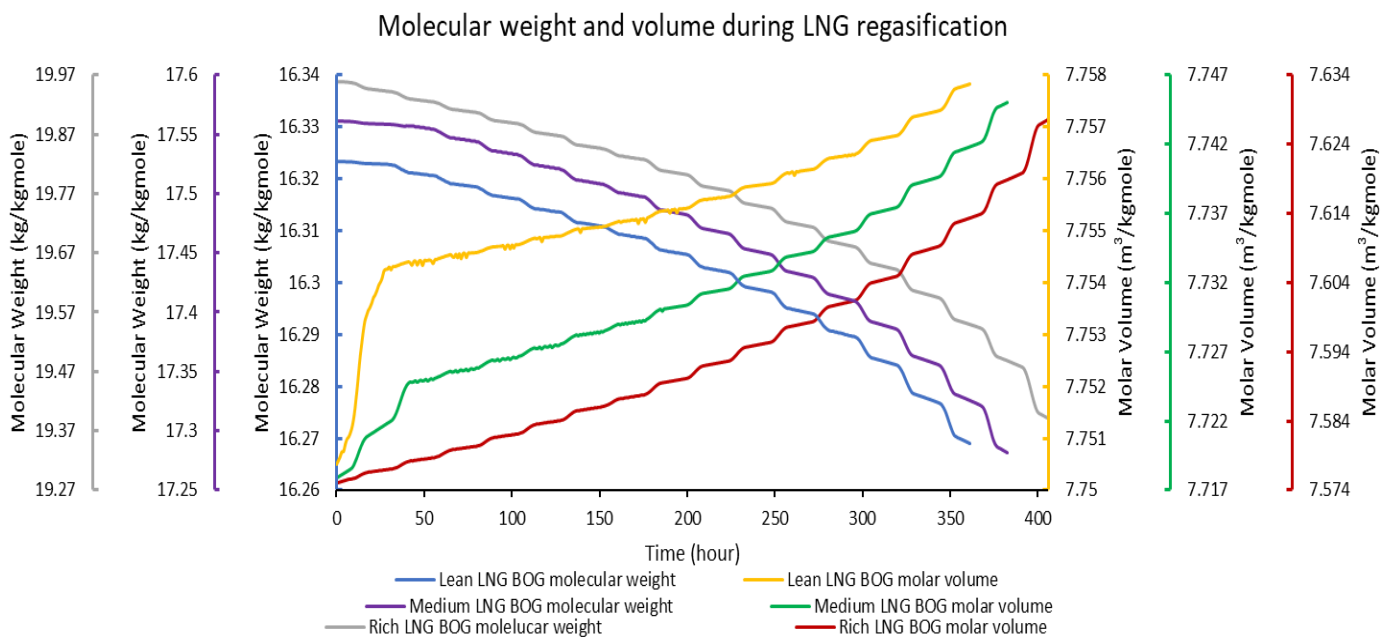


Figure 45. Molecular weight and volume changes during lean LNG regasification.

During the regasification process, the molar volume of BOG inside the storage tank changes significantly based on the type of LNG and the presence of solar radiation. For lean LNG, the molar volume rose rapidly in the first 29 hours due to the rapid increase in LNG temperature and the lack of BOG excess release. The BOG components expanded to compensate for the temperature rise, causing the molar volume to increase. Until the 300th hour, the molar volume rose gently with occasional small drops whenever the temperature inside the tank decreased due to the release of BOG excess during low heat ingress times, mostly without solar radiation. The molar volume continued to rise with larger increases during solar radiation presence and moderate increases without solar radiation until the end of regasification. Similarly, for medium LNG, the molar volume rose rapidly in the first 44 hours and continued to rise gently until the 189th hour, with similar patterns of temperature-driven expansion and BOG excess release. For rich LNG, the molar volume rose gently in the first 5 hours and continued to rise with magnified increases during solar radiation and high heat leakage until the end of regasification. In all cases, the molar volume changes were largely affected by LNG temperature changes, with rises in temperature causing BOG component expansion and vice versa.

4.2.2.2. Ships unloading

During ships unloading, molecular weight and volume changes of LNG and BOG inside the storage tank has been studied for each LNG namely lean, medium, and rich LNG.

Ships unloading started with approximately 10% LNG in tank for each LNG after the regasification and BOG was occupying 90% of the storage tank in equilibrium. Filling LNG inside the tank to 95% of the storage tank volume lasted for almost 15 hours and a quarter with small minutes difference due to different rates of evaporation for different LNG in rundown lines and storage tank but the pumping rate was the same. The loaded LNG composition and properties altered due to regasification of part of LNG so as molecular weight and volume as summarized in the table 13 below.

Table 13. Initial and final molecular weight and volume of LNG during storage tank loading from ships.

	Lean		Medium		Rich	
	Initial	Final	Initial	Final	Initial	Final
Molecular Weight (kg/kgmole)	16.25649	16.25672	17.53309	17.53362	18.84567	18.85013
Molar Volume (m ³ /kgmole)	0.03821	0.03820	0.03888	0.03885	0.03944	0.03937

The molecular weight of the LNG increases for the part LNG components especially lighter turned unto vapor phase due to heat leakage inside pumps, pipelines, and storage tank and incoming LNG. Therefore, this leads to LNG rich in heavier components as well as larger molecular weight. Molar volume decreased even though part of LNG components especially lighter depleted. The molar volume decreased due to molecular shrinkage as result of decrease in LNG temperature (i.e. from -159.89°C to -159.93°C , -160.28°C to -160.5°C , and -162.28°C to -162.83°C for lean, medium, and rich LNG respectively) due to incoming cold LNG and a slight scarcity of lighter components which can swell easily. For the large part of lighter components had evaporated, the remaining LNG had shrunken to compensate with fallen LNG temperature as seen in table 13.

For BOG inside the storage tank during LNG unloading from ships, molecular weight rose and molar volume decrease rapidly during the start of unloading and they progressively became gentle to constant until the end of storage tank filling as noticeable in figure 46. This happens because of not only heat ingress in rundown lines and storage tank but also temperature and compositional differences between incoming and remained LNG inside the storage tank. The incoming LNG and BOG was enriched in lighter components and cold while the stored LNG and BOG was depleted in lighter components and hot. The mixture of the two enhance the LNG evaporation intensity in the beginning and reduce as the composition and temperature of the two get close at the end of ships unloading so does increase BOG molecular weight but also decrease molar volume for the BOG continuously cool down as well as shrinking. The changes for molecular weight and molar volume magnified as heavier as LNG is. This is due to the fact that as heavier as the LNG is, the more enriched it is in nitrogen. Nitrogen is the major component in BOG for it is light and evaporates more and before other LNG components.

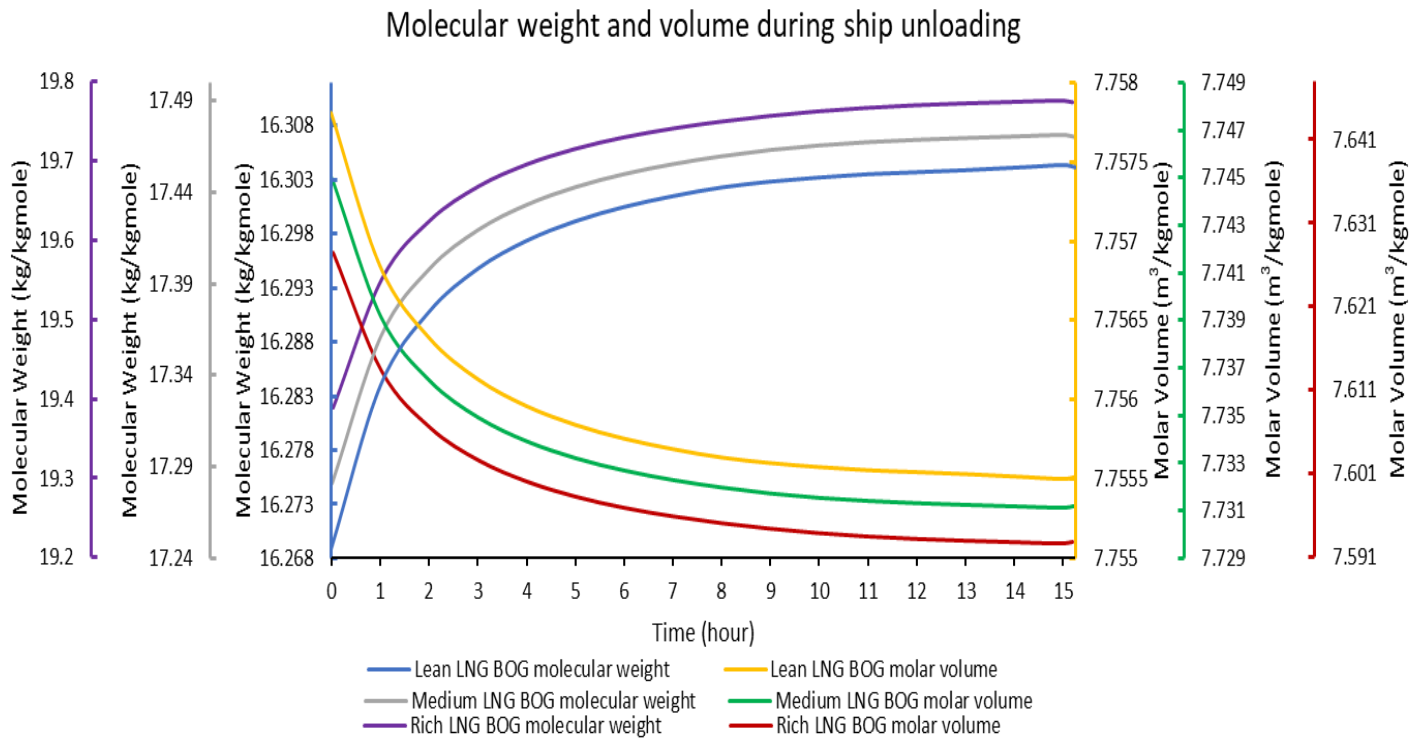


Figure 46. Molecular weight and volume changes during LNG storage tank filling.

4.2.2.3. Holding mode

During LNG storage tank holding mode, molecular weight and volume changes of LNG and BOG inside the storage tank has been studied for each LNG namely lean, medium, and rich LNG.

Storage tank holding started with approximately 95% LNG in tank for each LNG after being filled and BOG was occupying 5% of the storage tank in equilibrium. Holding LNG inside the tank was done for twenty-four hours, a day for each LNG. The loaded LNG composition and properties altered due to regasification of part of LNG due to heat leakage inside the tank so as molecular weight and volume as summarized in the table 14 below.

Table 14. Initial and final molecular weight and volume of LNG during storage tank holding mode.

	Lean		Medium		Rich	
	Initial	Final	Initial	Final	Initial	Final
Molecular Weight (kg/kgmole)	16.25672	16.25671	17.53362	17.53364	18.85013	18.84995
Molar Volume (m ³ /kgmole)	0.0382008	0.0382010	0.0388473	0.0388487	0.0393679	0.0393707

The molecular weight of the LNG decreases in lean and rich while it increases in medium LNG. This is due to the part LNG components especially lighter turned into vapor phase due to heat leakage inside storage tank. The lean constitutes of large amount lighter components than others such as methane and nitrogen and they are prone to vaporise. Although the rich LNG constitutes of heavier components but also has a large portion of nitrogen which is more prone to vaporise. While the medium LNG evaporated moderately especially for lighter components such as nitrogen and methane leaving behind LNG enriched in heavier components. Therefore, lean and rich LNG evaporated more during storage tank holding mode than medium LNG which is composed of moderate quantity of lighter components hence the decrease of molecular weight. Molar volume increased even though part of LNG components especially lighter depleted. The molar volume increased due to molecular expansion to compensate with heat ingress inside storage tank as noticeable in table 14 above.

The molecular weight and molar volume of BOG from LNG as noticeable in figure 47 change independently for they change based on different factors.

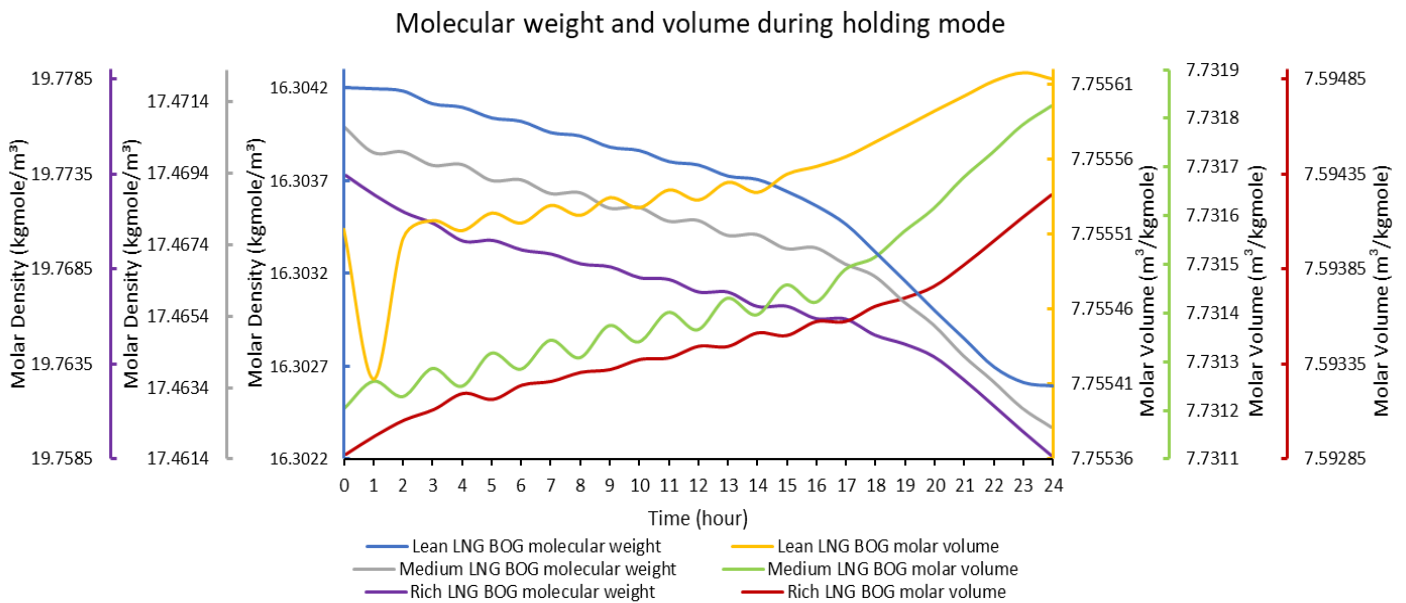


Figure 47. Molecular weight and volume changes during holding mode for lean LNG.

The molecular weight of BOG inside the tank decreased progressively as LNG was evaporating due to heat leakage in tank. It decreased for the large part of evaporated vapours was mostly lighter components which have less molecular weight and largely decreased whenever there was a BOG

excess release for a part of BOG was being taken out of the tank especially in period with high heat ingress in tank like from 14th to 23rd, first hour and from 16th to 24th and first two hours and from 19th to 24th holding hours with solar radiation presence as observable in figure 45. The molar volume was generally increasing mostly whenever there was a BOG excess release such as from fourteenth to the end of holding mode. It was also reducing whenever there was no BOG released from the tank. BOG is a gas, whenever there was a release of BOG, a large space to occupy was available hence increase of molar volume and vice versa as noticeable in figure 47.

4.2.3. Density

Molar and mass density changes for LNG and BOG in storage tank during LNG regasification, ships unloading and holding mode has been analysed independently for each LNG. Since the stored LNG was continuously changing because of evaporation of its small part to compensate with heat leakage so did molar and mass density of LNG and BOG continuously changed.

4.2.3.1. LNG regasification

The molar density of lean, medium, and rich LNG and mass density of lean LNG while medium and rich LNG mass density increased. Molar density of LNGs have decreased for part of LNG molecules have changed into vapours (BOG) and the remaining LNG molecules have swollen to compensate with heat leaked inside the storage tank. Mass density of lean LNG has decreased due to evaporation of part of LNG mass and a swell of non-evaporated LNG due to heat leaked inside the tank. While medium and rich LNG's mass density increased for large part evaporated mass was of lighter components, leaving behind heavier components so did the mass density increased as observable in table 15.

Table 15. Initial and final mass and molar density of LNG during LNG regasification.

	Lean LNG		Medium LNG		Rich LNG	
	Initial	Final	Initial	Final	Initial	Final
Molar Density (kgmole/m ³)	26.18425	26.17364	25.75943	25.7202	25.42487	25.35597
Mass Density (kg/m ³)	425.6737	425.4915	451.6531	450.9925	479.3205	477.8582

The BOG molar and mass density also decreased during lean, medium, and rich LNG regasification as noticeable in figure 48 below.

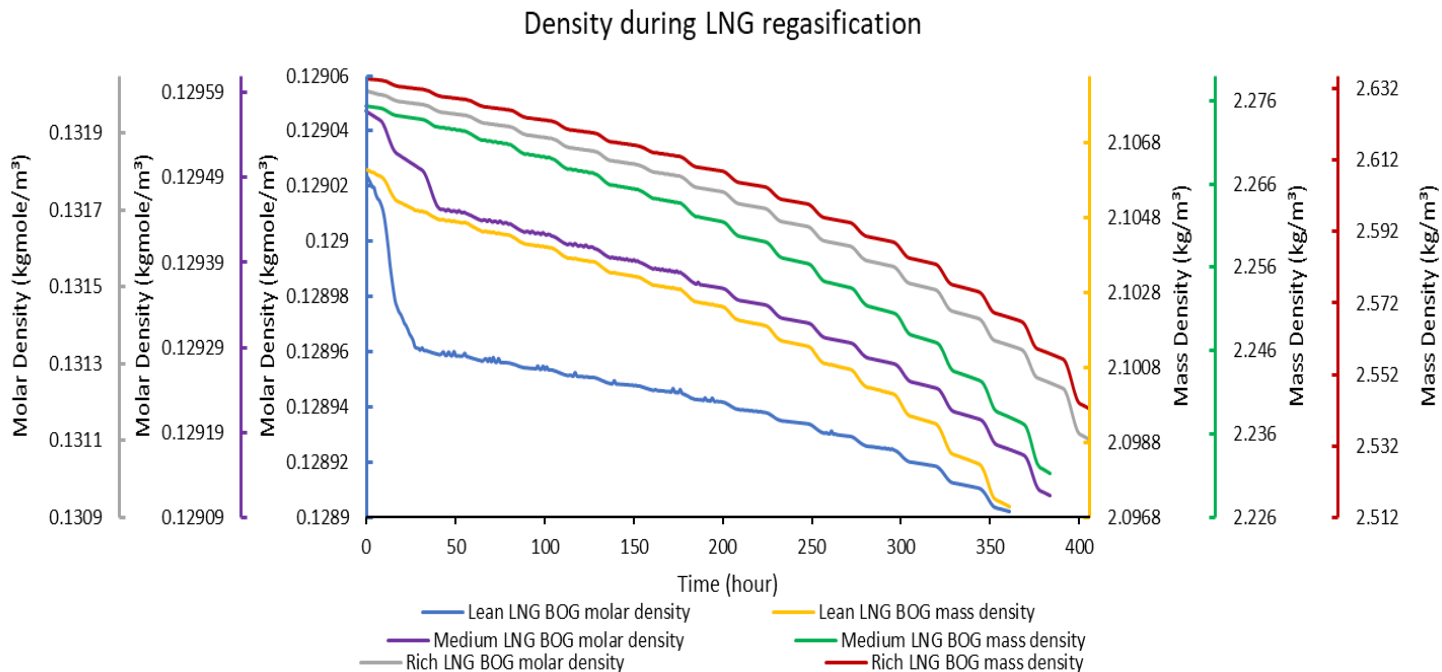


Figure 48. BOG molar and mass density changes during LNG regasification.

During the beginning of lean LNG regasification within the first 29 hours, the mass and molar BOG densities suddenly decreased as observable in figure 48. In this period, there was no BOG excess release, and the pressure remained below the set point. The 200,000 kg hourly lean LNG regasification continually left a large gap for the BOG to occupy, with heat ingress starting to build up before reaching a point where it evaporated more than the hourly LNG removal. This increase created a larger gap for small BOG moles and masses to occupy, leading to significant decreases in molar and mass BOG densities. The densities then gently decreased over time, with small increases due to continuous evaporation and BOG release. Rapid decreases in densities during solar radiation presence began from the 50th hour for molar density and the 200th hour for mass density, continuing until the end of the lean LNG regasification period. Small sudden density increases occurred between the 30th and 200th hours and the 30th and 300th hours during periods without solar radiation, resulting from successive hourly BOG excess releases followed by no release, causing densities to rise as vapors built up inside the tank. For medium LNG, within the first 44 hours, mass BOG density suddenly decreased while molar density gently decreased initially. Similar patterns of density changes occurred, with rapid decreases during solar radiation from the start of the regasification period, and small increases during non-solar periods between the 44th and 180th hours for molar density and the 44th and 191st hours for mass density. For rich

LNG, the initial decrease in densities was gentle but grew over time, with similar rapid decreases during solar radiation presence from the start of the regasification period, and gentle decreases during non-solar periods. Overall, changes in BOG molar and mass densities were largely influenced by the evaporation of lighter components and the presence of solar radiation, as shown in figure 48.

4.2.3.2. Ships unloading

During ships unloading and LNG storage tank loading, densities of LNG and BOG inside the tank increased progressively to the end until the storage tank was filled with LNG to 95% of its volume capacity as noticeable in table 16, and figure 49.

Table 16. Initial and final mass and molar density of LNG during storage tank loading.

	Lean LNG		Medium LNG		Rich LNG	
	Initial	Final	Initial	Final	Initial	Final
Molar Density (kgmole/m ³)	26.17366	26.17748	25.72087	25.74183	25.35601	25.40141
Mass Density (kg/m ³)	425.4918	425.5599	450.9664	451.3474	477.851	478.8201

The former LNGs with reduced densities due to LNG regasification increased their density as observable in table 16 due an enrichment of fresh and cool lean, medium, and rich LNG rich in heavier and lighter components which has not been swollen.

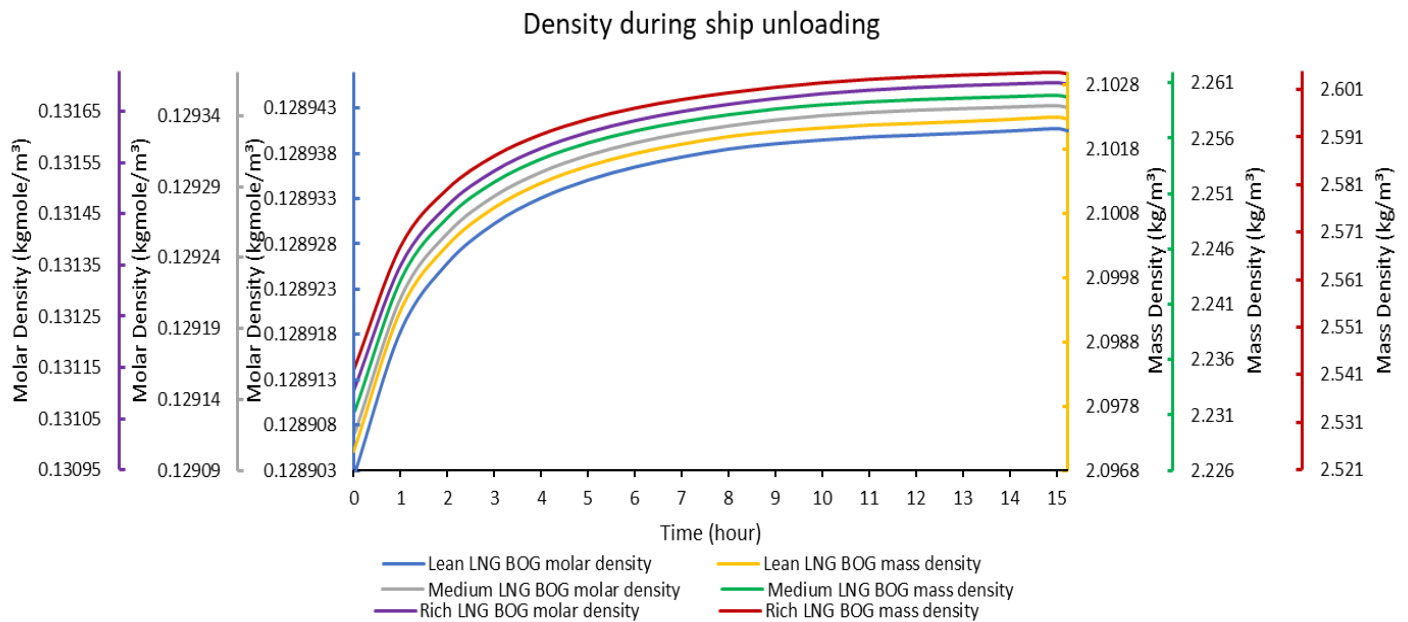


Figure 49. BOG molar and mass density changes during LNG ships unloading.

As lean, medium, and rich LNG was being filled into the tank, the BOG volume was being reduced but also enriched with additional BOG formation due to heat ingress in pumps, pipes, and storage tank hence the increase of mass and molar densities as observable in figure 49 for lean, medium, and rich LNG unloading from ships.

4.2.3.3. Holding mode

During LNG holding mode, densities of LNG and BOG inside the tank decreased to the end of holding mode in 24 hours for each LNG as noticeable in table 17, and figure 50.

Table 17. Initial and final mass and molar density of LNG during holding mode.

	Lean LNG		Medium LNG		Rich LNG	
	Initial	Final	Initial	Final	Initial	Final
Molar Density (kgmole/m ³)	26.17748	26.17731	25.74183	25.74087	25.40141	25.39962
Mass Density (kg/m ³)	425.5599	425.5569	451.3474	451.3311	478.8201	478.7816

The LNG molar and mass densities for each LNG during holding mode decreased as noticeable in table 17 for part of its moles and mass became vapours and LNGs swelled because of heat ingress into the storage tank.

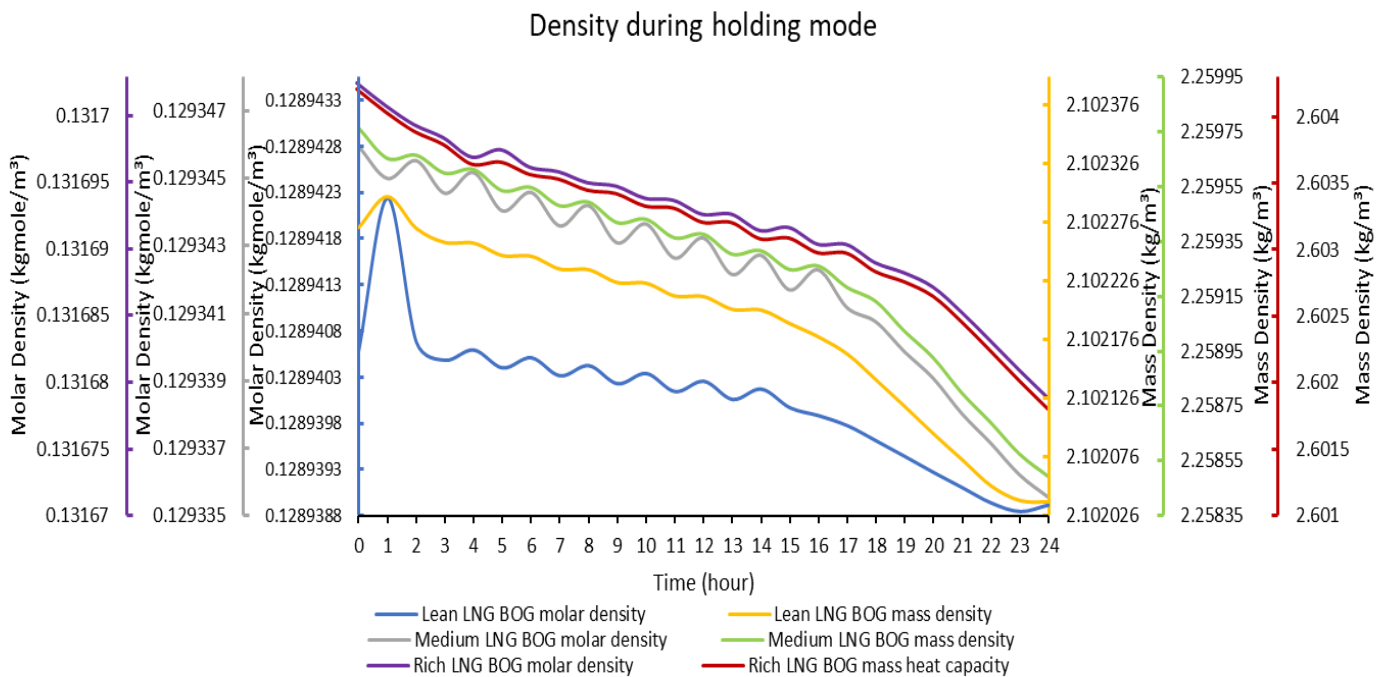


Figure 50. BOG molar and mass density changes during LNG holding mode.

The molar and mass density of BOG from lean, medium, and rich LNG holding generally decreased due to the evaporation of lighter components. For lean LNG, densities gently decreased with sudden increases and decreases whenever there was no BOG excess released and when BOG was released from the storage tank, respectively. This pattern was due to the enrichment of vapor moles and mass inside the tank during periods of no BOG release, causing density increases, and the depletion of moles and mass during BOG release, creating large empty volumes for BOG to occupy. Initially, a high heat ingress and no BOG release led to high molar and mass densities in the first hour. Similar patterns were observed for medium LNG, with densities gently decreasing and showing sudden increases and decreases based on BOG release conditions. For rich LNG, the decrease in densities was gentler, with very small increases and decreases in the absence of solar radiation. Overall, the densities of BOG decreased as lighter components evaporated over time, as observable in figures 50.

Therefore, the density continuously falls during LNG regasification and holding mode due to nitrogen reduction (Huang et al., 2022).

4.2.4. Heat capacity

Specific and mass heat capacity changes for LNG and BOG in storage tank during LNG regasification, ships unloading and holding mode has been analysed independently for each LNG. Since the stored LNG was continuously changing because of evaporation of its small part due to heat leakage so did Specific and mass heat capacity of LNG and BOG continuously changed.

4.2.4.1. LNG regasification

During LNG regasification mode, specific and mass heat capacity of LNG and BOG inside the tank increased until the end of regasification for each LNG whereby the LNG stored reached to approximately 10% of the tanks volume as noticeable in table 18, and figure 51.

Table 18. Initial and final heat capacities of LNG during LNG regasification.

	Lean LNG		Medium LNG		Rich LNG	
	Initial	Final	Initial	Final	Initial	Final
Specific Heat Capacity (kJ/kgmole.C)	55.98567	56.0013	55.88506	55.93524	55.85639	55.9388
Mass Heat Capacity (kJ/kg.C)	3.443819	3.444858	3.187329	3.189999	2.962823	2.968209

The specific and mass heat capacity of each LNG regasification mode increased as noticeable in table 18 for part of became vapours because of heat ingress into the storage tank leaving behind LNG rich in heavier components which require large heat to change their unit temperature.

During the initial regasification of lean LNG, within the first 29 hours, the specific heat capacity of BOG decreased rapidly during solar radiation presence, while the mass-specific heat capacity slightly decreased, as shown in figure 49. There was no BOG excess formed or released, causing BOG to accumulate, raising pressure and temperature. After the 29th hour, both specific and mass heat capacities increased continuously until the end of regasification, with significant increases during solar radiation, as BOG excess formed and was released, and lighter components depleted.

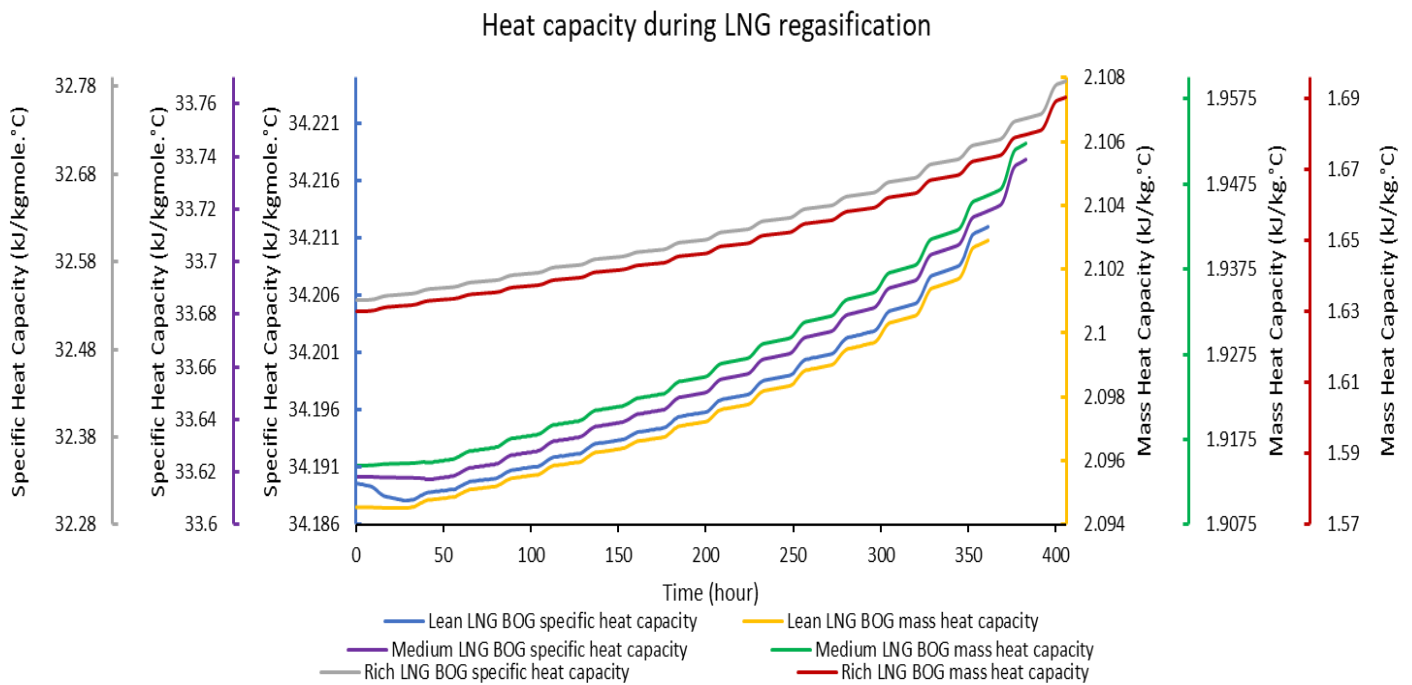


Figure 51. BOG specific and mass heat capacity changes during LNG regasification mode.

For medium LNG, within the first 44 hours, the specific heat capacity of BOG slightly decreased rapidly during solar radiation, while the mass-specific heat capacity slightly increased. No BOG excess formed or released, leading to pressure and temperature buildup. After the 44th hour, specific and mass heat capacities increased continuously, with notable rises during solar radiation. For rich LNG, specific and mass heat capacities increased continuously throughout regasification, with significant increases during solar radiation. BOG excess release cooled and depressurized the

tank, leading to an increase in specific and mass heat capacities due to the depletion of lighter components and the accumulation of heavier ones, as depicted in figure 51.

4.2.4.2. Ships unloading

During ships unloading mode, specific and mass heat capacity of LNG and BOG inside the tank decreased as noticeable in table 19, and figure 52.

Table 19. Initial and final heat capacities of LNG during ships unloading mode.

	Lean LNG		Medium LNG		Rich LNG	
	Initial	Final	Initial	Final	Initial	Final
Heat Capacity (kJ/kgmole-C)	56.00127	55.99615	55.93503	55.90848	55.93889	55.8843
Mass Heat Capacity (kJ/kg-C)	3.444856	3.444492	3.190255	3.188645	2.968262	2.964663

The specific and mass heat capacity of LNG inside the tank decreased due to the loading of fresh lean, medium, and rich LNG enriched in lighter components which have low heat capacities hence lowering specific and mass heat capacities as it can be seen in table 19 above.

The specific and mass heat capacity of BOG inside the tank also decreased as fresh lean, medium, and rich was being loaded in storage tank as shown in figure 52.

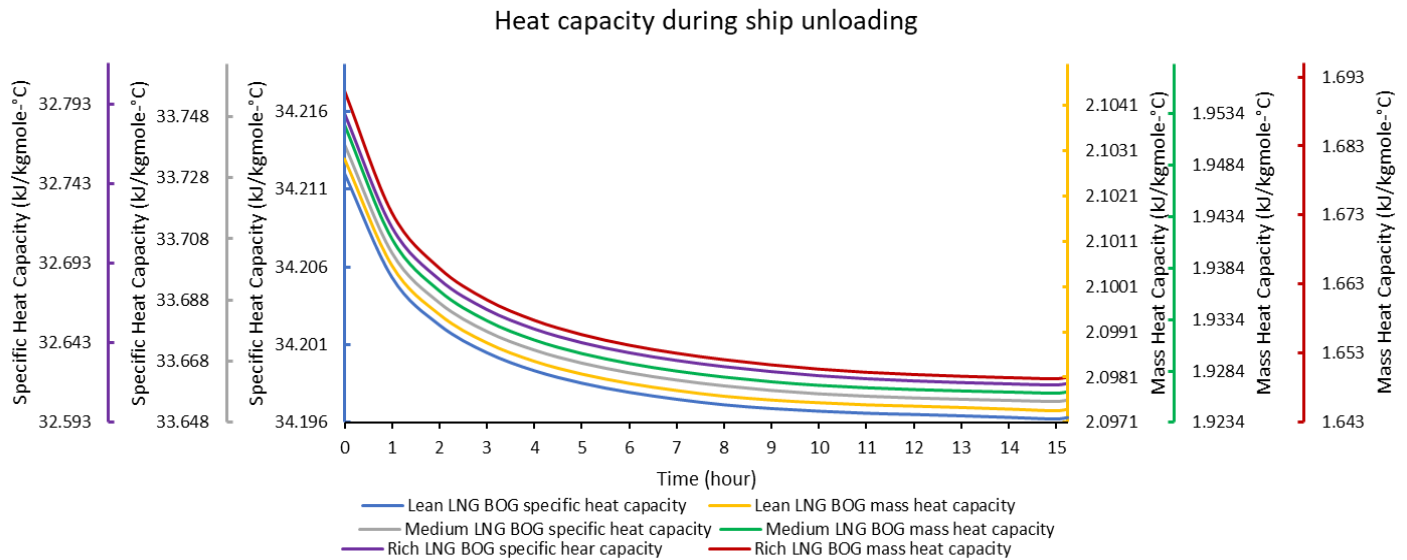


Figure 52. BOG specific and mass heat capacity changes during LNG unloading from the ship.

The decrease of specific and mass heat capacity of BOG inside the tank is a result of continuous BOG supply from pumps and pipeline enriched in lighter components and fresh LNG feed enrich

stored LNG with lighter components so does the BOG from it becomes rich in lighter components. Lighter components require less heat to change their unit temperature hence the decrease of specific and mass heat capacity of BOG as it gets enriched in lighter components.

4.2.4.3. Holding mode

During holding mode, specific and mass heat capacity of LNG and BOG inside the tank increased as noticeable in table 20, and figure 53.

Table 20. Initial and final heat capacities of LNG during holding mode.

	Lean LNG		Medium LNG		Rich LNG	
	Initial	Final	Initial	Final	Initial	Final
Heat Capacity (kJ/kgmole-C)	55.99615	55.99637	55.90848	55.90967	55.8843	55.88643
Mass Heat Capacity (kJ/kg-C)	3.444492	3.444509	3.188645	3.18871	2.964663	2.964805

The specific and mass heat capacity of each LNG during holding mode increased as noticeable in table 20 for part of became vapours because of heat ingress into the storage tank leaving behind LNG rich in heavier components which require large heat to change their unit temperature.

The specific and mass heat capacity of BOG during holding mode generally increased as it can be seen in figure 53. This is because the lighter components continually declined in BOG for it was being depleted in LNG and for it was being released out of the tank to safely keep the tank from overpressure.

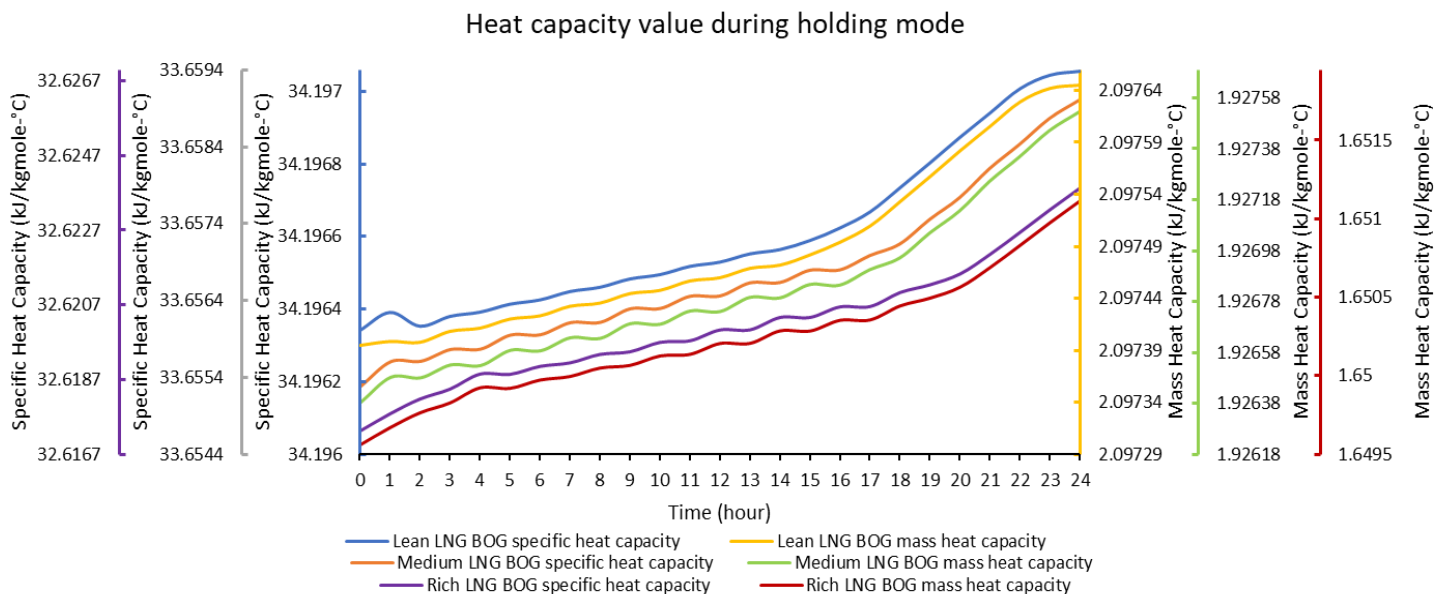


Figure 53. BOG specific and mass heat capacity changes during LNG holding mode.

For BOG from lean LNG, the specific heat capacity rose rapidly and mass heat capacity gently during the first hour. This initial rise was due to the rapid increase of heavier components in BOG, which required high heat capacity to change the temperature by a unit. Heat capacities continued to rise whenever there was no BOG excess released from the tank, due to the accumulation of a large mass and molecules inside the tank, necessitating larger heat capacities to increase BOG unit temperature. For BOG from medium LNG, both specific and mass heat capacities continually rose with sudden small decreases during BOG release times, due to the continual increase of heavier components in BOG and the cooling and depressurization as BOG was released, which required high heat capacity to change the temperature by a unit. Similarly, for BOG from rich LNG, specific and mass heat capacities continually rose with small decreases during BOG release times. During the first four hours of holding mode, heat capacities of BOG rose unceasingly due to the rapid increase of heavier components in BOG, requiring high heat capacity for temperature change.

4.2.5. Heating value

Lower and higher heating value changes for LNG and BOG in storage tank during LNG regasification, ships unloading and holding mode has been analysed independently for each LNG. Since the stored LNG was continuously changing as a result of evaporation of its small part due to heat leakage so did lower and higher heating value of LNG and BOG continuously changed.

4.2.5.1. LNG regasification

During lean, medium and rich LNG regasification, lower and higher heating value of LNG and BOG inside the tank increased as noticeable in table 21, and figure 54 and 55.

Table 21. Initial and final heating values of LNG during LNG regasification.

	Lean LNG		Medium LNG		Rich LNG	
	Initial	Final	Initial	Final	Initial	Final
HHV Molar Basis (kJ/kgmole)	893427	893692.5	948018.9	949476.5	998782.1	1001791
HHV Mass Basis (kJ/kg)	54956.93	54974.51	54068.99	54148.86	52978.97	53156.75
LHV Molar Basis (kJ/kgmole)	810898.5	811142.3	862226	863567	910069.3	912829.9
LHV Mass Basis (kJ/kg)	49880.39	49896.52	49175.9	49249.42	48273.33	48436.31

The heating value of LNG inside the storage tank increased as noticeable in table 21 as the LNG part enriched in lighter component was vaporising (i.e. mainly nitrogen) leaving behind heavier components (i.e. rich in heating value) hence the increase of heating value.

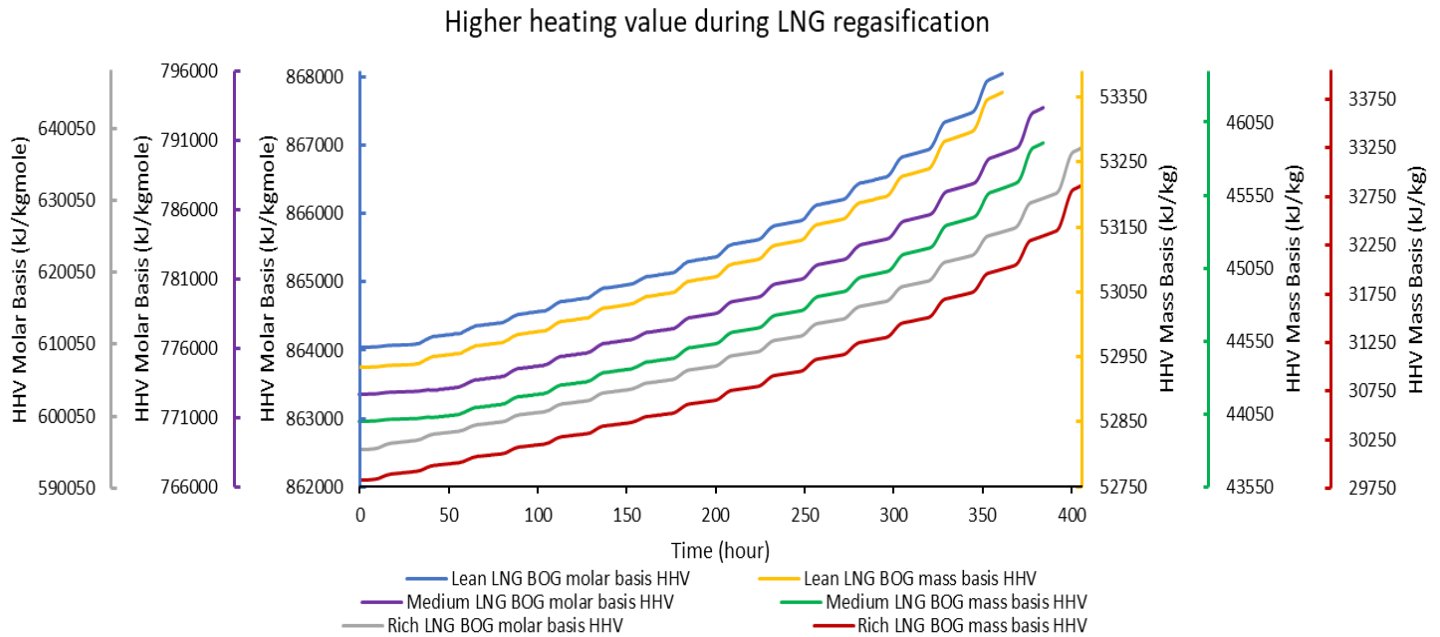


Figure 54. Higher heating value changes during LNG regasification mode.

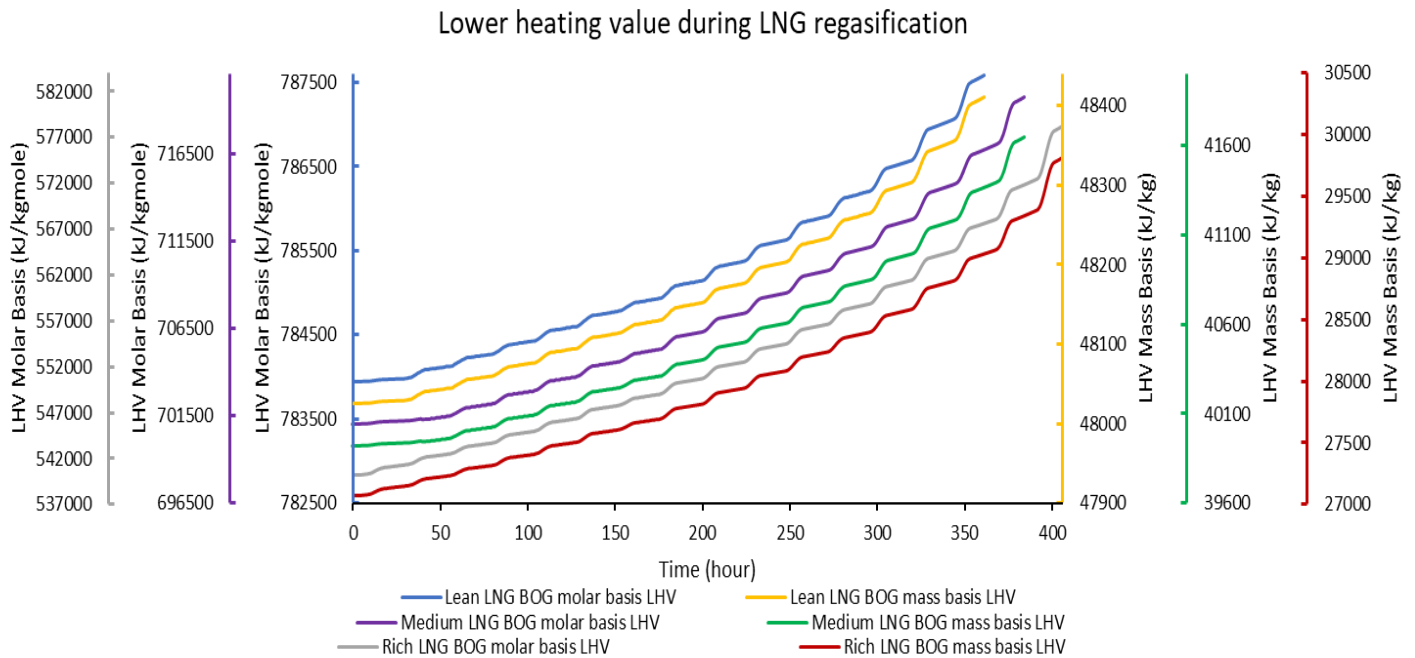


Figure 55. Lower heating value changes during LNG regasification mode.

Heating values of BOG inside the storage tank growingly increased continuously with a sudden higher rise during the presence of solar radiation. This was due to the growingly enrichment of hydrocarbons in BOG while nitrogen continuously depleting in BOG and heating value has risen higher in solar radiation presence due to large heat ingress and evaporation in such periods as noticeable in figure 54 and 55 above.

4.2.5.2. Ships unloading

During lean, medium and rich ships unloading, lower and higher heating value of LNG and BOG inside the tank decreased as noticeable in table 22, and figure 56, and 57.

Table 22. Initial and final heating values of LNG during ships unloading.

	Lean LNG		Medium LNG		Rich LNG	
	Initial	Final	Initial	Final	Initial	Final
HHV Molar Basis (kJ/kgmole)	893692.5	893518.3	949406.6	948469.1	1001800	999798.6
HHV Mass Basis (kJ/kg) [kJ/kg]	54974.51	54963.01	54149.41	54094.32	53158.1	53039.34
LHV Molar Basis (kJ/kgmole)	811142.3	810982.3	863501.4	862639.9	912837.8	911001.8
LHV Mass Basis (kJ/kg)	49896.52	49885.97	49249.81	49199.2	48437.53	48328.66

The heating value of LNG inside the storage tank decreased as noticeable in table 22 for the fresh lean, medium and rich LNG rich in lighter component (i.e. poor in heating value) was continuous added to the tank (i.e. mainly nitrogen) hence the decrease of heating value.

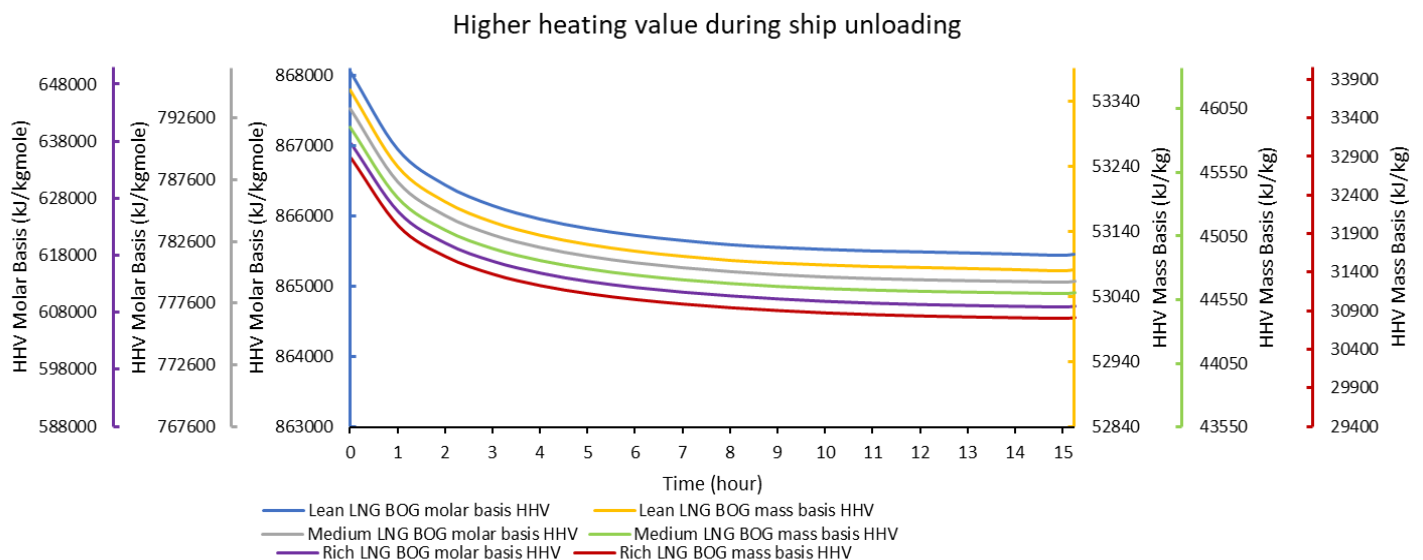


Figure 56. Higher heating value changes during LNG ships unloading mode.

Lower heating value during ship unloading

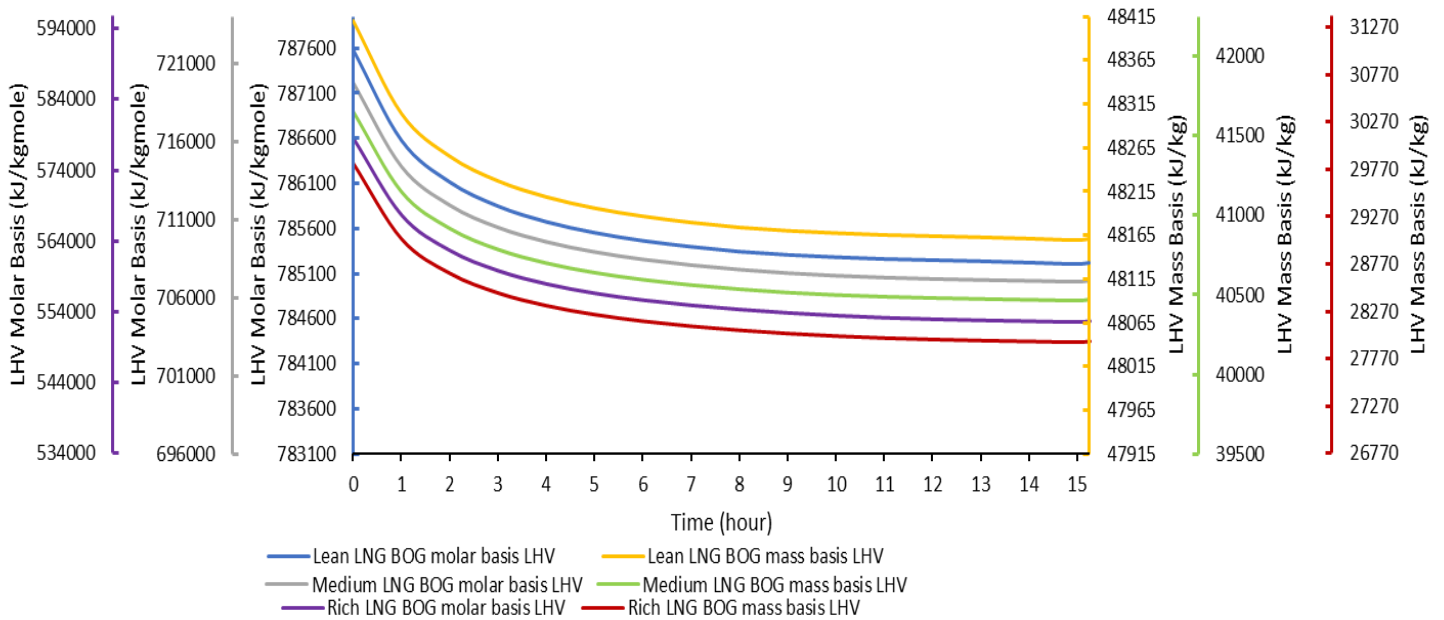


Figure 57. Lower heating value changes during LNG ships unloading mode.

Heating values of BOG inside the storage tank growingly decreased as LNG was being filled into storage tank for the BOG enriched in nitrogen (i.e. poor in heating value) was being added continuously from ship pumps, rundown lines and continuously nitrogen enriching LNG inside the storage tank as noticeable in figure 56 and 57 above.

4.2.5.3. Holding mode

During lean, medium and rich LNG holding mode, lower and higher heating value of LNG and BOG inside the tank increased as noticeable in table 23, and figure 58 and 59.

Table 23. Initial and final heating values of LNG during holding mode.

	Lean LNG		Medium LNG		Rich LNG	
	Initial	Final	Initial	Final	Initial	Final
HHV Molar Basis (kJ/kgmole)	893518.3	893526	948469.1	948513.2	999798.6	999877.2
HHV Mass Basis (kJ/kg) [kJ/kg]	54963.01	54963.53	54094.32	54096.78	53039.34	53044.02
LHV Molar Basis (kJ/kgmole)	810982.3	810989.4	862639.9	862680.5	911001.8	911073.8
LHV Mass Basis (kJ/kg)	49885.97	49886.45	49199.2	49201.46	48328.66	48332.96

The heating value of LNG inside the storage tank increased as noticeable in table 23 as the LNG part enriched in lighter component was vaporising (i.e. mainly nitrogen) leaving behind heavier components (i.e. rich in heating value) hence the increase of heating value.

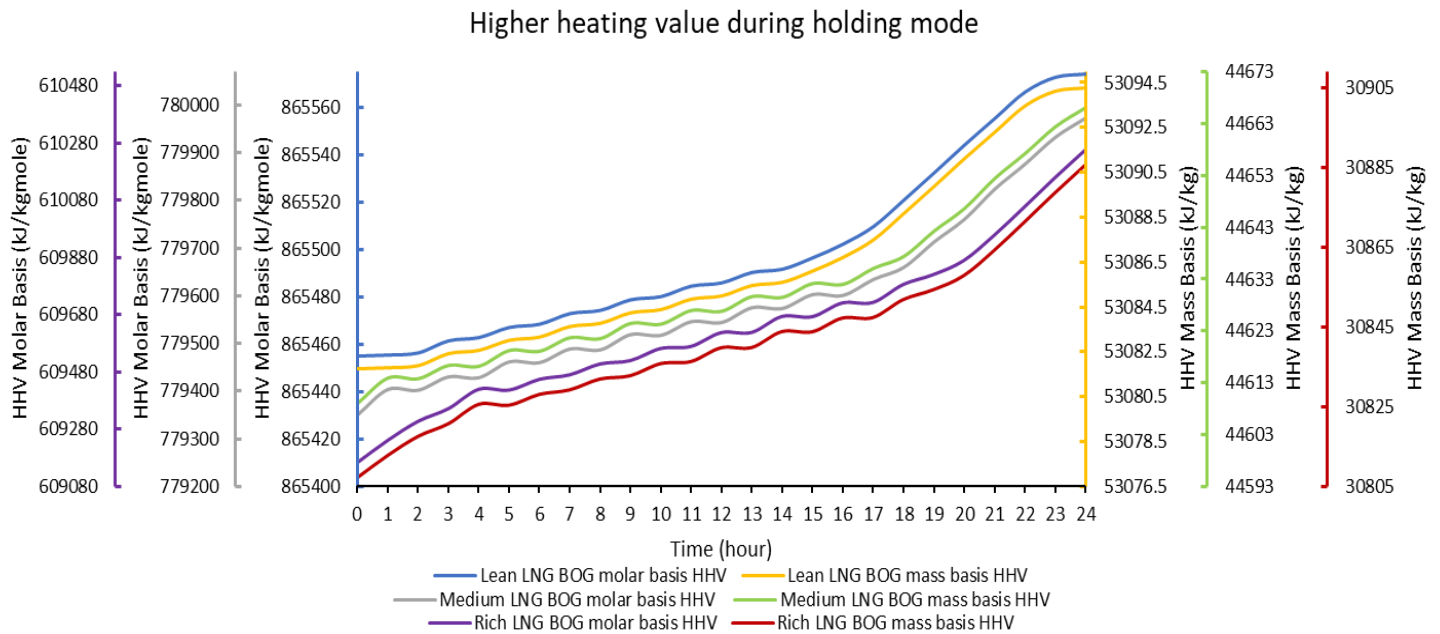


Figure 58. Higher heating value changes during LNG holding mode.

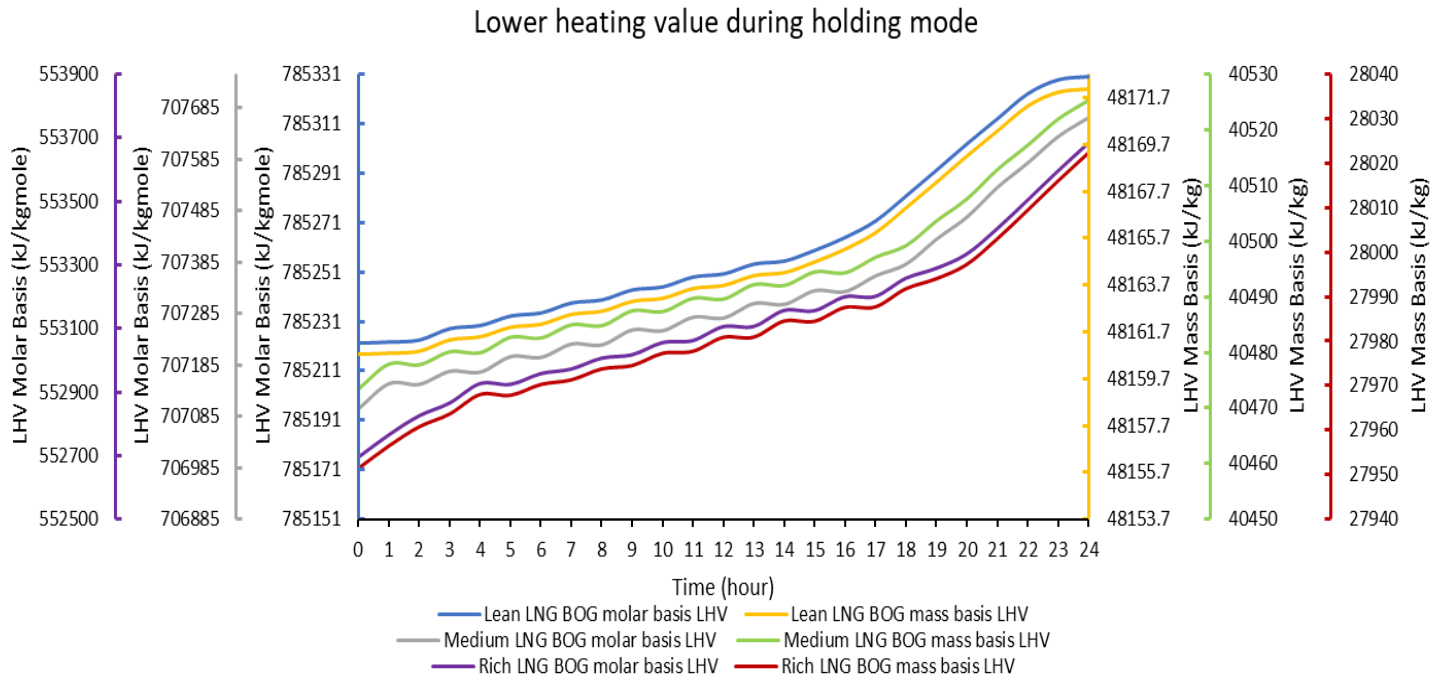


Figure 59. Lower heating value changes during LNG holding mode.

Heating values of BOG inside the storage tank growingly increased continuously with a sudden higher rise during BOG excess formation and release times. This was due to the growingly enrichment of hydrocarbons in BOG while nitrogen continuously depleting in BOG and heating value has risen higher during BOG release periods due to large hydrocarbons evaporation in such periods as noticeable in figure 58 and 59 above.

4.2.6. Thermal conductivity

Thermal conductivity changes for LNG and BOG in storage tank during LNG regasification, ships unloading and holding mode has been analysed independently for each LNG. Since the stored LNG was continuously changing because of evaporation of its small part to compensate with heat leakage so did thermal conductivity of LNG and BOG continuously changed.

4.2.6.1. LNG regasification

Thermal conductivity of lean, medium, and rich LNG has reduced during the LNG regasification period. While a 200,000kg of LNG was being regasified hourly, heat from ambient was leaking in the storage tank and change part of LNG into BOG. Therefore, as part of LNG components was changing, the remaining LNG continually depleted in thermal conductivity associated with evaporated LNG due to heat ingress as observable in table 24 below.

Table 24. Initial and final thermal conductivity of LNG during LNG regasification.

	Lean LNG		Medium LNG		Rich LNG	
	Initial	Final	Initial	Final	Initial	Final
Thermal Conductivity (W/m. K)	0.193362	0.193236	0.194395	0.193946	0.197099	0.196275

The thermal conductivity of the LNG has slightly reduced during regasification of each LNG as shown in the table 24 above. This is due to molecular expansion of LNG molecules as they absorb heat hence LNG reduces its density as well as thermal conductivity.

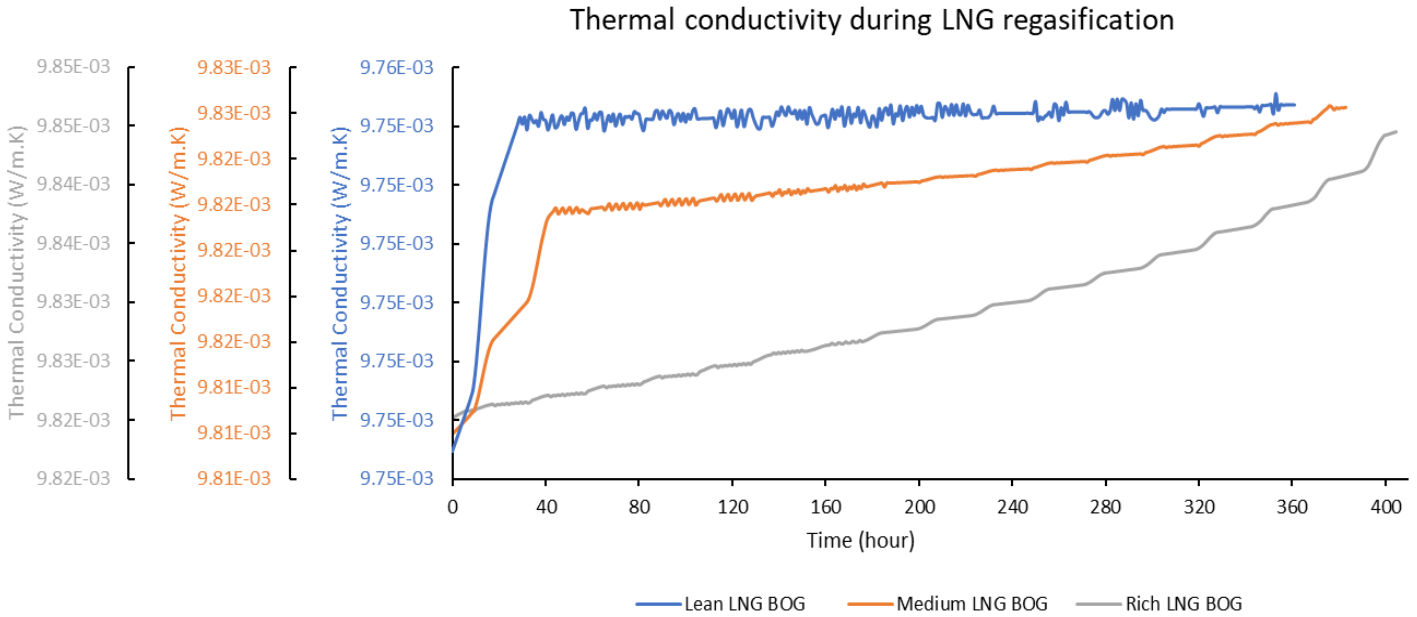


Figure 60. Thermal conductivity of BOG during LNG regasification.

During lean LNG regasification, the BOG thermal conductivity rapidly increased in the first 29 hours, then gently rose with sudden small fluctuations, as observable in figure 60. In the first 29 hours, the BOG density rose steeply during solar radiation, causing BOG buildup inside the storage tank without being released, leading to the rapid increase in thermal conductivity. The sudden small rises and drops in thermal conductivity afterward were due to changes in BOG density as BOG built up and was expelled to avoid overpressure. During medium LNG regasification, the BOG thermal conductivity rapidly increased in the first 44 hours and then gradually rose, with sudden small fluctuations. In the first 44 hours and later from the 300th hour to the end, BOG density rose steeply during solar radiation due to BOG buildup and rapid evaporation, leading to a rapid increase in thermal conductivity. The fluctuations in thermal conductivity between the 45th and 192nd hours resulted from changes in BOG density as BOG built up and was released. During rich LNG regasification, the thermal conductivity of BOG steadily increased over time with higher rises during solar radiation, as shown in figure 60. The BOG density increased as heavier hydrocarbons rose in BOG, with rapid increases during solar radiation due to intense heat leakage, causing the thermal conductivity to rise.

4.2.6.2. Ships unloading

The thermal conductivity of the LNG has increased during ships unloading for each LNG as shown in the table 25 below. The additional of fresh LNG feed cooled and shrunk LNG inside the storage tank hence increased the density as well as thermal conductivity.

Table 25. Initial and final thermal conductivity of LNG during ships unloading.

	Lean LNG		Medium LNG		Rich LNG	
	Initial	Final	Initial	Final	Initial	Final
Thermal Conductivity (W/m.K)	0.193236	0.193274	0.193945	0.194169	0.196277	0.196817

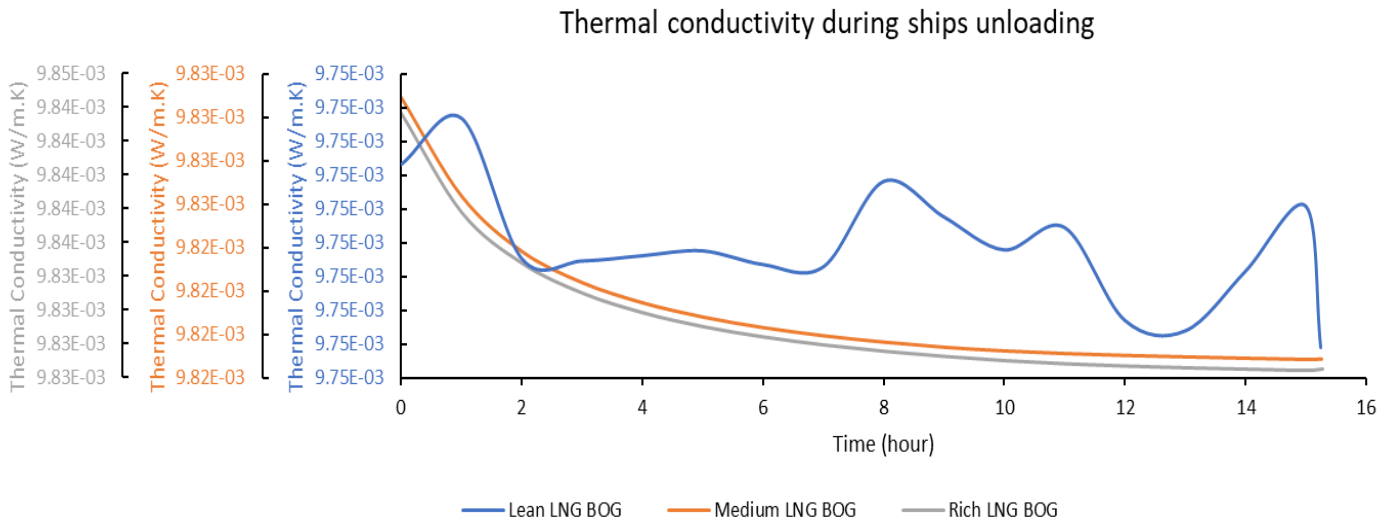


Figure 61. Thermal conductivity of BOG during LNG ships unloading mode.

During lean LNG unloading from ships to the storage tank, the thermal conductivity of BOG varied from time to time with a general diminishing trend. The incoming lean LNG evaporated due to heat leakage in the pumps, pipeline, and from the storage tank with varying ambient temperature as shown in figure 61 above hence widely varying the resulted BOG as well as its thermal conductivity. The less variations of thermal conductivity took place when there were not much ambient temperature variations between the second and seventh unloading hour and large variations during large variations of ambient temperature as well as solar radiation presence from 7th hour to the end of ships unloading. This was due to not much variation of BOG formation from pumps, pipeline, and from the storage tank for the ambient temperature variation was close. The presence of large ambient temperature variation as well as solar radiation boosted the BOG

formation with different rates and composition from pumps, pipeline, and from the storage tank for the lean LNG source was varying as it passed through rundown lines to the tank. The resulted BOG varied time to time hence its thermal conductivity variations.

The thermal conductivity of BOG inside storage tank during medium and rich LNG filling reduced as noticeable in figure 61 above. This was due to a continuous enrichment of nitrogen rich medium and rich LNG inside the tank hence the enrichment of nitrogen in BOG as well as decline of thermal conductivity.

4.2.6.3. Holding mode

The thermal conductivity of the LNG has slightly reduced during holding mode of each LNG as shown in the table 26 below. This is due to molecular expansion of LNG molecules as they absorb heat hence LNG reduces its density as well as thermal conductivity.

Table 26. Initial and final thermal conductivity of LNG during holding mode.

	Lean LNG		Medium LNG		Rich LNG	
	Initial	Final	Initial	Final	Initial	Final
Thermal Conductivity (W/m.K)	0.193274	0.193269	0.194169	0.19416	0.196817	0.196796

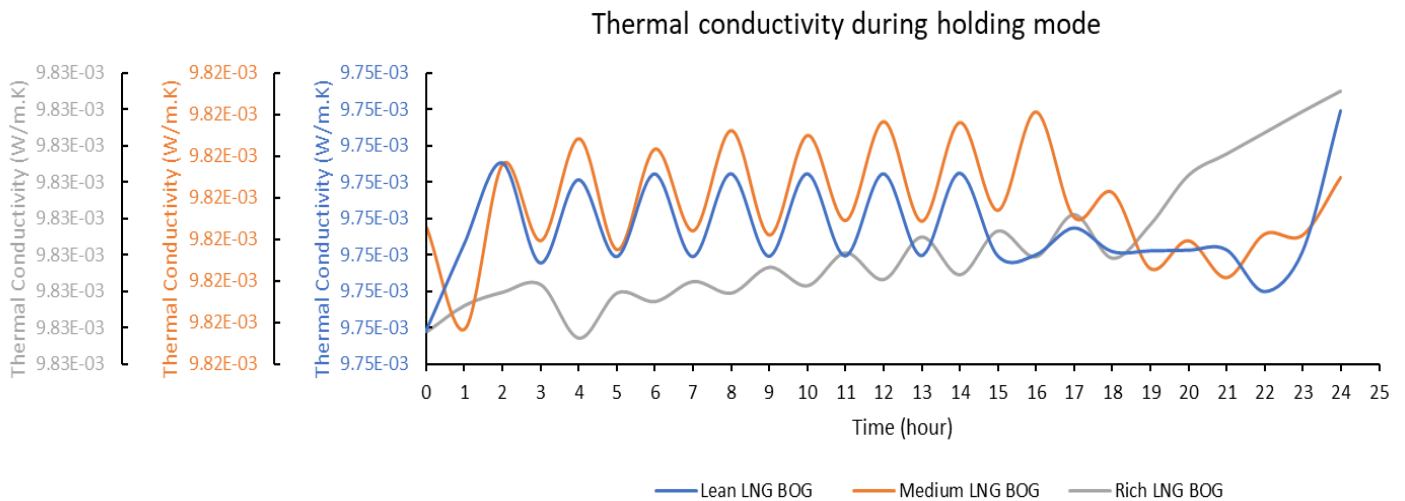


Figure 62. Thermal conductivity of BOG during LNG holding mode.

During the first fifteen hours of lean LNG holding, the thermal conductivity rose and fell sequentially due to the release and retention of BOG inside the storage tank, causing fluctuations in BOG mass, density, and thermal conductivity. From the 15th to the 22nd hour, thermal

conductivity barely changed before rising rapidly to the end of the holding mode, mainly due to significant heat ingress from solar radiation, leading to large LNG evaporation and increased BOG mass, density, and thermal conductivity. For medium LNG, during the first seventeen hours, thermal conductivity similarly rose and fell due to BOG release and retention. From the 17th hour to the end of the holding mode, thermal conductivity remained steady before rapidly increasing with a slight drop, correlating with heat ingress and large LNG evaporation during solar radiation periods. For rich LNG, thermal conductivity rose in the first three hours and from the 18th hour to the end of the holding mode, with large heat ingress from solar radiation driving LNG evaporation and increasing BOG mass, density, and thermal conductivity. Between the third and eighth hours of rich LNG holding, thermal conductivity fluctuated due to sequential BOG release and retention, affecting BOG mass, density, and thermal conductivity, as shown in figure 62 above.

4.3. Recoverable BOG

BOG continuously form because of heat ingress through piping, pumping and storage tank. BOG formation is a way the LNG cools itself by evaporating a small LNG portion. Not all BOG formed are able to be retrieved back. Even though the BOG forms continuously since the heat ingress continuously, the storage tank at receiving terminal can hold the formed boil-off gas until the set-point pressure is reached inside the tank. At the reach of set point, the tank releases a portion of the BOG out to avoid overpressure that may cause accident. In this work, the storage tank pressure was set to 117 kPa. During LNG pumping and piping from the ship to the storage tank at the receiving terminal, the portion of the released BOG is sent to the ship to maintain pressure and temperature in ship tank during storage tank filling mode and the remaining portion is recoverable. While during LNG regasification and holding mode, the released BOG is recoverable.

During LNG regasification mode, the starting volume of the LNG in the storage tank was simulated to be 95% of storage tank volume for all LNGs which is 190000m³. The initial mass differs for each LNG because of their compositional differences. The LNG gasification mode was simulated to evaporate 200,000kg of LNG hourly until the LNG volume in storage tank reaches to 10% of storage tank volume. Regasification was simulated to start at the same time for all LNGs at 00:00' AM, 26th June, 2024 and lasted differently. LNG regasification mode lasted 15 days and 1 hours, 15 days and 22 hours, and 16 days and 21 hours for lean, medium and rich respectively. This is due to the heaviness of the LNG, the more the heavier the LNG is, the more it will last longer

during regasification. The recovered BOG released from the storage tank is 315913.51kg, 290373.34kg, and 307147.70kg from lean, medium and rich LNG storage tank respectively. The lean LNG evaporate more than the rest for it is constituted of large quantity of lighter components. The rich LNG releases more BOG for it last longer and more prone to heat ingress and contains large quantity of nitrogen which is lighter and more prone to evaporate than for medium LNG.

During storage tank loading mode, the starting volume of the LNG in the storage tank was simulated to be 10% of storage tank volume for all LNGs which is 20000m³. The initial mass differs for each LNG because of their compositional differences. The LNG storage tank loading mode was simulated to pump 1400m³/h of LNG hourly per each pump for eight pumps submerged into LNG cargo ship and through two run-down lines with four pumps feeding each until the LNG volume in storage tank reaches to 95% of storage tank volume. Storage tank loading or ships unloading was simulated to start at after the reach of 10% of LNG storage tank volume and lasted for 16 hours for all LNGs but with small LNG quantity loaded at the last hour to fill to 95% storage tank volume. LNG storage tank loading mode started at 1:00' AM on 10th June, 11:00' PM on 10th June, and 11:00' PM on 11th June, 2024 for lean, medium and rich respectively. Not all the LNG pumped was reaching into the storage tank as LNG, some portion reach to the tank in gas form due to heat ingress into pumping and piping. During pumping and piping LNG into storage tank from ships, 168628.30kg, 140249.76kg, and 159199.1kg of BOG was formed from lean, medium and rich LNG pumping and piping. The other part of BOG is produced from heat ingress inside the storage tank during pumping and loading of LNG into storage tank. The recoverable BOG released from the storage tank during pumping and piping after diverting a part of it to stabilise temperature and pressure inside ship tanks is 186482.32kg, 156570.73kg, and 173210.30kg from lean, medium and rich LNG storage tank loading mode respectively. The lean LNG produced more BOG than others for it is lighter and constitutes of large quantity of lighter components compare to other LNGs. The rich LNG produced more BOG than medium LNG even though it is heavier for it contains more nitrogen than medium LNG and nitrogen is lighter and evaporate faster than hydrocarbon components of LNG.

During LNG storage tank holding mode, the starting volume of the LNG in the storage tank was simulated to be 95% of storage tank volume for all LNGs. The initial mass differs for each LNG because of their compositional differences. The LNG storage tank holding mode was simulated

for a storage tank at receiving terminal to hold LNG without loading and unloading for a day. Holding mode was simulated to start after the end of storage tank loading mode whereby the storage tank was filled to approximately 95% of its volume for all LNGs. It started at 05:00' PM of 10th June, 03:00' PM of 11th June, and 02:00' PM of 12th June 2024 for lean, medium and rich LNG respectively and it lasted for 24 hours. The recoverable BOG released from the storage tank during holding mode is 22462.53kg, 22370.38kg, and 19279.79kg from lean, medium and rich LNG storage tank respectively. The lean LNG evaporate more than the rest for it is constituted of large quantity of lighter components, followed by the medium LNG, and rich LNG is the least to produce BOG for it is heavier than others.

4.4. BOG management

The recovered BOG from each mode were designed to be converted into CNG. According to the literature and industrial operations, the CNG were simulated to be at 250 bars at ambient temperature. Each LNG compositional type was simulated independently throughout all modes; LNG regasification, ships unloading, and LNG holding mode.

The recoverable BOG was firstly sent to the storage tank before multistage compressors. The tank served as the intermediary BOG storage for BOG excess do not get released always hence to avoid running compressors with no BOG and as a knockout drum for by liquids that may be released with BOG. Three successive compressors and coolers have been used. The compression ratio of 6.055 for each compressor was set to be and the cooling was independent for each LNG towards the final resulted CNG at ambient temperature (i.e., ideally assumed to be 25⁰C).

In each of three stages, the recovered overall BOG from lean, medium, and rich LNG during LNG regasification, ships unloading mode and holding mode was compressed and cooled independently. The CNG pressure was increased with 8.5 kPa for the sake pressure loss that can take happen during the CNG loading into storage tanks as noticeable in table 27 below.

Table 27. BOG conversion to CNG simulation results.

Mode	Total BOG mass inlet (kg)	Total energy (kW)						Overall CNG pressure (kPa)	Overall CNG temperature (°C)
		Compressor			Cooler				
		1st stage	2nd stage	3rd stage	1st stage	2nd stage	3rd stage		

Lean LNG	LNG regasification	315913.51	14699.08	21197.63	24517.66	5651.56	18265.96	20289.17	25008.5	25
	Ships unloading	186482.32	8678.81	12515.32	14474.09	3336.95	10785.69	11980.77	25008.5	25
	LNG holding	22462.53	1045.18	1507.25	1743.31	401.85	1298.80	1442.67	25008.5	25
Medium LNG	LNG regasification	290373.34	12638.19	18483.34	22225.05	4770.69	15094.82	16563.76	25008.5	25
	Ships unloading	156570.73	6819.06	9971.84	11987.40	2574.28	8146.36	8940.12	25008.5	25
	LNG holding	22370.38	973.24	1423.46	1711.89	367.36	1162.27	1423.32	25008.5	25
Rich LNG	LNG regasification	307147.70	11704.45	17535.40	22315.35	4315.05	13257.98	18123.86	25008.5	25
	Ships unloading	173210.30	6617.51	9910.26	12600.91	2440.23	7500.89	10259.13	25008.5	25
	LNG holding	19279.79	734.91	1100.98	1400.97	270.94	832.51	1138.12	25008.5	25

The resulted simulation results as observable in table 27 above have shown that the different BOG quantity recovered in different mode for each LNG consumed different energy. Even though the intended pressure and temperature of CNG was the same, the energy consumption was different as the quantity recovered was.

The resulted performance of the BOG conversion to CNG via multistage compressor have been summarised in the table 28 below. The energy consumption continually increased from first to the third stage of compression and cooling. As the stage increase the energy consumption also increased for the gas needed to be pressurised higher and needed to be cooled for as it got hotter due to compression.

Table 28. Conversion performance assessment.

	Mode	Total CNG mass produced (kg)	Energy used (kW)	Energy per CNG mass produced (kW/kg)	CNG mass produced (kg/h)
Lean LNG	LNG regasification	315913.51	104621.08	0.331169994	875.10668
	Ships unloading	186482.32	61771.63	0.331246575	12228.3491
	LNG holding	22462.53	7439.07	0.331177018	935.938543
Medium LNG	LNG regasification	290373.34	89775.84	0.309173829	758.154945
	Ships unloading	156570.73	48439.07	0.309374975	10266.9332

	LNG holding	22370.38	7061.55	0.315665082	932.099345
	LNG regasification	307147.70	87252.10	0.284072119	756.521425
	Ships unloading	173210.30	49328.93	0.284792114	11358.05246
Rich LNG	LNG holding	19279.79	5478.43	0.284153858	803.3247742

Throughout lean, medium, and rich LNG simulated modes, the performance of BOG conversion summarised in table 40 reveals that the ships unloading mode for lean and rich LNG consumed large energy per CNG produced while for medium LNG, it was BOG conversion during LNG holding mode. BOG conversion from lean LNG ships unloading mode has consumed a lot of energy per CNG mass produced. This is due to compositional cause mainly nitrogen content and heavier hydrocarbons content which added more compression and cooling energy requirement.

During lean, medium, and rich LNG simulated modes, the performance of BOG conversion summarised in table 28 reveals that the ships unloading mode has produced large quantity of CNG per hour especially for lean LNG. This was due to large hourly BOG excess formation during ships unloading especially for lean LNG from ship pumps, rundown lines and storage pumps while storage tank is the only BOG excess formation place for other modes. The lean LNG constitutes of large quantity of lighter components hence the large BOG excess formation. LNG regasification mode for all LNG has generated less BOG as well as CNG for large BOG quantity generated did not get released out of the tank but rather continually replaced the withdrawn LNG inside the tank.

For a storage tank of 200,000m³, at least 35 CNG dedicated vehicles of 25 kilograms storage capacity can be supplied hourly and up to 489 vehicles hourly during ships unloading can be fed.

4.5. CNG properties

The resulted CNG composition and properties for each LNG in each simulated mode have been summarised in the table 29 and 30 below. CNG properties include the simulated results and calculate properties such as Wobbe, methane number (i.e., using GasCalc), and rough estimation of MON based on empirical formulas.

Table 29. The resulted CNG composition for each LNG in all simulated modes.

Lean LNG	Medium LNG	Rich LNG
Mole fraction	Mole fraction	Mole fraction

Component	LNG regasification mode	Ships unloading mode	LNG holding mode	LNG regasification mode	Ships unloading mode	LNG holding mode	LNG regasification mode	Ships unloading mode	LNG holding mode
Methane	0.9782	0.9785	0.9782	0.8817	0.8825	0.8811	0.6888	0.692433	0.6892
Ethane	2.6E-05	2.6E-05	2.6E-05	9.2E-05	9.2E-05	9.2E-05	9.8E-05	9.91E-05	9.81E-05
Propane	2.5E-08	2.5E-08	2.5E-08	2.8E-07	2.8E-07	2.8E-07	2.9E-07	2.99E-07	2.95E-07
n-Butane	6.1E-11	6.2E-11	6.2E-11	1.3E-09	1.3E-09	1.3E-09	1.1E-09	1.13E-09	1.11E-09
n-Pentane	0.0E+00	0.0E+00	0.0E+00	2.7E-12	2.7E-12	2.7E-12	2.3E-12	2.33E-12	2.29E-12
Nitrogen	0.0218	0.0215	0.0217	0.1183	0.1174	0.1188	0.3111	0.307468	0.310702

The produced CNG in each LNG differs from one mode to the other. CNG produced from lean LNG vaporised BOG had a high methane content, low heavier hydrocarbons and nitrogen content as its LNG source is. The rich LNG vaporised BOG has provided a lowest methane and rich in heavier hydrocarbon and nitrogen content while CNG from BOG of medium LNG displayed medium value of the methane, heavier hydrocarbons and nitrogen as the LNG sources was. The ships unloading mode provided CNG rich in hydrocarbons mainly methane and low in nitrogen content among other modes for all LNG sources. This was due to the BOG contribution from a fresh feed LNG from ships. As it has described in the literature, CNG typical is made of methane of 85-95%, ethane of 1-10%, propane of 0-2%, traces of heavier hydrocarbon, and nitrogen of 1-3%. The CNG composition can be less or more to the typical CNG composition. As the resulted CNG revealed, CNG from lean and rich LNG's BOG was away the range due to the methane and nitrogen components while CNG from medium LNG's BOG do meet the typical CNG compositional range as shown in table 29 above.

Produced CNG properties have been summarized in table 30 with comparison to the typical CNG properties from literature. The CNG produced from rich LNG's BOG fell off the range due to its very low heating value and heat capacity which highly limit its performance as a fuel (Graham et al., 1998; Kouroussis & Karimi, 2006). This is due to its high content of nitrogen and very low methane. Thus, CNG produced from BOG of rich LNG cannot be an option to be used as fuel unless blended to increase its heating and heat capacity value. The CNG from BOG of lean and medium LNG have shown good properties compare to typical CNG properties whereby the CNG from lean LNG's BOG is far better as a fuel with good heating value. Therefore, the CNG from lean and medium LNG' BOG can be good fuel.

Table 30. Produced CNG properties and its comparison to typical CNG properties' range.

Properties	Mode									Typical CNG range from literature
	LNG regasification			Ships unloading			LNG holding			
	Lean	Medium	Rich	Lean	Medium	Rich	Lean	Medium	Rich	
Molecular Weight	16.304	17.460	19.768	16.300	17.449	19.725	16.303	17.466	19.763	16-20
Molar Density (kgmole/m³)	11.995	11.597	10.930	11.997	11.603	10.949	11.995	11.594	10.932	-
Mass Density (kg/m³)	195.559	202.488	216.077	195.550	202.465	215.960	195.557	202.504	216.061	150 - more than 200
Act. Volume (m³)	1615.441	1434.024	1421.472	953.631	773.321	802.047	114.865	110.469	89.233	-
Specific Heat Capacity (kJ/kgmole.C)	55.451	53.097	48.821	55.460	53.121	48.908	55.452	53.081	48.831	-
Mass Heat Capacity (kJ/kg.C)	3.401	3.041	2.470	3.402	3.044	2.480	3.401	3.039	2.471	2.9-3.2
LHV Molar Basis (Std) (kJ/kgmole)	785259.898	707840.243	553036.409	785490.033	708538.123	555959.847	785279.252	707402.875	553363.367	-
HHV Molar Basis (Std) (kJ/kgmole)	865496.959	780165.067	609543.274	865750.608	780934.251	612765.404	865518.291	779683.012	609903.639	-

HHV Basis (kJ/kg)	53086.137	44683.817	30834.392	53112.872	44754.536	31065.858	53088.385	44639.540	30860.229	-
LHV Basis (kJ/kg)	48164.715	40541.425	27975.932	48188.972	40605.589	28185.941	48166.754	40501.253	27999.374	-
Molar Volume (m³/kgmole)	0.083	0.086	0.091	0.083	0.086	0.091	0.083	0.086	0.091	~0.1-0.12
Thermal Conductivity (W/m. K)	0.073	0.068	0.060	0.073	0.068	0.060	0.073	0.068	0.060	0.04-0.07
LHV (MJ/Nm³)	35.870	31.640	24.720	35.870	31.680	24.840	35.870	31.600	24.720	≈32-35
HHV (MJ/Nm³)	39.850	35.130	27.440	39.850	35.170	27.580	39.850	35.110	27.460	35-40
Compressibility factor	0.998	0.998	0.999	0.998	0.998	0.999	0.998	0.998	0.999	0.85-1
Stoichiometric air/fuel ratio (Vol/Vol)	9.530	8.400	6.560	9.530	8.410	6.600	9.530	8.400	6.570	9 to 10
Stoichiometric air/fuel ratio (Mass/Mass)	17.200	13.940	9.620	17.200	13.960	9.690	17.200	13.920	9.630	17-18
Specific gravity (relative to air)	0.554	0.603	0.683	0.554	0.602	0.681	0.554	0.603	0.682	0.55-0.75
Wobbe index (MJ/Nm³)	48.190	40.750	29.930	48.190	40.810	30.100	48.190	40.690	29.930	44-55
Methane number	100.000	103.000	102.000	100.000	103.000	102.000	100.000	103.000	102.000	70-130+
Motor octane number ≈	825.000	849.000	841.000	825.000	849.000	841.000	825.000	849.000	841.000	-

4.6. Validation

The model was validated with comparison of the model results obtained by Adom & Ji (2010). Adom & Ji (2010) has used LKP and BWRS models to BOG generation and the methane percentage of the LNG in various LNG storage tanks with different sizes. The model focused on the effect of methane percentage in LNG to the amount of BOG produced daily for various storage tank sizes. For validation purpose, one of the LNG storage tank sizes and two methane content percentage within the studied scope were used. However, there is discrepancies in the heat leakage, an out of the box methane percentage was added in comparison, and only LNG holding operational mode was validated. The resulted data of 200,000m³ storage tank were extracted and plotted with the current study results in the figure below.

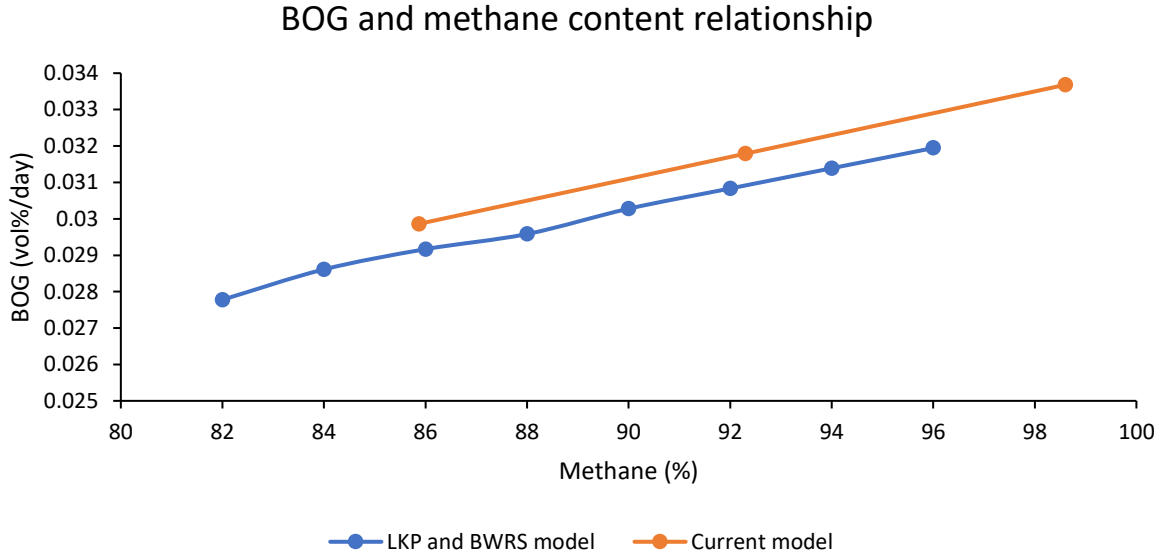


Figure 63. Study results comparison of BOG generation and methane content relationship during holding mode.

BOG generation and methane content relationship comparison revealed the same behaviour despite different operating conditions. As the methane content increases, the BOG generation increases as well. Since they all have linear behaviour, the BOR estimation was calculated by using their slopes. BOR for Adom & Ji (2010) and current study turned out to be 0.029% and 0.03% respectively for the same storage tank size.

CHAPTER V.

CONCLUSION AND RECOMMENDATION

5.1. Conclusion

With increasing global energy demand and environmental concerns, LNG is favored as a cleaner fossil fuel, driving continuous enhancements in the LNG supply chain for economic and environmental efficiency. Measures such as BOG reliquefaction, using BOG as fuel for LNG regasification, and compressing BOG into natural gas distribution have significantly reduced BOG wastage, despite occasional flaring and high energy requirements. Converting BOG into CNG fuel for local vehicles is proposed. BOG generation, depending on terminal operations and facilities, is managed using above-ground full containment LNG tanks to minimize energy consumption. Studies on LNG compositions and operational modes at a terminal in Maputo reveal that ship unloading generates the most BOG due to additional heat leakage. Converting BOG into CNG is effective, but rich LNG's BOG may need blending for vehicle fuel use. A detailed economic and market analysis is recommended before implementing this solution. The adopted Boil-Off Gas (BOG) management method involves converting BOG into CNG. This process, implemented at the studied receiving terminal, avoids flaring BOG. Each BOG recovery was conducted during the seasonal transition period, with a multistage compressor used for conversion. Energy consumption was lower during LNG regasification and higher during ship unloading. While CNG from lean and medium LNG BOG met specifications, CNG from rich LNG BOG was off-spec due to a low lower heating value and may require blending for vehicle fuel. Despite promising findings for managing BOG, ensuring environmental friendliness and efficient resource use, a detailed economic and market analysis is recommended before full implementation.

5.2. Future study recommendation

This study serves as a starting point for converting BOG into vehicle fuel, offering insights into BOG generation influenced by climate, facilities, and LNG composition. It provides a basis for BOG recovery, conversion into CNG, and associated energy consumption. Future studies should simulate different LNG compositions, operating conditions, and storage tank types to assess climate effects and efficiency. Economic and energy analyses, budget assessments, and experimental studies are needed to refine and validate the model, improve BOG management efficiency, and enhance CNG fuel quality through blending.

REFERENCES

- AccuWeather. (2024, June). *Weather forecast*. AccuWeather. <https://www.accuweather.com/en/mz/maputo/242431/weather-forecast/>
- Adom, E., & Ji, X. (2010). Modelling of Boil-Off Gas in LNG Tanks: A Case Study. In *International Journal of Engineering and Technology* (Vol. 2, Issue 4).
- Agarwal, R., Rainey, T. J., Ashrafur Rahman, S. M., Steinberg, T., Perrons, R. K., & Brown, R. J. (2017). LNG regasification terminals: The role of geography and meteorology on technology choices. *Energies*, *10*(12). <https://doi.org/10.3390/en10122152>
- Al Ghafri, S. Z. S., Perez, F., Heum Park, K., Gallagher, L., Warr, L., Stroda, A., Siahvashi, A., Ryu, Y., Kim, S., Kim, S. G., Seo, Y., Johns, M. L., & May, E. F. (2021). Advanced boil-off gas studies for liquefied natural gas. *Applied Thermal Engineering*, *189*. <https://doi.org/10.1016/j.applthermaleng.2021.116735>
- Alexandra, J., & Antunes, S. (2018). *Simulation and Design of a Boil-Off Gas Re-liquefaction System in a Small-Scale LNG Supply Chain Case Study of Trafaria*.
- Alyami, H., Lee, P. T. W., Yang, Z., Riahi, R., Bonsall, S., & Wang, J. (2014). An advanced risk analysis approach for container port safety evaluation. *Maritime Policy and Management*, *41*(7), 634–650. <https://doi.org/10.1080/03088839.2014.960498>
- Ashok, B., & Nanthagopal, K. (2018). Eco friendly biofuels for CI engine applications. In *Advances in Eco-Fuels for a Sustainable Environment* (pp. 407–440). Elsevier. <https://doi.org/10.1016/B978-0-08-102728-8.00015-2>
- Aslam, M. U., Masjuki, H. H., Kalam, M. A., Abdesselam, H., Mahlia, T. M. I., & Amalina, M. A. (2006). An experimental investigation of CNG as an alternative fuel for a retrofitted gasoline vehicle. *Fuel*, *85*(5–6), 717–724. <https://doi.org/10.1016/j.fuel.2005.09.004>
- Backhaus, H. W., & Friedrichs, K. (1980). A New Concept of an Offshore LNG-tanker Loading and Unloading System. In *Underwater Technology* (pp. 93–108). Elsevier. <https://doi.org/10.1016/b978-0-08-026141-6.50012-0>
- Badger, J., Bauwens, I., Casso, P., Davis, N., Hahmann, A., Hansen, S. B. K., Hansen, B. O., Heathfield, D., Knight, O. J., Lacave, O., Lizcano, G., Bosch i Mas, A., Mortensen, N. G.,

- Olsen, B. T., Onninen, M., Potter Van Loon, A., & Volker, P. (2024). *Mozambique mean wind speed at 100m*. <https://globalwindatlas.info>
- Benito, A. (2009). *Accurate determination of LNG quality unloaded in Receiving Terminals: An Innovative Approach*.
- Bisen, V. S., Karimi, I. A., & Farooq, S. (2018). Dynamic Simulation of a LNG Regasification Terminal and Management of Boil-off Gas. In *Computer Aided Chemical Engineering* (Vol. 44, pp. 685–690). Elsevier B.V. <https://doi.org/10.1016/B978-0-444-64241-7.50109-9>
- British Petroleum, & International Gas Union. (2011). *Guidebook to Gas Interchangeability and Gas Quality*. <https://www.igu.org/resources/guidebook-to-gas-interchangeability-and-gas-quality-august-2011/>
- Coyle, D. A., & Patel, V. (2005). Processes and Pump Services in the LNG Industry. *The 22nd International Pump Users Symposium*, 179–185. <https://doi.org/10.21423/R18H4F>
- Dobrota, Đ., Lalić, B., & Komar, I. (2013). Problem of Boil - off in LNG Supply Chain. *Transactions on Maritime Science*, 2(2), 91–100. <https://doi.org/10.7225/toms.v02.n02.001>
- EPA. (2023, November 1). *Importance of Methane*. Global Methane Initiative. <https://www.epa.gov/gmi/importance-methane>
- Finlayson-Pitts, B. J., & Pitts Jr., J. N. (2000). *Chemistry of the Upper and Lower Atmosphere*. Academic Press.
- Foss, M. M. (2012). *Introduction to LNG: An overview on liquefied natural gas (LNG), its properties, the LNG industry, and safety considerations*. www.beg.utexas.edu/energyecon/lng
- Geman, H., & Ohana, S. (2009). Forward curves, scarcity and price volatility in oil and natural gas markets. *Energy Economics*, 31(4), 576–585. <https://doi.org/10.1016/j.eneco.2009.01.014>
- Gomes, J., Damasceno, A., Carrilho, C., Lobo, V., Lopes, H., Madede, T., Pravinrai, P., Silva-Matos, C., Diogo, D., Azevedo, A., & Lunet, N. (2014). The effect of season and temperature variation on hospital admissions for incident stroke events in Maputo, Mozambique. *Journal of Stroke and Cerebrovascular Diseases*, 23(2), 271–277. <https://doi.org/10.1016/j.jstrokecerebrovasdis.2013.02.012>

- Graham, J. P., Stockwell, R. T., & Montez, A. M. (1998). A New CNG Engine Test for the Evaluation of Natural Gas Engine Oils Author(s): Wim van Dam. In *Journal of Fuels and Lubricants* (Vol. 107).
- Hafner, M., & Luciani, G. (2022). *The Palgrave Handbook of International Energy Economics* (M. Hafner & G. Luciani, Eds.). Palgrave Macmillan. <https://doi.org/10.1007/978-3-030-86884-0>
- Hannah, R., Pablo, R., & Max, R. (2024). Energy Production and Consumption. *Our World in Data*.
- Huang, B., Li, J., Fu, C., Guo, T., & Feng, S. (2022). A Comprehensive Review of Stratification and Rollover Behavior of Liquefied Natural Gas in Storage Tanks. In *Processes* (Vol. 10, Issue 7). MDPI. <https://doi.org/10.3390/pr10071360>
- Hyundai. (2007). HYUNDAI-JC CARTER-SNECMA LNG marine pumps. In *HYUNDAI-JC CARTER-SNECMA LNG marine pump*. Motralec. www.motralec.com
- IGU. (2024). *2024 World LNG report*.
- International Energy Agency. (2023). *World Energy Outlook 2023*. www.iea.org/terms
- Kaplan, A., & Yang, C. (2003). *Design Considerations for an LNG Receiving Terminal*. 1–9. <https://doi.org/doi:10.2118/84257-ms>
- Khan, M. I., Yasmin, T., & Shakoor, A. (2015). Technical overview of compressed natural gas (CNG) as a transportation fuel. In *Renewable and Sustainable Energy Reviews* (Vol. 51, pp. 785–797). Elsevier Ltd. <https://doi.org/10.1016/j.rser.2015.06.053>
- Khan, M. Ibrahim., & Islam, R. (2007). *The petroleum engineering handbook: sustainable operations*. Gulf Pub.
- Khan, M. S., Qyyum, M. A., Ali, W., Wazwaz, A., Ansari, K. B., & Lee, M. (2020). Energy saving through efficient BOG prediction and impact of static boil-off-rate in full containment-type LNG storage tank. *Energies*, 13(21). <https://doi.org/10.3390/en13215578>
- Kim, D., Sohn, Y., Lee, K., Yoon, I., & Yang, Y. (2010, November 14). Design of Samcheok LNG Receiving Terminal of Korea Gas Corporation. *ISOPE-2010*.

- Kouroussis, D., & Karimi, S. (2006). Alternative Fuels in Transportation. *Bulletin of Science, Technology & Society*, 26(4), 346–355. <https://doi.org/10.1177/0270467606292150>
- Kramer, U., Lorenz, T., Hofmann, C., Ruhland, H., Klein, R., & Weber, C. (2017). Methane Number Effect on the Efficiency of a Downsized, Dedicated, High Performance Compressed Natural Gas (CNG) Direct Injection Engine. *SAE Technical Papers, 2017-March*(March). <https://doi.org/10.4271/2017-01-0776>
- Kurle, Y. M., Wang, S., & Xu, Q. (2017). Dynamic simulation of LNG loading, BOG generation, and BOG recovery at LNG exporting terminals. *Computers and Chemical Engineering*, 97, 47–58. <https://doi.org/10.1016/j.compchemeng.2016.11.006>
- Lembrechts, J. J., van den Hoogen, J., Aalto, J., Ashcroft, M. B., De Frenne, P., Kemppinen, J., Kopecký, M., Luoto, M., Maclean, I. M. D., Crowther, T. W., Bailey, J. J., Haesen, S., Klinges, D. H., Niittynen, P., Scheffers, B. R., Van Meerbeek, K., Aartsma, P., Abdalaze, O., Abedi, M., ... Lenoir, J. (2022). Global maps of soil temperature. In *Global Change Biology* (Vol. 28, Issue 9, pp. 3110–3144). John Wiley and Sons Inc. <https://doi.org/10.1111/gcb.16060>
- Li, Y., & Li, Y. (2016). Dynamic optimization of the Boil-Off Gas (BOG) fluctuations at an LNG receiving terminal. *Journal of Natural Gas Science and Engineering*, 30, 322–330. <https://doi.org/10.1016/j.jngse.2016.02.041>
- Liu, C., Zhang, J., Xu, Q., & Gossage, J. L. (2010). Thermodynamic-analysis-based design and operation for boil-off gas flare minimization at LNG receiving terminals. *Industrial and Engineering Chemistry Research*, 49(16), 7412–7420. <https://doi.org/10.1021/ie1008426>
- Long, Bob., & Garner, Bob. (2004). *Guide to storage tanks & equipment : the practical reference book and guide to storage tanks and ancillary equipment with a comprehensive buyers' guide to worldwide manufacturers and suppliers*. Professional Engineering.
- Lu, H., Ma, G., Li, X., & Wu, S. (2018). Stress analysis of LNG storage tank outlet pipes and flanges. *Energies*, 11(4). <https://doi.org/10.3390/en11040877>
- Milojević, S., Gordić, D., & Pešić, R. (2012). *MVM2012-066 Natural Gas as a Safe Technology for Clean Urban Vehicles*.

- Mokhatab, S., Mak, J. Y., Valappil, J. V., & Wood, D. A. (2014). *Handbook of Liquefied Natural Gas* (1st ed.). Gulf Professional Publishing. <http://elsevier.com/locate/permissions>,
- Naji, S. Z., Abd, A. A., & Hashim, A. S. (2019a). Tracking boil off gas generation into liquefied natural gas supply chain using HYSYS simulator. *IOP Conference Series: Materials Science and Engineering*, 579(1). <https://doi.org/10.1088/1757-899X/579/1/012019>
- Naji, S. Z., Abd, A. A., & Hashim, A. S. (2019b). Tracking boil off gas generation into liquefied natural gas supply chain using HYSYS simulator. *IOP Conference Series: Materials Science and Engineering*, 579(1). <https://doi.org/10.1088/1757-899X/579/1/012019>
- NEED. (2018). *Forms of Energy What Is Energy?* www.NEED.org
- Pandit, V. (2017, April 22). Pressurized TM CNG-advanced Material Grade for High Pressure CNG Fuel Line Applications. *IOGPC2017*. <http://www.asme.org/about-asme/terms-of-use>
- Phalen, T., Prescott, C. N., Zhang, J., & Findlay, T. (2007). Update on subsea LNG pipeline technology. *Offshore Technology Conference, Proceedings, 1*, 313–322. <https://doi.org/10.4043/18542-ms>
- Pindyck, R. S. (2004). Volatility in Natural Gas and Oil Markets. In *Source: The Journal of Energy and Development* (Vol. 30, Issue 1).
- Poling, B. E., Thomson, G. H., Friend, D. G., Rowley, R. L., & Wilding, W. V. (2008). *Perry's Chemical Engineers' Handbook*. The McGraw-Hill Companies.
- Querol, E., Gonzalez-Regueral, B., García-Torrent, J., & García-Martínez, M. J. (2010). Boil off gas (BOG) management in Spanish liquid natural gas (LNG) terminals. *Applied Energy*, 87(11), 3384–3392. <https://doi.org/10.1016/j.apenergy.2010.04.021>
- Rahmania, A., & Purwanto, W. W. (2020). Simulation of boil-off gas effect along LNG supply chain on quantity and quality of natural gas. *AIP Conference Proceedings*, 2223. <https://doi.org/10.1063/5.0000853>
- Rehnlund, B. (2008). *Outlook on standardization of alternative vehicle fuels* (M. van Walwijk, Ed.). www.atrax.se

- Robinson, D. B., Peng, D. Y., & Ng, H. J. (1977). Applications of the Peng-Robinson Equation of State. *ACS Symposium Series*, 60, 200–220. <https://doi.org/10.1021/bk-1977-0060.ch008>
- Rötzer, Josef. (2016). *Design and Construction of LNG Storage Tanks* (Konrad. Bergmeister, Frank. Fingerloos, & J. Dietrich. Wörner, Eds.). Ernst & Sohn.
- Sedlaczek, R. (2008). *Boil-Off in Large and Small Scale LNG Chains* [NTNU]. <http://www.ipt.ntnu>
- Shammazov, I., & Karyakina, E. (2023). The LNG Flow Simulation in Stationary Conditions through a Pipeline with Various Types of Insulating Coating. *Nurse Researcher*, 8(2). <https://doi.org/10.3390/fluids8020068>
- Smitherman, B. T., Porter, D., & Craddick, C. (2013). *Regulations for Compressed Natural Gas and Liquefied Natural Gas*. www.rrc.state.tx.us.
- Speight, J. G. (2019). Recovery, storage, and transportation. In *Natural Gas* (pp. 149–186). Elsevier. <https://doi.org/10.1016/b978-0-12-809570-6.00005-9>
- Tarakad, R. R. . (2000). *LNG receiving and regasification terminals : an overview of design, operation, and project development considerations*. Zeus Development Corp.
- The World Bank. (2022). *2022 Global Gas Flaring Tracker Report*. www.worldbank.org
- The World Bank. (2023). *Global Gas Flaring Tracker Report*. www.worldbank.org
- Turbaningsih, O., & Yuanita, N. (2014). Vessel mooring analysis and ignition range dispersion analysis for LNG jetty facilities. *Jurnal Teknologi (Sciences and Engineering)*, 69(7), 173–180. <https://doi.org/10.11113/jt.v69.3284>
- Tutiempo network. (2024, June). *Solar radiation*. Tutiempo. <https://en.tutiempo.net/solar-radiation/maputo>
- Włodek, T. (2019). Analysis of boil-off rate problem in Liquefied Natural Gas (LNG) receiving terminals. *IOP Conference Series: Earth and Environmental Science*, 214(1). <https://doi.org/10.1088/1755-1315/214/1/012105>
- World Bank. (2007). *Environmental, Health, and Safety Guidelines for Liquefied Natural Gas (LNG) Facilities*. www.ifc.org/ifcext/enviro.nsf/Content/EnvironmentalGuidelines

- World Bank. (2017). *Environmental, Health, and Safety Guidelines for Liquefied Natural Gas Facilities*. www.ifc.org/ehsguidelines.
- Wu, M., Zhu, Z., Sun, D., He, J., Tang, K., Hu, B., & Tian, S. (2019). Optimization model and application for the recondensation process of boil-off gas in a liquefied natural gas receiving terminal. *Applied Thermal Engineering*, *147*, 610–622. <https://doi.org/10.1016/j.applthermaleng.2018.10.117>
- Xiong, L., Liao, H.-L., & Li, M.-S. (2014, August 28). The flutter performance study for a suspension bridge based on numerical analysis and wind-tunnel test. *ACEM14*.
- Yang, Y.-M. (2006). *Development of the World's Largest Above-ground Full Containment LNG Storage Tank*.
- Zakaria, M. S., Osman, K., Saadun, M. N. A., Manaf, M. Z. A., & Mohd Hanafi, M. H. (2013). Computational simulation of boil-off gas formation inside liquefied natural gas tank using evaporation model in ANSYS fluent. *Applied Mechanics and Materials*, *393*, 839–844. <https://doi.org/10.4028/www.scientific.net/AMM.393.839>
- Zakaria, Z., Baslasl, M. S. O., Samsuri, A., Ismail, I., Supee, A., & Haladin, N. B. (2019). Rollover Phenomenon in Liquefied Natural Gas Storage Tank. *Journal of Failure Analysis and Prevention*, *19*(5), 1439–1447. <https://doi.org/10.1007/s11668-019-00739-2>

ANNEXES

I. Depicted temperature and solar radiation

Table 31. Used temperature and solar radiation (AccuWeather, 2024; Tutiempo network, 2024).

Date	Time (hour)	Solar radiation (W/m ²)	Temperature (°C)	Date	Time (hour)	Solar radiation (W/m ²)	Temperature (°C)	Date	Time (hour)	Solar radiation (W/m ²)	Temperature (°C)
26 May, 2024	0:00	0	19	2 June, 2024	0:00	0	20	9 June, 2024	0:00	0	14
	1:00	0	19		1:00	0	19		1:00	0	14
	2:00	0	18		2:00	0	19		2:00	0	14
	3:00	0	18		3:00	0	19		3:00	0	14
	4:00	0	18		4:00	0	18		4:00	0	14
	5:00	0	18		5:00	0	18		5:00	0	14
	6:00	0	19		6:00	0	18		6:00	0	14
	7:00	15	19		7:00	34	18		7:00	14	15
	8:00	77	19		8:00	219	20		8:00	106	15
	9:00	354	21		9:00	397	22		9:00	245	17
	10:00	542	24		10:00	533	24		10:00	382	18
	11:00	639	26		11:00	613	26		11:00	489	19
	12:00	657	27		12:00	637	27		12:00	538	20
	13:00	610	28		13:00	594	28		13:00	529	21
	14:00	502	28		14:00	488	29		14:00	451	22
	15:00	342	28		15:00	331	28		15:00	306	21
	16:00	148	28		16:00	140	27		16:00	129	21
	17:00	1	25		17:00	1	25		17:00	0	20
	18:00	0	24		18:00	0	25		18:00	0	18
	19:00	0	23		19:00	0	24		19:00	0	17
20:00	0	22	20:00	0	23	20:00	0	16			

	21:00	0	22		21:00	0	23		21:00	0	15
	22:00	0	22		22:00	0	23		22:00	0	15
	23:00	0	21		23:00	0	23		23:00	0	15
27 May, 2024	0:00	0	21	3 June, 2024	0:00	0	23	10 June, 2024	0:00	0	15
	1:00	0	20		1:00	0	22		1:00	0	15
	2:00	0	20		2:00	0	22		2:00	0	14
	3:00	0	20		3:00	0	21		3:00	0	14
	4:00	0	19		4:00	0	20		4:00	0	13
	5:00	0	19		5:00	0	20		5:00	0	14
	6:00	0	19		6:00	0	20		6:00	0	14
	7:00	43	19		7:00	33	20		7:00	13	15
	8:00	234	21		8:00	218	21		8:00	85	15
	9:00	417	22		9:00	399	22		9:00	225	17
	10:00	555	24		10:00	536	24		10:00	381	18
	11:00	636	25		11:00	618	25		11:00	499	20
	12:00	652	26		12:00	637	26		12:00	563	21
	13:00	606	26		13:00	592	27		13:00	550	22
	14:00	500	25		14:00	486	27		14:00	467	22
	15:00	340	25		15:00	329	26		15:00	318	21
	16:00	147	25		16:00	139	26		16:00	134	20
	17:00	1	24		17:00	0	25		17:00	0	18
	18:00	0	23		18:00	0	25		18:00	0	17
	19:00	0	23		19:00	0	24		19:00	0	16
	20:00	0	23		20:00	0	23		20:00	0	16
	21:00	0	22		21:00	0	23		21:00	0	15
	22:00	0	21		22:00	0	22		22:00	0	15
23:00	0	20	23:00	0	22	23:00	0	15			
28 May, 2024	0:00	0	19	4 June, 2024	0:00	0	21	11 June, 2024	0:00	0	15
	1:00	0	19		1:00	0	21		1:00	0	14
	2:00	0	19		2:00	0	20		2:00	0	14

	3:00	0	18		3:00	0	19		3:00	0	13
	4:00	0	18		4:00	0	18		4:00	0	13
	5:00	0	18		5:00	0	18		5:00	0	13
	6:00	0	17		6:00	0	17		6:00	0	14
	7:00	41	18		7:00	32	17		7:00	25	14
	8:00	232	19		8:00	216	17		8:00	203	15
	9:00	414	21		9:00	396	19		9:00	382	18
	10:00	552	23		10:00	534	21		10:00	520	20
	11:00	582	24		11:00	616	23		11:00	603	22
	12:00	499	26		12:00	635	24		12:00	623	22
	13:00	500	26		13:00	590	25		13:00	580	23
	14:00	489	26		14:00	485	25		14:00	477	23
	15:00	333	26		15:00	328	25		15:00	323	24
	16:00	145	25		16:00	138	24		16:00	135	23
	17:00	1	23		17:00	0	23		17:00	0	22
	18:00	0	22		18:00	0	22		18:00	0	21
	19:00	0	21		19:00	0	21		19:00	0	20
	20:00	0	21		20:00	0	20		20:00	0	19
	21:00	0	21		21:00	0	19		21:00	0	18
	22:00	0	20		22:00	0	18		22:00	0	17
	23:00	0	19		23:00	0	18		23:00	0	17
29 May, 2024	0:00	0	19	5 June, 2024	0:00	0	16	12 June, 2024	0:00	0	16
	1:00	0	19		1:00	0	16		1:00	0	15
	2:00	0	19		2:00	0	15		2:00	0	14
	3:00	0	18		3:00	0	15		3:00	0	14
	4:00	0	18		4:00	0	14		4:00	0	14
	5:00	0	16		5:00	0	14		5:00	0	13
	6:00	0	15		6:00	0	14		6:00	0	13
	7:00	35	20		7:00	31	14		7:00	24	13
	8:00	138	18		8:00	214	15		8:00	202	15

	9:00	396	20		9:00	394	18		9:00	381	18
	10:00	549	23		10:00	532	21		10:00	518	20
	11:00	630	25		11:00	613	23		11:00	601	22
	12:00	649	26		12:00	632	25		12:00	621	24
	13:00	602	26		13:00	584	26		13:00	579	25
	14:00	496	27		14:00	470	27		14:00	476	26
	15:00	337	27		15:00	324	26		15:00	322	27
	16:00	144	27		16:00	134	25		16:00	135	25
	17:00	1	24		17:00	0	24		17:00	0	24
	18:00	0	22		18:00	0	22		18:00	0	22
	19:00	0	22		19:00	0	21		19:00	0	21
	20:00	0	21		20:00	0	20		20:00	0	20
	21:00	0	21		21:00	0	19		21:00	0	19
	22:00	0	20		22:00	0	18		22:00	0	18
23:00	0	19	23:00	0	17	23:00	0	17			
30 May, 2024	0:00	0	19	6 June, 2024	0:00	0	16	13 June, 2024	0:00	0	21
	1:00	0	19		1:00	0	16		1:00	0	20
	2:00	0	18		2:00	0	15		2:00	0	19
	3:00	0	17		3:00	0	14		3:00	0	20
	4:00	0	17		4:00	0	14		4:00	0	21
	5:00	0	16		5:00	0	14		5:00	0	20
	6:00	0	17		6:00	0	14		6:00	0	20
	7:00	39	17		7:00	29	14		7:00	23	21
	8:00	227	19		8:00	205	15		8:00	200	23
	9:00	408	22		9:00	373	18		9:00	380	24
	10:00	546	22		10:00	489	21		10:00	516	28
	11:00	628	24		11:00	543	24		11:00	599	26
	12:00	646	25		12:00	538	27		12:00	619	23
	13:00	600	27		13:00	468	28		13:00	578	26
14:00	494	28	14:00	352	29	14:00	475	25			

	15:00	335	29		15:00	260	29		15:00	321	26
	16:00	143	28		16:00	117	28		16:00	136	27
	17:00	1	26		17:00	0	26		17:00	0	25
	18:00	0	25		18:00	0	24		18:00	0	24
	19:00	0	24		19:00	0	22		19:00	0	24
	20:00	0	23		20:00	0	21		20:00	0	23
	21:00	0	22		21:00	0	20		21:00	0	22
	22:00	0	21		22:00	0	22		22:00	0	21
	23:00	0	20		23:00	0	18		23:00	0	21
31 May, 2024	0:00	0	19	7 June, 2024	0:00	0	18				
	1:00	0	19		1:00	0	17				
	2:00	0	19		2:00	0	16				
	3:00	0	19		3:00	0	16				
	4:00	0	18		4:00	0	15				
	5:00	0	18		5:00	0	15				
	6:00	0	17		6:00	0	15				
	7:00	37	17		7:00	23	16				
	8:00	225	19		8:00	154	17				
	9:00	406	22		9:00	311	19				
	10:00	544	24		10:00	445	21				
	11:00	625	26		11:00	538	23				
	12:00	644	27		12:00	575	24				
	13:00	598	29		13:00	549	24				
	14:00	492	28		14:00	460	24				
	15:00	334	28		15:00	310	23				
	16:00	142	27		16:00	129	23				
17:00	1	26	17:00	0	22						
18:00	0	24	18:00	0	21						
19:00	0	23	19:00	0	21						
20:00	0	23	20:00	0	20						

	21:00	0	22		21:00	0	19
	22:00	0	21		22:00	0	18
	23:00	0	21		23:00	0	18
1 June, 2024	0:00	0	20	8 June, 2024	0:00	0	16
	1:00	0	20		1:00	0	16
	2:00	0	20		2:00	0	15
	3:00	0	19		3:00	0	16
	4:00	0	19		4:00	0	16
	5:00	0	19		5:00	0	16
	6:00	0	18		6:00	0	16
	7:00	27	18		7:00	27	17
	8:00	115	19		8:00	206	17
	9:00	200	21		9:00	383	18
	10:00	268	23		10:00	519	19
	11:00	308	25		11:00	601	20
	12:00	375	26		12:00	620	21
	13:00	404	27		13:00	578	22
	14:00	370	28		14:00	475	22
	15:00	283	28		15:00	318	22
	16:00	130	27		16:00	132	21
	17:00	1	26		17:00	0	21
	18:00	0	24		18:00	0	20
	19:00	0	23		19:00	0	18
	20:00	0	23		20:00	0	18
	21:00	0	22		21:00	0	17
	22:00	0	21		22:00	0	16
23:00	0	21	23:00	0	15		

II. Collected Maputo average wind speed

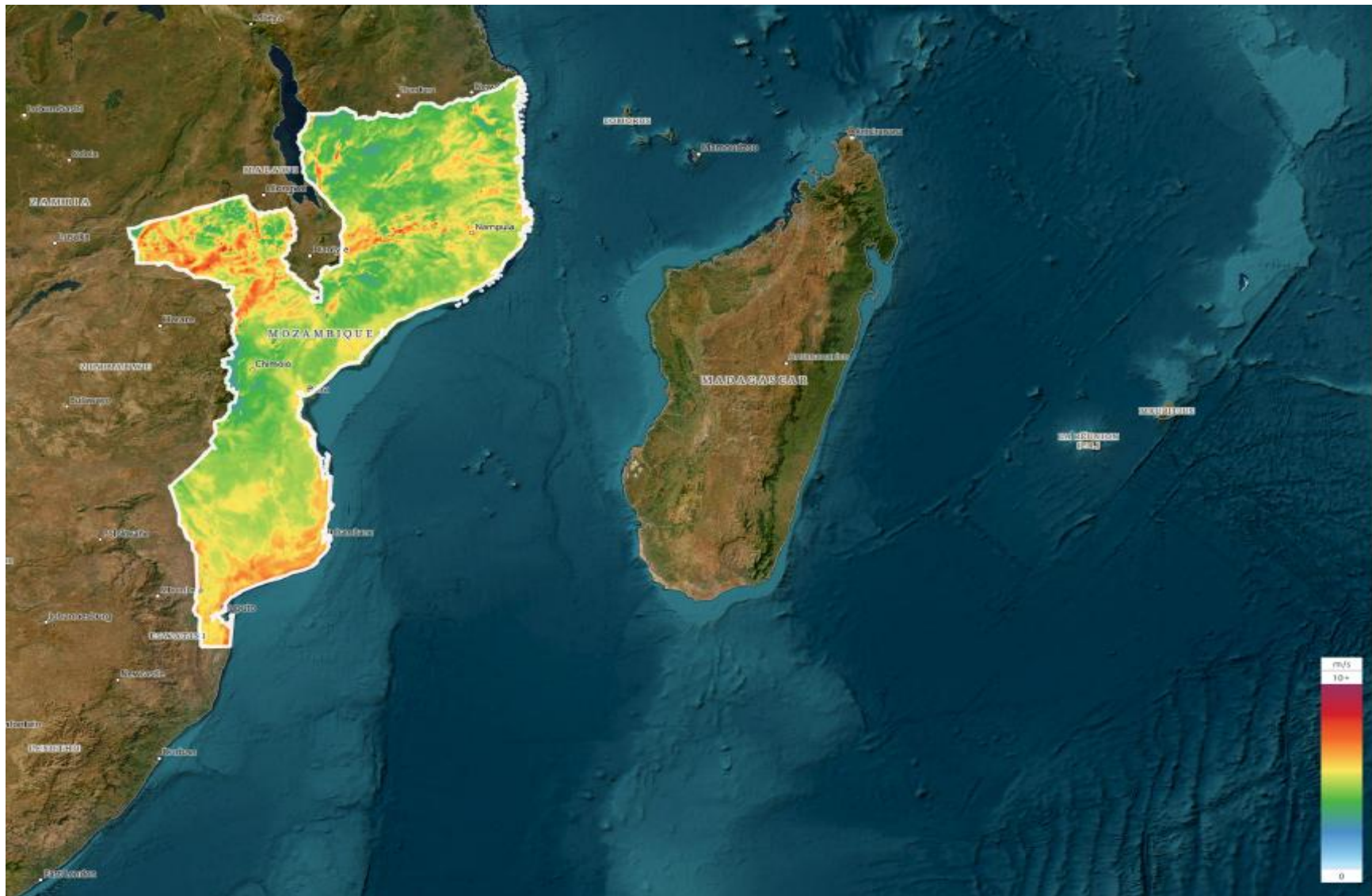


Figure 64. Mozambican map of average wind speed at 100m (Badger et al., 2024).

Emmanuel

NGIRUWONSANGA

Dedicated to exploration of natural resources and hydrocarbon processing in sustainable and environmentally friendly manner towards sustainable development.

Experience

March- June 2024

Processing Engineer

Intern at the SASOL Petroleum Temane in Central Processing Facility responsible for Processing Engineer's duties in plant and have worked to handle liquids especially water and condensate.

June – July 2022

Geologist

Responsible of development and exploration of a mine for FXB- TUGIRANUBUMWE in sustainable and environmentally friendly manner with complying on mining rules and regulations.

September 2019 – February 2022

Digital Records Administrator

Digitalization of Rwandan mining and geological archive since the beginning of exploration and mining in Rwanda in Rwanda Mines, Petroleum, and Gas Board.

Education

2022 – 2024

Hydrocarbon Processing Engineer

Universidade Eduardo Mondlane

2015 – 2019

Applied Geology

University of Rwanda

Skills

- Modelling
- Design
- Creativity
- Entrepreneurship
- Exploration
- Processing
- Reserve estimation
- Mining

Contact

KN4 Nyarugenge
Kigali, Rwanda
+250788907475
nskyler.ne@gmail.com